Thesis for the Degree of Doctor of Philosophy

Functional Analysis of Two 4-Hydroxy-3-methylbut-2-enyl diphosphate reductase (Hdr) Isozymes in *Burkholderia glumae* BGR1

***Burkholderia glumae*에서 2벌의 Hdr에 대한 기능 연구**

February 2013

Department of Agricultural Biotechnology

Seoul National University

권 문 혁

Thesis for the Degree of Doctor of Philosophy

Functional Analysis of Two 4-Hydroxy-3-methylbut-2-enyl diphosphate reductase (Hdr) Isozymes in *Burkholderia glumae* BGR1

***Burkholderia glumae*에서 2벌의 Hdr에 대한 기능 연구**

Advisor: Soo Un Kim

Moonhyuk Kwon

February 2013

Functional Analysis of Two 4-Hydroxy-3-methylbut-2-enyl diphosphate reductase (Hdr) Isozymes in *Burkholderia glumae* BGR1

*Burkholderia glumae*에서 2벌의 Hdr에 대한 기능 연구

지도교수: 김 수 언

이 논문을 농학박사학위논문으로 제출함
2013 년 1 월

서울대학교 대학원
농생명공학부 응용생명화학전공
권 문 혁

권문혁의 박사학위논문을 인준함
2013 년 1 월

위 원 장 _____ 인

부위원장 _____ 인

위 원 _____ 인

위 원 _____ 인

위 원 _____ 인

Functional Analysis of Two

4-Hydroxy-3-methylbut-2-enyl diphosphate reductase (Hdr)

Isozymes in *Burkholderia glumae* BGR1

Advisor: Soo Un Kim

A dissertation submitted in partial fulfillment
of the requirement for the degree of

DOCTOR OF PHILOSOPHY

to the Faculty of
Department of Agricultural Biotechnology
at

SEOUL NATIONAL UNIVERSITY

by

Moonhyuk Kwon

Date Approved

_____ _____

_____

_____

_____

_____

ABSTRACT

The terpenoids are biosynthesized by polymerization of isoprenoid units consisting of isopentenyl diphosphate (IPP) and dimethylallyl diphosphate (DMAPP). The Hdr (4-Hydroxy-3-methylbut-2-enyl diphosphate reductase) is the ultimate enzyme in MEP pathway converting (*E*)-4-hydroxy-3-methylbut-2-enyl diphosphate (HMBPP) to IPP and DMAPP. Despite most free-living bacteria have a trend of genome size reduction in evolution from generalist to specialist, *Burkholderia glumae,* a Gram negative rice-pathogenic bacterium, harbors 2 *hdr* isogenes while lacking isopentenyl diphosphate isomerase (*idi*). Molecular and genetics analysis of *hdr* gene region suggest that each *hdr* isogene was found in respective putative operon. The *Bghdr1* gene and FKBP-type peptidyl-prolyl cis-trans isomerase (*slp*) were polycistronic, as were the *Bghdr2* gene and hopanoids associated radical *S*-adenosyl methionine (SAM) domain containing protein (*hpnH*). Hdr2 isozyme was placed in a clade different from Hdr1, and only 56.1 % identity was found between them. Nevertheless, both *hdr* genes could complement *E. coli hdr* deletion mutant (DYTL1). BgHdr1 and BgHdr2 catalyzed reduction of HMBPP into IPP and DMAPP at a virtually same ratio of 2:1, in contrast to 5:1 ratio of other bacterial Hdrs so far characterized *in vitro* enzyme assay. The k_{cat} and K_m values of BgHdr1 and BgHdr2 were 187.0 min^{-1} and 6.0 μM and 66.6 min^{-1} and 21.2 μM, respectively. Therefore, Hdr1 was 10 times more efficient than Hdr2: k_{cat}/K_M of Hdr1 was 31.1 μM^{-1} min^{-1} and Hdr2 3.1 μM^{-1} min^{-1}. The transcript message level of *hdr2* was 1.6 ~

1.8 folds higher than *hdr1* at 6 and 10 h after inoculation. The different expression level was further confirmed by Northern blot throughout whole growth phase. To identify the physiological role of each isogene, *hdr* knock-out (KO) mutants were constructed. On LB medium, the growth rates of 2 mutants were not different from that of BGR1 (wild-type). The colony size of *hdr1* knock-out mutant (HDR1KO) was smaller than that of BGR1 and *hdr2* knock-out mutant (HDR2KO). The HDR1KO grew slower than HDR2KO and BGR1 under conditions such as minimal nutrient, high temperature, acidic environment, and in planta. Especially, in rice plant, the HDR1KO was less virulent than due to the reduced colonization ability. The difference in phenotype was evident in protein composition of the KO mutants. In SDS-PAGE, several cellular protein bands of HDR1KO moved faster than those of HDR2KO and BGR1. The proteins that showed electrophoretic mobility shift was identified through LC MS/MS. The major change was observed in GroEL, which exhibited acetylation at Lys390 upon disruption of *hdr1*. To answer if the change was cued by the differential function of *hdr* isogenes or by the regulation in the promoter level, HDR1KO complementation assay was performed as follows. The 6 plasmids were constructed by combination of putative *hdr1* promoter, *hdr1* operon promoter, and *hdr2* promoter and two *hdr* open-reading frames (ORF).The GroEL acetylation of HDR1KO was rescued by the vectors harboring putative *hdr1* operon promoter, regardless of *hdr* ORF, The same vectors also rescued hypersensitive reaction (HR) ability of HDR1KO. The *hdr2* upstream region, the putative *hdr2* operon promoter, was predicted to have a ToxR (LysR-type regulator)

binding site by genome anlaysis. By electrophoretic mobility shift assay and yeast-1-hybride assay, ToxR was confirmed to bind and activate *hdr2* operon. The overall regulation points in MEP pathway were shown in transcriptome analysis. 4-Diphosphocytidyl-2-C-methyl-D-erythritol kinase (*cmk*) was up-regulated in both KO mutants, whereas (*E*)-4-hydroxy-3-methyl-but-2-enyl 4-diphosphate synthase (*hds*) was down regulated in HDR2KO. Upregulation of undecaprenyl diphosphate phosphatase (*upp*) and undecaprenyl diphosphate synthase (*ups*) and downregulation of squalene synthase1 (*sqs1*) and squalene synthase2 (*sqs2*) were found in HDR2KO. The most positively affected in the HDR1KO was *tox* operon genes that were responsible for toxoflavin biosynthesis. The toxin accumulation in the cell was higher in *hdr1* KO mutant than *hdr2* KO or BGR1. In the HDR2KO, the most up-regulated were stress-related ribosomal protein and SAM decarboxylase genes. .

Keywords; acetylation, *Burkholderia glumae*, GroEL, heat shock response, separated regulation, 4-hydroxy-3-methylbut-2-enyl diphosphate reductase (Hdr), 2-*C*-methyl-D-erythritol 4-phosphate (MEP) pathway.

Student Number; 2005-21628

CONTENTS

LIST OF FIGURES

LIST OF TABLES

LIST OF ABBREVIATIONS

AACT	Acetoacetyl CoA thiolase
AT	3-Amino-1,2,4-triazole
Bp	Base pair
CDP-ME	4-Diphosphocytidyl-2-*C*-methyl-D-erythritol
CDP-ME2P	4-Diphosphocytidyl-2-*C*-methyl-D-erythritol-2-phosphate
CFU	Colony forming unit
Cmek	CDP-ME kinase
DMAPP	Dimethylallyl diphosphate
DOXP	1-Deoxy-D-xylulose-5-phosphate
Dxr	DOXP reductoisomerase
Dxs	DOXP synthase
*Ec*LytB	*E. coli* LytB protein
FAD	Flavin adenine dinucleotide
FPP	Farnesyl diphosphate
FMN	Flavin mononucleotide
G-3-P	Glyceraldehyde 3-phosphate
GGPP	Geranylgeranyl diphosphate
gDNA	Genomic DNA
Hdr	HMBPP reductase
Hds	HMBPP synthase

HMBPP	1-Hydroxy-2-methyl-2-(*E*)-butenyl 4-diphosphate
HMG-CoA	3-Hydroxy-3-methylglutaryl coenzyme A
Hmgr	HMG-CoA reductase
Hmgs	HMG-CoA synthase
Idi	Isopentenyl diphosphate isomerase
Ids	Isopentenyl diphosphate / dimethylallyl diphosphate synthases
IPP	Isopentenyl diphosphate
kDa	Kilodalton
DMAPP	Dimethylallyl diphosphate
LB	Luria-Bertani
MEP	2-*C*-Methyl-D-erythritol 4-phosphate
MEcPP	2-*C*-Methyl-D-erythritol-2, 4-cyclodiphosphate
MVA	Mevalonic acid
Mvk	MVA kinase
MVP	Phosphomevalonate
MVPP	Diphosphomevalonate
NADH	Nicotinamide adenine dinucleotide hydeogen
NADPH	Nicotinamide adenine dinucleotide phosphate hydrogen
OD	Optical density
ORF	Open reading frame
PCR	Polymerase chain reaction
Pmd	MVPP decarboxylase

Pmk	MVP kinase
PMSF	Phenylmethylsulphonylfluoride
SDS-PAGE	Sodium dodecyl sulfate - polyacrylamide gel electrophoresis
Sqc	Squalene cyclase
Sqs	Squalene synthase
Upp	Undecaprenyl diphosphate phosphatase
Ups	Undecaprenyl diphosphate synthase
UV	Ultra-violet
RT-qPCR	Reverse quantity transcription-polymerase chain reaction
Y1H	Yeast one-hybrid
3M2B1ol	3-methyl-2-buten-1-ol
3M3B1ol	3-methyl-3-buten-1-ol
6×His	Hexa-histidine tag

INTRODUCTION

The isoprene C_5 units isopentenyl diphosphate (IPP) and dimethylallyl diphosphate (DMAPP) are the building blocks for the essential biological molecules such as steroids, hormones, and ubiquinones as well as the terpene secondary metabolites (Lange et al., 2000). There are two pathways producing isoprene building blocks (Hunter, 2007). The mevalonate (MVA) pathway, discovered more than half a century ago, starts from acetyl CoA as a precursor to finally produce IPP. The IPP is then converted into DMAPP by isopentenyl diphosphate isomerase (Idi) to meet the need for DMAPP. The pathway exists in animal, as well as in some eubacteria, archea, fungi, and plants (Oldfield et al., 2012).

On the other hand, another isoprene unit-producing pathway, the so-called non-mevalonate pathway or 2-*C*-methyl-D-erythritol 4-phosphate (MEP) pathway, was discovered only about 20 years ago (Rohmer, 1999). This pathway, existing in plants and most eubacteria, utilizes glycealdehyde-3-phosphate and pyruvic acid to finally produce IPP and DMAPP (Rohmer, 1999).

The terpenoids mostly used for drugs are biosynthesized by plants (Kirby et al., 2009). Furthermore, the essential hormones of isoprenoid origin in plants are very important objects of study for plant physiology (Hemmerlin et al., 2012). Therefore, the terpene synthases and terpene biosynthesis regulatory mechanisms were well-defind in plants, although the enzyme properties are still to be elucidated (Coroda et al., 2009). Among the studies about genes of terpene pathways, the isogene function is one of the main interests. The duplication events have played an essential role in

genome evolution of plants (Flagel et al., 2009). The results of duplication are isotype genes, and many plants use these isogenes to specific purposes (Lohr et al., 2005). The specific functions of isozyme in two pathways are especially known through plants isogenes research (Hemmerlin et al., 2012). Plants produce terpenoids as house-keeping as well as stress-inducible metabolites. Each isogene is envolved in the production of specific terpenoids and the isogenes were expressed differentially (Sando et al., 2008). In the MEP pathway, *1-deoxy-D-xylulose 5-phosphate synthase* (*dxs*), *1-deoxy-D-xylulose 5-phosphate reductase* (*dxr*), *hdr* and *idi* studies were known to exist as multicopy genes, and the function of the isogenes are distinctive from housekeeping to stress responsive by primary or secondary metabolite flux (Van der Fits et al., 2000; Walter et al., 2002; Kim et al., 2006; Kobayashi et al., 2007; Kim et al., 2008; Phillips et al., 2008; Sando et al., 2008; Seetang-Nun Y et al., 2008). Among the isogenic MEP pathway genes, *hdr* isogenes are not well characterized in contrast to *dxs*, *dxr* and *idi* isogenes (Kim et al., 2008; Kim et al., 2009; Hemmerlin et al., 2012). Moreover, studies on Hdr were mostly performed at a transcriptional level. Therefore, the exact function of Hdr isozyme is still unknown (Hemmerlin et al., 2012).

In contrast, in bacteria, the isogene function of MEP pathway isogenes has not been reported (Gräwert et al., 2011). The reason for the lack of the study is summarized as follows. One is that MEP pathway has become the new target of antibiotic and herbicide discovery (Rodríguez-Concepción, 2004). Therefore, the enzyme properties and structure were the main concern. The other is that genome

reduction has occurred during evolution from environmental bacteria to host specific bacteria (Hayden et al., 2012). This renders the bacterial isozyme very rare. Besides, bacterial terpenes are mostly primary metabolites. Thus bacteria have few useful terpenes for practical application (Daum et al., 2009; Odom, 2011).

Nevertheless, the understanding of bacterial MEP pathway is essential from the following perspective. Firstly, the regulatory mechanism of bacterial MEP pathway is unknown. Unlike MVA pathway research, only limited information is available for the regulation of MEP pathway (Hemmerlin et al., 2012). Secondly, the bacteria can be engineered as factory for terpene production (Kirby et al., 2009). To increase terpene productivity, it is important to modify host genome. But the modification was mostly done at the level of fermentation improvement and genetic construction (Keasling, 2012). Thirdly, since MEP pathway is of prokaryotic origin (Lange et al., 2000; Gophna et al., 2006; Bhattacharya et al., 2007; Gould et al., 2008), studies on MEP pathway in bacteria could give a key to understand MEP pathway in eukaryotes, i.e. plants.

Burkholderia glumae is a Gram-negative bacterium causing rice grain rot and seedling rot (Cottyn et al., 1996; Suzuki et al., 1998; Kim et al., 2004). Recently, spreading of this disease into the expanding temperate region due to global warming has become a serious concern in rice cultivation regions (Ham et al., 2011). *B. glumae* interestingly harbors two *hdr* genes, and is devoid of isopentenyl diphosphate isomerase (*idi*). So this bacterium was a good target to study *hdr* isogene.

All of Burkholderia species and some eubacteria have 2 *hdr* isogenes, with each *hdr* isogene neighbors specific genes to form an operon. This indicates that the function of *hdr*-containing operon could have specific function. Each *hdr*-containing operon seems to be regulated by an independent signal. The present study was performed to elucidate function of each Hdr isozyme. To this end, the reverse genetics approach of *B. glumae* was employed. In addition, the product ratio and kinetic parameters were determined to provide explanation on the presence of two genes of *hdr* in *B. glumae*.

LITERATURE REVIEW

1. The rice pathogenic bacterium *Burkholderia glumae*.

Burkholderia glumae is a gram negative bacterium and a pathogen in rice species. The symptoms are grain rot, seedling rot and wilt diseases that cause severe yield losses (Cottyn et al., 1996; Suzuki et al., 1998; Kim et al., 2004; Jeong et al., 2003). The diseases of *B. gluame* are prevalent at many countries that grow rice as important crop, and the region was spread quickly to a whole world, due to the global warming (Ham et al., 2011; Lim et al., 2009; Shahjahan et al., 2000).

The weapon that leads to serious symptoms and plant growth reduction is toxoflavin (Nagamatsu, 2001; Sato et al., 1989). Toxoflavin is biosynthesized by *toxABCDE* operon genes and transported using *toxFGHI* genes (Kim et al., 2004) (Fig. 1). The other virulence factor is lipase related with type II secretion systems. These two factors are regulated by quorum-sensing signals (Boekema et al., 2007; Ham et al., 2011). For the rest of what?, type III secretion effectors, so called hrp, flagella-dependent motility (swimming and swarming ability), and exopolysaccharides (EPSs) could also contribute to virulence of *B. glumae* against host plants (Kang et al., 2008; Kim et al., 2007; Jeong et al., 2003; Schaad., 2001).

By whole genome sequencing, 2 chromosomes and 4 plasmids of the BGR1 strain were read, and the genes were annotated (Lim et al., 2009). *B. glumae*-related species, *B. pseudomallei,* is a severe pathogen to human. The high homology

between these species warrants the importance of sudy in *B. glumae*.

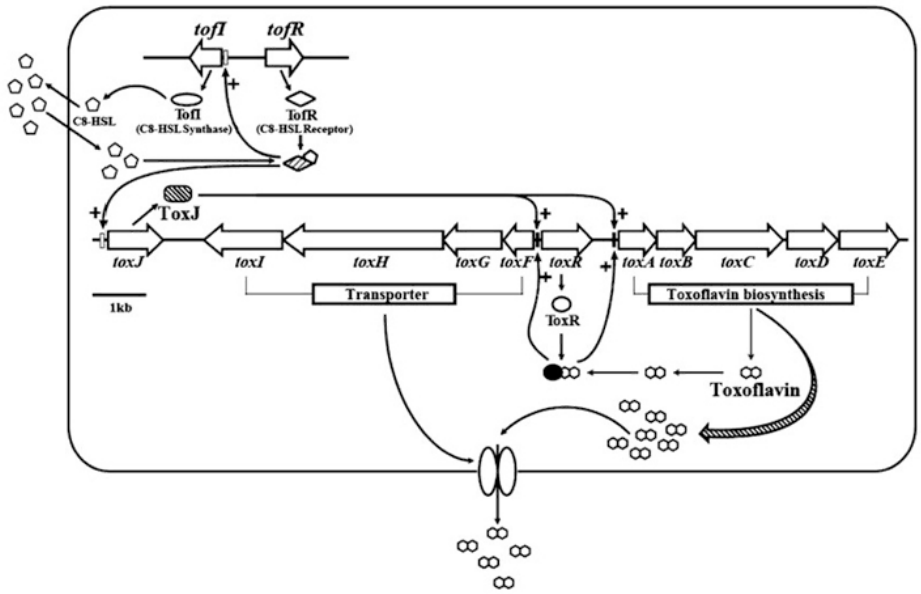

Figure 1. The toxoflavin production and regulation circuits in *B. glumae*.

The toxoflavin biosynthesis operon is composed with *toxABCDE*, and transport operon is composed with *toxFGHI*. The ToxR is a LsyR-type regulator, which activates 2 operons with co-inducer, toxoflavin. The Quorum-sensing signal molecule is C8-HSL, and this binds TofR at certain concentration. C8-HSL-TofR activates *toxJ* gene and then, ToxJ activates both tox operon with ToxR.

2. The MEP pathway.

The isoprene C5 unit is necessary to continue life in all of organisms (Sacchettini et al., 1997; Christianson, 2008). The isoprene was polymerized to terpenes thorough prenylation (Kellogg et al., 1997; Kuzuyama et al., 2003). The terpenes are classified into monoterpe (C10), sesquiterpene (C15), diterpene (C20), triterpene (C30), and so on, according to carbon numbers (Hemmerlin et al., 2012). Terpenes are used not only as cell component, hormons, protein modification and signal molecules but also as defense mechanisms material and other many secondary metabolites (Fraenkel, 1959; Rohmer et al., 1993; Penuelas et al., 1995; Briskin, 2000; Daum et al., 2009; Yazaki et al., 2009) (Fig. 3). Besides, the terpene also can be used for the defense mechanisms as secondary metabolites (Pichersky et al., 2000; Wink, 2003). Terpenoids have been used as drugs such as antimallarial, anticancer and antibiotics for human and also essential material for own organisms to survival and growth (Rodríguez-Concepción, 2004; Rohmer et al., 2004).

The isoprene units exist as 2 isomeric forms: isopentenyl pyrophosphate (IPP) and dimethylallyl pyrophosphate (DMAPP) (Flesch et al., 1988; Zhou et al., 1991). In the biosynthesis of terpene, polymerization of IPP and DMAPP by prenylases (GPP synthase, FPP synthase, GGPP synthase and so on) (Kellogg et al., 1997; Kuzuyama et al., 2003) initiates the process. After prenylation, specific terpene synthase modifies skeleton of terpenoids by rearrangement or cyclyzation, and then derivatives are attached or modification by oxidation occurs (Sacchettini et al.,

1997; Kuzuyama et al., 2003). Many kinds of specific tepene synthases and P450 genes have been identified in various organisms (Jacobsen et al., 1999).

2.1. Two pathways for biosynthesis isoprene unit.

At first, the MVA pathway was known as the only road to isoprene unit synthesis (Goodwin, 1958; Modi et al., 1961; Durr et al., 1964). Acetyl-coA is starting material, and after 6 enzyme (AACT, Hmgs, Hmgr, Mvk, Pmk and Pmd) reaction steps, IPP is synthesized. Then IPP isomerase converts IPP to its isomer DMAPP (Grochowski et al., 2006) (Fig. 2). This old pathway has been studied thoroughly in enzyme kinetics, structure, mechanisms, and regulation (Hemmerlin et al., 2012).

Recently, another IPP-producing pathway, MEP pathway, was discovered. Pyruvate and glyceraldehyde-3-phosphate (G-3-P) are converted to IPP and DMAPP as final products (Disch et al., 1988, Rohmer et al., 1993). This pathway has 7 steps involving 7 enzymes (Dxs, Dxr, Mect, Cmek, Mecs, Hds and Hdr) (Eisenreich et al., 2004; Vranová et al., 2011) (Fig. 2). Idi is the optional enzyme (Harn et al 1999). Some organisms have only one of the two pathways. For example, fungi, archaeal, and animals biosynthesize isoprene unit via MVA pathway, while most eubacteria through MEP pathway (Lange et al., 2000; Eisenreich et al., 2004). Only plants have both pathways. Plants use each pathway to make different carbon number products: MVA pathway for C15 and C30 whereas MEP pathway for C10,

C20 and C40) (Modi et al., 1961; Chappell, 1995; Thai et al., 1999; Wu et al., 2006). Because animals do not have MEP pathway, MEP pathway is potentially good drug target to comtrol infection by bacterial pathogen (Rodríguez-Concepción, 2004; Rohmer et al., 2004). However, despite of continuous research, many things were still unknown (López-Juez, 2007). However, MEP pathway in bacterial system has been receiving less attention compared to plant (Hemmerlin et al., 2012; Heuston et al., 2012).

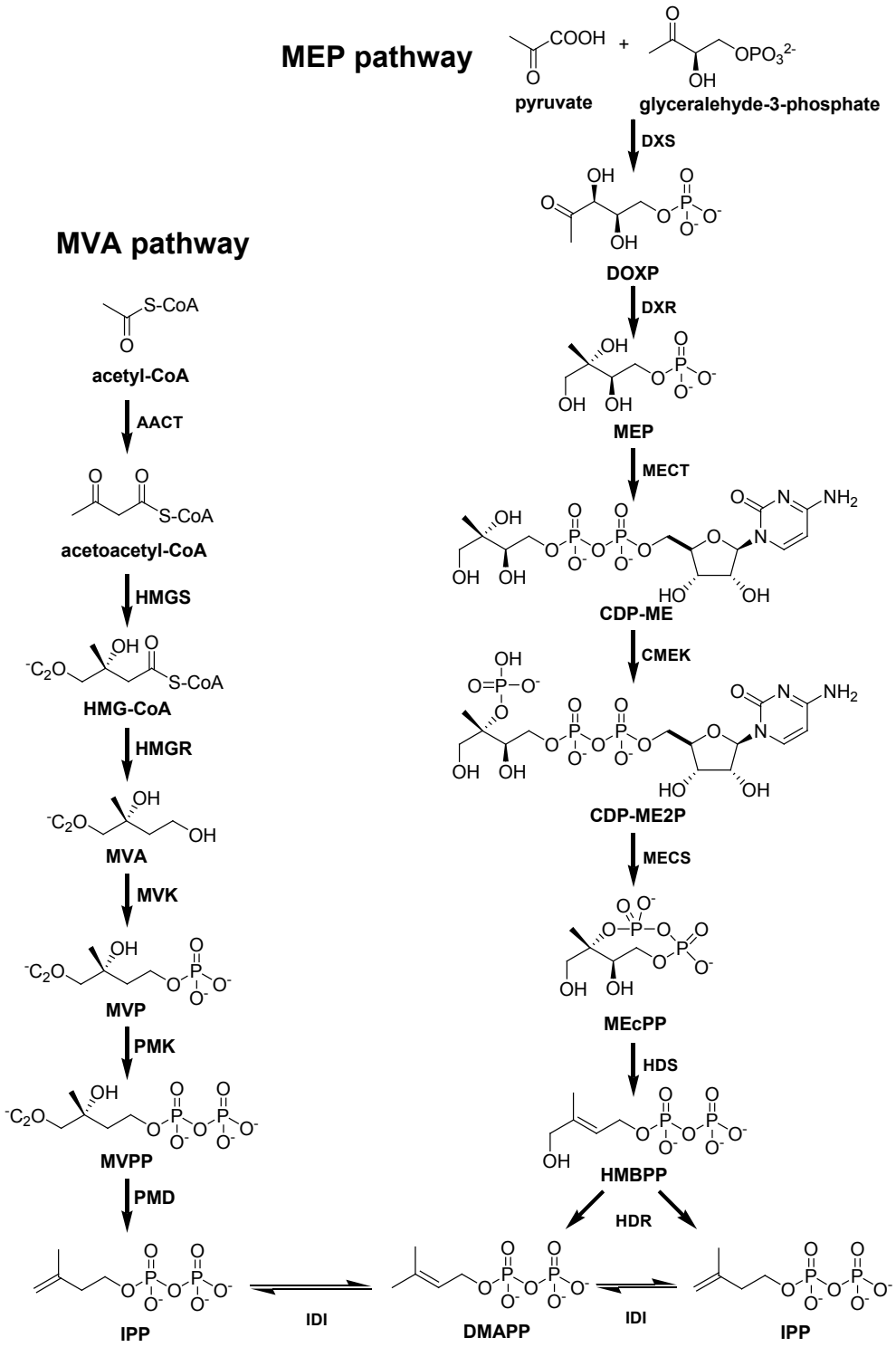
MEP pathway
pyruvate
glyceralehyde-3-phosphate
DXS
DOXP
DXR
MEP
MECT
CDP-ME
CMEK
CDP-ME2P
MECS
MEcPP
HDS
HMBPP
HDR
IPP
IDI
DMAPP
IDI
IPP
MVA pathway
acetyl-CoA
AACT
acetoacetyl-CoA
HMGS
HMG-CoA
HMGR
MVA
MVK
MVP
PMK
MVPP
PMD
IPP

Figure 2. Isoprenoids biosynthesis pathways.

The old MVA pathway discovered in mammals, fungi and plant plastid use acetyl-CoA as starting material. The recent MEP pathway is from pyruvate and glyceraldehyde-3-phosphate to isoprenoids.

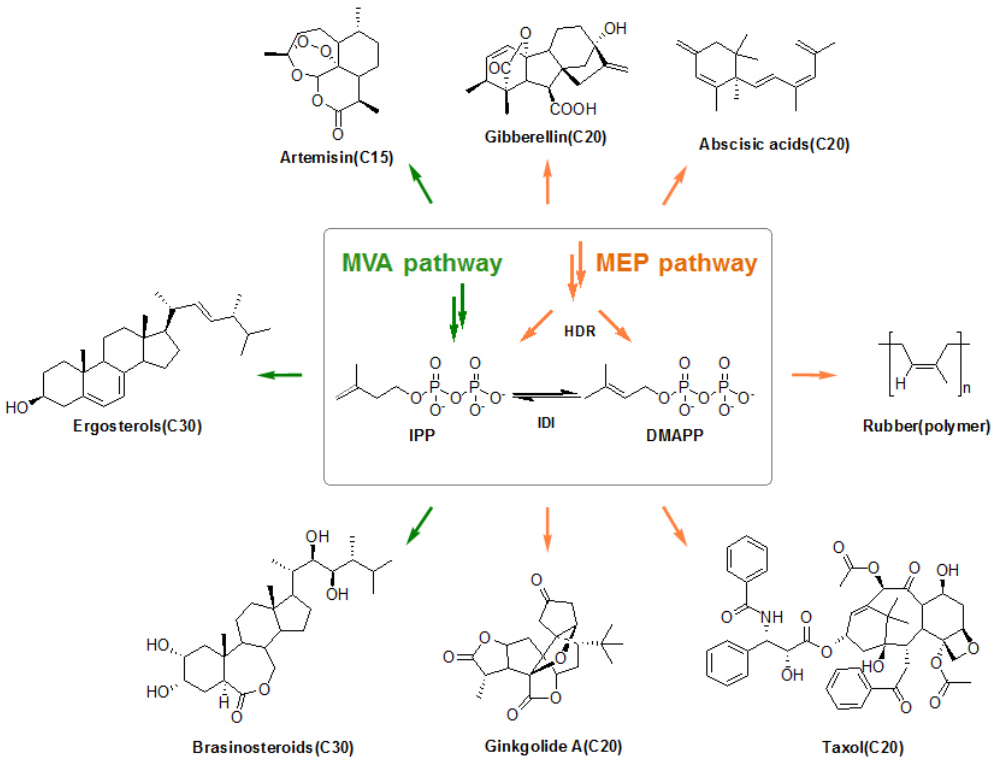

Figure 3. Isoprenoids flux via MVA and MEP pathways.

Terpenoids biosynthesis starts with IPP and DMAPP. Terpenoids precursors (GPP, FPP and GGPP) are synthesized by prenylation of DMAPP with IPP. The green arrows indicate the flux of tepenoids (C15 and C30) via MVA pathway, while orange arrows indicate the flux of C10 and C20 terpenoids via MEP pathway.

2.2. Hdr, the final enzyme of MEP pathway

The crystal structure and enzymatic properties of MEP pathway enzymes have been reported (Coroda et al., 2009; Erosh, 2006) (Table 1). The final enzyme of MEP pathway, Hdr, contains iron-sulfur clusters, which renders Hdr sensitive against oxygen (Gräwert et al., 2010; Wolff et al., 2003). Hence, the experiment must be done in anaerobic chamber which make it difficult to isolate intact Hdr proteins (Altincicek et al., 2002; Wolff et al., 2003). Therefore, the earlier studies of Hdr were performed through *in vivo E. coli* systems (Rohdich et al., 2002). To answer if Hdr produces both DMAPP and IPP as products, feeding experiment with ^{13}C-labeled 1-deoxy-D-xylulose, D-xylulokinase converted the deoxy sugar into ^{13}C-labeled 1-deoxy-D-xylulose 5-phosphate, the substrate of Dxr, and then the products of Hdr were detected as ^{13}C-labeled DMAPP and IPP in *E. coli* extracts (Hintz et al., 2001).

Later, *in vitro* Hdr enzyme assay was attempted (Adam et al., 2002; Altincicek et al., 2002; Gräwert et al., 2004; Wolff et al., 2003). According to *in vitro* enzyme assay, the reaction of Hdr was reduction of HMBPP so that the electron donor had to exist. The artificial electron doneors used were deazaflavin and reduced methylviologen (Altincicek et al., 2002; Gräwert et al., 2004; Wolff et al., 2003). Actually, flavodoxin is the physiological electron donor in Gram-negative bacteria, whereas plants use ferredoxin (Puan et al., 2005; Sancho, 2006). *E. coli* and *Aquifex aeolicus* Hdr's were characterized by *in vitro* enzyme assays (Adam et al., 2002;

Altincicek et al., 2002; Gräwert et al., 2004; Wolff et al., 2003) (Fig. 4). These Hdr's could catalyze HMBPP to IPP and DMAPP at the ratio of 5:1 ~ 6:1 (Table 3). Idi treatment makes the ratio from 2.2:1 to 13:1 at equilibrium. However, there is no report on plant Hdr product ratio (Ramos-Valdivia et al., 1997; Rohdich et al., 2003; Street et al., 1990).

Table 1. The characterization of MEP pathway enzymes.

The prokaryotic enzymes of MEP pathway were studied to know the reaction mechanisms and structure. Despite some reports were studied, many enzyme reaction were still unknown exactly.

Protein	Organism	Enzymatic properties	Crystal structure
Dxs	*B. subtilis*	[129]	
	D. radiodurans		[42]
	E. coli	[26, 27]	[42]
IspC	*E. coli*	[28]	[55, 133–136]
	M. tuberculosis	[131]	[137, 138]
	P. falciparum	[49]	[139]
	T. maritima		[140]
	Synechocytis sp. PCC6803	[132]	
	Z. mobilis		[141]
IspD	*A. thaliana*		[144]
	E. coli	[72]	[145, 146]
	M. tuberculosis	[142, 143]	
IspE	*A. aeolicus*	[147]	[84, 85, 147]
	A. tumefaciens	[148]	
	E. coli	[73]	[149]
	T. thermophilus		[150]
IspF	*A. thaliana*		[152]
	E. coli	[74]	[81, 153, 154]
	H. influenzae		[155]
	P. falciparum	[151]	
	T. thermophilus		[156]
	M. smegmatis		[157]
IspDF	*C. jejuni*	[158]	[158]
	A. tumefaciens	[148]	
	M. loti	[159]	
IspG	*A. aeolicus*		[116]
	E. coli	[100]	
	T. thermophilus	[105]	[160]
IspH	*A. aeolicus*	[106]	[120]
	E. coli	[103]	[118, 119]

2.3. The function and regulation of isogenes in MEP pathway.

The 3-hydroxy-3-methylglutaryl coenzyme A reductase (Hmgr) is classified into 2 types by their different functions, and has a role in isoprenoids fux regulation in MVA pathway (Hemmerlin et al., 2012). Hmgr1 was used to synthesize constitutive metabolites (phytosterols), but Hmgr2 is engaged in sesquiterpenoids biosynthesis and so-called stress-mediated compound production (Hemmerlin et al., 2004; Maldonado-Mendoza et al., 1997; Merret et al., 2007; Sando et al., 2008). In many plants, Hmgr isoforms have differential expression and regulation among tissues types, development stages, stress condition (Learned et al., 1997; Ohyama et al., 2007; Suzuki et al., 2004) (Table 2).

The initial studies of MEP pathway isogenes were focused on *dxs* isogenes. (Coroda et al., 2012). Two classes of *dxs* gene in plants are separately regulated by independent signals under the specific conditions in Arabidopsis (Araki et al., 2000). The multiple *dxs* gene functions were studied in other plants such as *Ginkgo biloba* (Kim et al., 2005; Kim et al., 2006, 2009) and *Oryza sativa* (Phillips et al., 2007; Walter et al., 2000, 2002). These studies accelerated the research on MEP pathway enzymes encoded as isogenes. For instance, *dxs1* knock-out in Arabidopsis resulted in albino phenotype (Mandel et al., 1996) due to blockade of photosynthetic carotenoids and chlorophyll synthesis. The other type of Dxs (Dxs2 and 3) could not complement the function of Dxs1 (Phillips et al., 2008). Dxs2 is involved in specific terpene secondary metabolism, and Dxs3 is expressed in specific tissues (Coroda et

al., 2012; Kim et al., 2005). This separated function of *dxs* isogenes is mirrored in the case of *dxr* gene in *Hevea brasiliensis* (Seetang-Nun et al., 2008) and *Populus trichocarpa* (Wiberley et al., 2009).

Recently, the other MEP pathway isozymes were studied in many plants. Cmk was found in *Ginkgo biloba* (Kim et al., 2008a), Mct and Mcs in *Hevea brasiliensis* (Sando et al., 2008), Mcs and Hds in *Populus trichocarpa* (Wiberley et al., 2009) (Table 2).

The *hdr* isogenes were identified in *Ginkgo biloba, oryza sativa,* and *Pinus taeda.* The expression of the isogenes was tissue-specific (Jung et al., 2008; Kim et al., 2008b; Kim et al., 2009) (Fig. 5). The gene *hdr1* was induced by light, while *hdr2* was expressed highly in the root or wood and have correlation with accumulation of diterpene (Jung et al., 2008; Kim et al., 2008b; Kim et al., 2009). Therefore, type1 Hdr is associated with primary metabolism, whereas type 2 Hdr with secondary metabolism (Hemmerlin et al., 2012). Idi also exists as iogenes, and the phenotype of each knock-out mutant was different (Phillips et al., 2008).

Isogene function of plant MEP pathway enzymes are not fully understood so far. Now it becoems clear that isogenes have specific role and regulation mechanism (Hemmerlin et al., 2012; Vranová et al., 2012). Although the first 2 enzymes (Dxs, Dxr) of MEP pathway was known as the most important regulation points, it is highly possible that Hdr is another regulation point (Hemmerlin et al., 2012) (Fig. 4) because Hdr is the final enzyme in MEP pathway (Kim et al., 2008b; Kim et al., 2009). However, few Hdr isozyme studies were reported (Hemmerlin et al., 2012).

Only gene expression study could tell the mechanism of isozyme regulation and function in MEP pathway (Coroda et al., 2012).

Table 2. **Isogenes in the previous studies in MEP pathway.**

At first, the isogene was studied about *dxs* gene. The function and regulation of *dxs, dxr, hdr* and *idi* isogene was distinguished to various types. This research was only studied at a transcript level in plants while enzyme properties were studies in prokaryotes. The bacterial isogenes was not introduced until now.

Enzyme	Plant species	Gene	Protein (type*)	Reference
DXS	*Arabidopsis thaliana*	*DXS*	DXS1 (1)	Estévez *et al.*, 2000
		DXL1	DXS2 (1)	Araki *et al.*, 2000
		DXL2	DXS3 (3)	Araki *et al.*, 2000
	Picea abies	*PaDXS1*	PaDXS1 (1)	Phillips *et al.*, 2007
		PaDXS2A	PaDXS2A (2)	Phillips *et al.*, 2007
		PaDXS2B	PaDXS2B (2)	Phillips *et al.*, 2007
	Medicago truncatula	*MtDXS1-like*	MtDXS1 (1)	Walter *et al.*, 2002*a*
		MtDXS2-like	MtDXS2 (2)	Walter *et al.*, 2002*a*
	Ginkgo biloba	*GbDXS1*	GbDXS1 (1)	Kim *et al.*, 2006
		GbDXS2	GbDXS2 (2)	Kim *et al.*, 2006
	Oryza sativa	*dxs1-like*	OsDXS1 (1)	Kim *et al.*, 2005
		dxs2-like	OsDXS2 (3)	Kim *et al.*, 2005
		dxs3	OsDXS3 (2)	Kim *et al.*, 2005
				Okada *et al.* 2007
	Zea mays	*dxs1*-like	DXS1 (1)	Walter *et al.*, 2000
		dxsL2-like	DXS2 (2)	Walter *et al.*, 2000
DXR	*Hevea brasiliensis*	*HbDXR1-like*	DXR1	Seetang-Nun *et al.*, 2008
		HbDXR2	DXR1	Seetang-Nun *et al.*, 2008
HDR	*Ginkgo biloba*	*GbIDS1*	GbHDR1	Kim *et al.*, 2008
		GbIDS2	GbIHDR2	Kim *et al.*, 2008
		GbIDS2-1-like	GbHDR2-1	Kim *et al.*, 2008
	Pinus taeda	*PtIDS1*	PtHDR1	Kim *et al.*, 2008
		PtIDS2	PtHDR2	Kim *et al.*, 2008

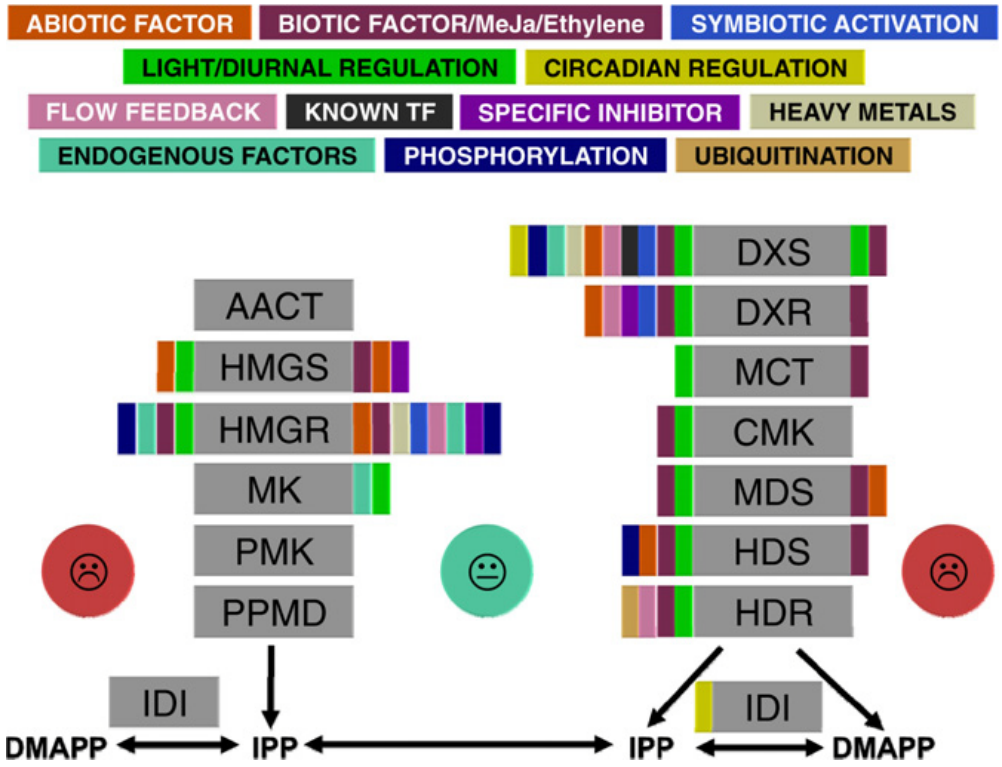

Figure 4. **The factors of regulation in isoprenoids biosynthesis.**

Hmgr is a core regulation point in MVA pathway. This old pathway was studied much more than the MEP pathway. The regulation of MEP pathway was studied in Dxs and Dxr, because these enzymes were known as key regulation point. Hdr was thought as key enzyme, but few information is available.

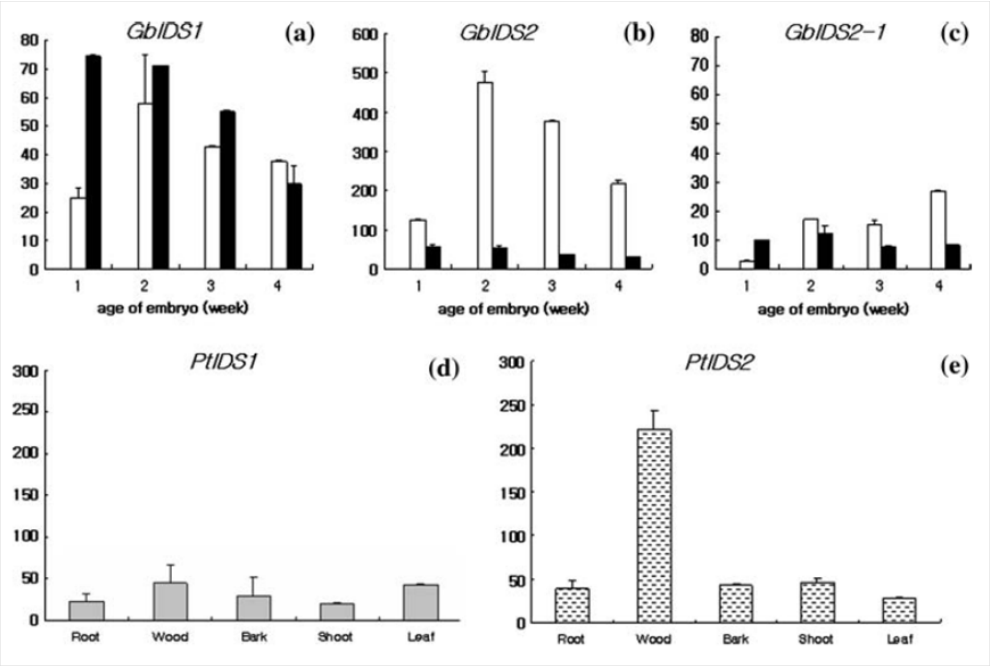

Figure 5. The tissue specific expression of *hdr* isogenes in plants.

The tissue specific Hdr expression meant that enzyme functions and terpene flux were distinguished in plants. Hdr isozymes were classified to 2 types, the type I was involved in primary metabolites in contrast the type II was associated with secondary metabolites.

3. Acetylation and deacetylation of enzyme in bacteria.

The regulation in bacteria appears at various steps. From DNA to metabolites, there are many regulation points; simply transcription, translation, and post-translational modification. Before transcription begins, the sigma factors recognize specific promoter and regulates initiation of transcription, and various kinds of sigma factors are in turn controlled by cell environments (Slonczewski et al., 2009).

In transcription, the efficiency is regulated by GC contents, and then ribosome can recognize the mRNA. After transcription, before binding with mRNA, ribosome can regulate translation by RNases which process rRNA degradation. Aminoacyl-tRNA transferases also regulate translation. And the final stage to produce functional proteins is post-translational modification. The translated proteins is folded and modified by phosphorylation, adenylation, and acetylation. Ribosome associated energy need is known to be about 40 % of total bacterial energy output (Slonczewski et al., 2009). Therefore, the production of protein is tightly regulated. To utilize the energy efficiently and to quickly respond to stress condition, activation/inactivation of protein by post-translational modification is important instead of maintaining pool of proteins by constant synthesis. Among the post-translational modification, acetylation and deacetylations are representative and common regulation methods in bacteria (Slonczewski et al., 2009).

The acetylation was first discovered in histone regulation of eukaryotes (Grunstein, 1997; Struhl, 1998), and later found also in bacteria (Smith et al., 2000). Production

of acetyl-CoA is essential under the starvation condition (Slonczewski et al., 2009). TCA cycle takes up acetyl CoA in quick response to meet energy demand of the cells. When the starvation is ended, acetyl-CoA production has to be stopped. Acetyl-CoA synthetase (Acs) is the enzyme that transfers CoASH to acetate to form acetyl-CoA (Starai et al., 2004). For a quick conversion of acetate, the lysine residue of Acs is acetylated for inactivation of the enzyme by protein acetyltransferase enzyme (Pat). On he other hand, at the time of starvation, acetylated Acs is changed to deacetylated active form by CobB protein in *Salmonella enterica* (Starai et al., 2004) (Fig. 6). The similar reaction is catalyzed by AcuA (acetylase) and AcuC (deacetylase) in *Bacillus subtilis* (Gardner et al., 2006). This set of reactions saves energy and respond quickly in bacteria against stress environment (Gardner et al., 2008). In the case of *E. coli*, evidence of protein acetylation is discovered by LC-MS analysis. The 125 lysine residues of 85 different proteins were ahown to be acetylated and these proteins can have varieties of functions; anabolism, catabolism, DNA stability, repair, and chaperones (Yu et al., 2008). The additional acetylation causes the inactivation of those proteins at stationary phase, whereas the activation of proteins is caused by the deacetylation at exponential phase to meet higher energy demand (Yu et al., 2008). *E. coli* can also have chemotaxis protein CheY regulatory mechanisms using acetylation and deacetylation for quick response (Soppa, 2010; Zhang et al., 2009)

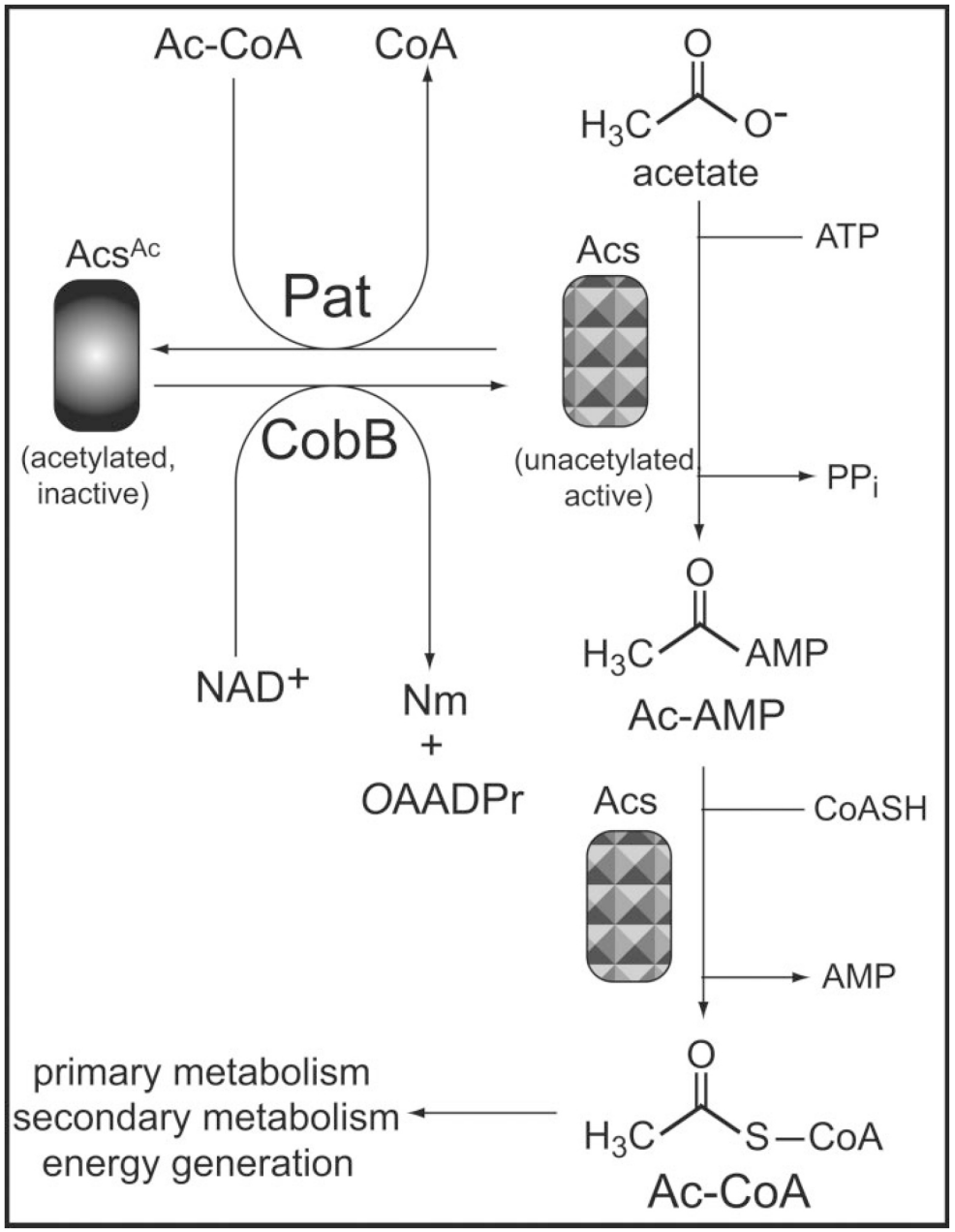
Ac-CoA
CoA
O
H3C
O-
acetate
AcsAc
Pat
Acs
ATP
(acetylated,
inactive)
CobB
(unacetylated,
active)
PPi
O
H3C
AMP
Ac-AMP
NAD+
Nm
+
OAADPr
Acs
CoASH
AMP
primary metabolism
secondary metabolism
energy generation
O
H3C
S—CoA
Ac-CoA

Figure 6. The regulation of Acs in *S. enterica* by acetylation.

The Acs was regulated by aectylation to use sudden response under the starvation environments. Many bacteria could save energy using acetylation of proteins.

MATERIALS AND METHODS

1. Bacterial strains and culture media

The bacterial strains and plasmids are presented in Table 3. *Burkholderia glumae* BGR1 and *E .coli* s-17 strain were kindly provided by Prof. I. Hwang (Department of Agricultural Biotechnology, Seoul National University). *B. glumae* for seed culture and all of *E. coli* strains were cultured in LB (Luria-Bertani) medium (1 % tryptone, 0.5 % yeast extract and 0.5 % NaCl). To measure growth of *B. glumae* and its knock-out mutants, they were cultured in M9 (minimal) medium (6 g/L Na_2HPO_4, 3 g/L KH_2PO_4, 0.5 g/L NaCl, 1 g/L NH_4Cl, 1 mg/L thiamine, 1 mM $MgSO_4$, 1 M $CaCl_2$ and 0.2 % glucose). For pH shock test, *B. glumae* was cultured in LB media buffered with 100 mM MES (pH 4 and 5), 100 mM MOPS (pH 7) or 100 mM bicine (pH 8.5). All of the bacterial cultures were done in LB medium at 37 ℃, except for heat shock condition at 42 ℃. LB medium for *B. glumae* contained 50 μg/mL rifampicin. Antibiotics were used at following concentrations; 100 μg/mL ampicillin, 50 μg/mL kanamycin, 25 μg/mL spectinomycin and 10 μg/mL tetracycline.

2. DNA and RNA extraction

Plasmids were extracted by miniprep kit (Dynebio, Korea), and gDNA was isolated and purified by Wizard Genomic DNA Purification Kit (Promega, USA). The total RNA was extracted by RiboPure^{TM}-Bacteria kit (Ambion,

http://www.ambion.com) for RT-PCR and Northern blot, and by RNeasy Mini Kit and RNAprotect Bacteria Reagent (QIAGEN, USA) for transcriptome sequencing.

3. Isolation of *B. glumae hdr* and *E. coli hdr* genes

The PCR was performed to clone *B. glumae hdrs* from gDNA of *B. glumae*. Primer pairs for *B. glumae hdr1* (bglu_1g28650) [5`-cggatccGATGAGCTCCACCGAT-3` (HDR1-F) and 5`-ggatccTCAGCCAGCGGGCG-3` (HDR1-R)] and *hdr2* (bglu_2g22170) [5`-cggatccGATGCGAGTCATTCTTG-3` (HDR2-F) and 5`-cggatccTTAAACTTCGCGGGC-3` (HDR2-R)] were designed from the previously published sequence data (Lim et al., 2009). The *hdr* of *E. coli* was similarly cloned with the following primers: 5`-cggatccGATGCAGATCCTGTTG-3` (EcHDR-F) and 5`-cggatccGTTAATCGACTTCACGAA-3` (EcHDR-R). PCR products were cloned into pGEMT-easy vector. The insert of the resulting plasmid was rescued as BamHI fragment and ligated into the same site of pMW118 vector (Nippon Gene, http://nippongene.com), harboring *lac* promoter in the opposite direction. To operon test, 265 bp DNA fragments for *hdr1* operon and 249 bp DNA fragments for *hdr2* operon were synthesized by PCR with cDNA. As a positive control, the gDNA was used as a template. As a negative control, the PCRs were performed using following primer set (HDR1OPERON-F: GACCTGATCGAGTTCAATGCG, HDR1OPERON-R: CGCTCGACGATCTCGATCG, HDR2OPERON-F: GCGAGGAAAAAGTCGAATTCAAG, HDR2OPERON-R:

GCTGGTTCAGGATCGGGT).

4. Complementation assay

The strain DLYT1 is a mutant of *E. coli* FS1576 with partial MVA pathway and knocked out *hdr*. It survives only in the presence of mevalonate in the medium (Kim et al., 2008). The strain was cultured in LB medium including 0.1 % mevalonate and ampicillin at 50 g/mL. The recombinant plasmids BgHDR1-pMW118, BgHDR2-pMW118, and EcHDR-pMW118 were transformed into DLYT1, and the transformants were cultured on LB medium containing kanamycin at 25 μg/mL and ampicillin at 50 μg/mL but with no mevalonate (37 ºC, 16 h) (Kim et al., 2008).

5. Over-expression and purification of His-Hdr

The *B. glumae hdr*s were cloned from gDNA of *B. glumae* by PCR, using the following primer pairs: for BgHdr1, 5`-cggttctggttctggccacATGAGCTCCACCGATACGCT-3` (HDR1pET-F) and 5`-gacggagctcgaattctcGCCAGCGGGCGGCAGATT-3` (HDR1pET-R); and for BgHdr2, 5`-cggttctggttctggccacATGCGAGTCATTCTTGCCCA-3` (HDR2pET-F) and 5`-gacggagctcgaattctcAACTTCGCGGGCGACAGC-3` (HDR2pET-R). The primers were designed to have short 16~18 nucleotide fragment (lettered in lower case in the above-mentioned primer) corresponding to the target pET-32a(+) sequence (Novagen, USA) for homologous recombination. The expression vector,

pET-32a(+), was digested by using *Msc*1 and *Eco*R1. This linearized vector and PCR product were reacted for 15 min at 50 ºC by using In-Fusion HD Enzyme Premix (Clontech, USA). The resulting recombinant plasmids were transformed into *E. coli* Stellar competent cells (Takara). After sequence confirmation, the plasmids were retransformed into *E. coli* BL21(DE3)pLysS (Invitrogen, USA). The transformed bacteria were cultured in LB medium at 28 ºC until OD_{600} reached 0.5. The IPTG was then added at the final concentration of 0.1 mM, and the culture was further incubated for 6 h at 28 ºC. The cells were harvested by centrifugation at 6,000 rpm (4 ºC, 5 min) on Beckman C0650 rotor, washed two times with washing buffer (20 mM Tris-HCl, pH 8.0 in 10 mM NaCl and 10 % glycerol), and resuspended in 10 mL of resuspension buffer (20 mM Tris-HCl, pH 8.0 in 10 mM NaCl and 10 % glycerol). The resuspended cells were sonicated 15 times (30 s pulses at 30 W with 30 s interval) under Ar gas on Misonix XL2000 (Qsonica, USA). After centrifugation of the sonicated cells at 11,000*g* for 25 min at 4 ºC, the supernatant was eluted through Ni-NTA column (Novagen) with 500 μL each of 50, 100, 150, 200 mM imidazole in the resuspension buffer. The purified proteins were enriched using centrifugal filter (Amicon® Ultra centrifugal filter 30 kDa). The concentration of protein was determined by using the Bradford assay (Bradford, 1976). All the protein harvesting procedures were performed under Ar atmosphere except for centrifugation.

6. Characterization of BgHdr proteins

Fe contents were determined by literature method as follows (Kennedy et al., 1984). Each 100 μL of 20 mM BgHdr protein solution was mixed with 100 μL of Solution A (1.35 g of sodium dodecyl sulfate in 30 mL of water, mixed with 0.45 mL of saturated NaOAc) and 100 μL of Solution B (270 mg of ascorbic acid and 9 mg sodium metabisulfate in 5.6 mL of water, mixed with 0.4 mL of saturated NaOAc). The mixture was incubated at 30 ºC for 15 min, after which 50 μL of Solution C (18 mg of 5,5`-[3-(2-pyridyl)-1,2,4-triazine-5,6-diyl]bis-2-furansulfonic acid disodium salt dissolved in 1 mL of water) was added. The absorbance of the sample and the standard $FeCl_2$ were measured at 593 nm.

7. Determination of product ratio

To produce enzymatic products, 2 μM of purified BgHdr protein was reacted with 2.7 mM HMBPP, 2.5 mM methyl viologen (MV), and 3.8 mM sodium dithionite (DT) in 300 μL of 50 mM Hepes buffer (pH 8.0) for 3 h at room temperature. The products were then converted into the corresponding alcohols, 3-methyl-2-buten-1-ol (3M2B1ol) and 3-methyl-3-buten-1-ol (3M3B1ol), by addition of concentrated ammonium hydroxide to the final concentration of 0.1 N followed by addition of 0.2 g of cerium oxide, and the mixture was reacted with gentle stirring at 40 ºC for 1 h (Tan et al., 2008). The mixture was then centrifuged at 10,000 *g* for 3 min, and the supernatant was extracted with 270 μL EtOAc. Alcohols were separated on an Agilent Technologies 7890A GC system equipped with FID detector and Agilent HP-5 column (30 m by 0.32 mm inside diameter by 0.25 μm thickness) using the

following temperature program: hold for 5 min at 40 ºC and raise at 1 ºC/min to final temperature of 150 ºC (elution gas, N_2; flow rate, 1 mL/min)

8. Kinetics studies

Four hundred nanomolar BgHdr was incubated with HMBPP (0-125 μM) in 50 mM Hepes buffer (pH 8.0) containing 2 mM MV and 0.4 mM sodium dithionite (DT) as reducing agent. Total volume of mixture was 450 μL. The reaction was monitored by measuring absorbance decrease of reduced MV at 732 nm (ε_{732} = 3,150 $M^{-1}cm^{-1}$).

9. Northern blot analysis

B. glumae was cultured in M9 medium, and from lag phase to stationary phase (from 10 h to 19 h after inoculation) the culture was sampled every 1 h and total RNA was extracted using RiboPure^{TM} –Bacteria kit (Ambion, USA). Northern blot analysis was performed with 2 μg of total RNA. After separating the total RNA on 1.2 % agarose formaldehyde gel, RNA was transferred onto GeneScreen Plus hybridization transfer membranes (Perkin-Elmer). DNA probes were prepared by PCR of gDNA with following primers (HDR1probe-F: CGCTCGTCACGAAGGTCCACGTC, HDR1probe-R: GTGACGAGCGCGACGCGCT, HDR2probe-F: CCCAGGCCGTCGAGCAGGACG, HDR2probe-R: CACCAGGATCACTTCGCCGGGAATT).

10. Construction of *Burkholderia glumae hdr*-disruptant

The cosmids that harbored *hdr1 or 2* were isolated by miniprep. The cosmids were cut at HindIII or SmaI site, and cloned into the pBluescript II ks(+) or pUC19. The cloned plasmids were cut at *Asi*SI or *Eco*RV site within *hdr1* and *hdr2*, the Ω cassette from pHP45Ω were inserted into the site. These plasmids were cut at *Hin*dIII or *Sma*I sites, the fragments were cloned into the pLAFR3. These vectors were introduced into *B. glumae* BGR1 to generate *hdr1*::Ω and *hdr2*::Ω (BGHDR1KO and BGHDR2KO) using marker-exchange mutagenesis by tri-mating with *E. coli* HB101 (Lee, 2006).

11. Swimming test

The BGR1 and *hdr* isogene mutants were cultured for 10 h, harvested and OD_{600} of the washed cells were normalized to 1.0. One microliter of each cell suspension was injected into LB plates containing 0.3 % bacto agar, then incubated at 28 ºC for 24 or 36 h.

12. Infection of rice

To observe virulence of *B. glumae* strains in wilt disease, rice seedlings were grown for 3 weeks in 28 °C chamber under the continuous illumination. Seedlings were sprayed with 10^8 – 10^9 cfu/mL of bacteria. For grain rot observation, rice plants were grown to the flowering stage in green house. Bacterial suspensions were diluted with water to the concentration of 10^8 – 10^9 cfu/ml and the rice panicles

were soaked. Then, 10 rice panicles were collected from each treatment, grinded and resuspended in 1 mL water. The resuspended bacteria cells were diluted to the 10^{-9} fold. Ten microliters of diluted suspension was spread on LB plate. After 24 h, colonies were counted. The disease symptom was observed after 7 days after inoculation. The severity of disease was determined by evaluating the Disease index from the disease score (Kim et al., 2004). Disease score in a scale of 5 was obtained by estimating the discolored area per panicle as follows: 0-20 % discolor = 1, 20-40 % discolor = 2, 40-60 % discolor = 3, 60-80 % discolor = 4, 80-100 % discolor = 5.

Diseae index = the sum of number of panicles per score × score / the sum of number of panicles.

13. Isolation of cellular protein

The proteomics approach was used to observe cellular protein patterns of mutants. The *B. glumae* was cultured in 50 mL of M9 medium, and cell was harvested at 6 and 10 h after inoculation. After centrifugation of the culture, the pellets were washed, and resuspended with 10 mL of 10 mM Tris-HCl (pH 8.0) and 0.1 mM PMSF, and the cells were sonicated using the following program: pulse on for 10 s, pulse off for 1 s and total processing time for 15 min) (550 Sonic Dismembrator, Fisher Scientific, USA). The disrupted cells were centrifuged at 10,000 rpm, 4 ºC on Beckman C0650 rotor for 1 h, and the supernatant was resuspended in 5 mL of 10 mM Tris-HCl (pH 8.0). The suspension was mixed with 20 mL of cold acetone, and

the mixture was incubated overnight at -20 ºC. After centrifugation at10,000 rpm, 4 ºC on Beckman C0650 rotor for 1 h, the precipitated proteins were resuspended in 1 mL of 10 mM Tris-HCl (pH 8.0), and separated by 10 % SDS PAGE. Three lanes per sample were run for the treatment of 3 digestive enzymes (trypsin, AspN, and chymotrypsin). The separated protein bands of interest were excised and washed twice with distilled water. Gels were then de-stained with 50 mM ammonium bicarbonate (ABC) in 50 % acetonitrile (MeCN) aqueous solution and further diced into size of about 1 mm^2. Subsequently, gels were dehydrated sequentially in 70 % and 100 % MeCN, reduced with dithiothreitol (DTT), and alkylated with iodoacetamide (IAA). Gels were once again washed with what? and dehydrated. After the gels had been fully dried, they were rehydrated with the enzyme solutions (25 ng/μL of trypsin, 1 ng/μL of AspN and 5 ng/μL of chymotrypsin, dissolved in their respective reaction buffers; trypsin, 50 mM ABC, 0.1 mM $CaCl_2$, pH 8.0, AspN, 100 mM ABC, pH 8.5, and chymotrypsin, 100 mM Tris-Cl, 10 mM $CaCl_2$, pH 7.8). For statistical analysis, each enzyme sets were prepared in triplicate. Any remaining solutions were discarded from the gels and 50 μL of additional reaction buffer was added. After incubation at 37°C for overnight (except for chymotrypsin, which was incubated at 30 °C), 100 μL of 10 % formic acid in 10 % MeCN solution was added and the digested peptides were extracted by ultrasonification. Peptides were then serially extracted by 100 μL of 0.1 % trifluoroacetic acid (TFA) in 50 % MeCN, 0.1 % TFA in 70 % MeCN and finally 0.1 % TFA in 100 % MeCN. Collected peptide extracts were dried in SpeedVac (Thermo Scientific, San Jose, CA,

USA) vacuum evaporator and reconstituted in 10 μL of 0.1 % formic acid in distilled water. Samples were centrifuged before injection.

14. Nano-LC-MS/MS analysis

The prepared peptide samples were analyzed using LTQ XL linear trap mass spectrometer (Thermo Scientific, San Jose, CA) equipped with nano-HPLC system (Eksigent, Dublin, CA). Five microliters of peptide sample was injected and loaded onto a C18 trap column (2.5 cm × 100 μm i.d., Upchurch Scientific, Oak Harbor, WA) using auto-sampler. Trapped samples were eluted and separated through in-line, homemade reverse-phase C18 micro column, which was packed in fused-silica nano-spray tip (column dimension, 10 cm × 100 μm i.d.; particle size, 5 μm; pore size, 300 Å; Nanobaume, Wildomar, CA). Peptides were eluted using the mobile phase gradient of solvent A (0.1 % formic acid in HPLC-grade water) and B (0.1 % formic acid in MeCN) with a flow rate of 200 nL/min. The gradient started with 2 % of solvent B and increased to 50 % in 100 min, then increased to 100 % in 105 min. After 5 minutes of maintaining 100 % solvent B (washing), the column was equilibrated to 98 % solvent A and 2 % solvent B for another 10 minutes. Eluted peptides were ionized by nanospray with a voltage of 1.4 kV and subjected to mass spectrometer. Peptide ions were first analyzed with full-MS scan in a range of *m/z* 300-2000, and the 7 most intense ions from the full-MS scan were data-dependently selected for the CID tandem MS analysis (normalized collision energy of 35 eV for 30 ms). Dynamic exclusion parameters of the data-dependent scan were; repeat

count = 2, repeat duration = 30 s, list size =300, exclusion duration = 180 s, low mass width = 0.8, high mass width = 2.2.

15. Database search

All MS/MS data were analyzed using Sorcerer-SEQUEST (version 3.5, Sage-N research, Milpitas, CA). Protein FASTA database was constructed by downloading the following protein search results from NCBI protein database (http://www.ncbi.nlm.nih.gov/protein). The search query was "*Burkholderia glumae* BGR1" and only proteins in the 'RefSeq' were selected. The database contained 5773 entries as of December 2, 2012. SEQUEST was set up to search the database assuming the digestion enzyme as trypsin (after K and R), AspN (before D) or chymotrypsin (after F, W, Y, M, and L but not before P) and parent ion mass range of 400-5000 Da. Each digestion was allowed up to 2 miss-cleavages. SEQUEST was searched with a fragment ion mass tolerance of 1.00 Da (monoisotopic mass) and a parent ion tolerance of 1.00 Da (average mass). Iodoacetamide derivative of cysteine was specified as a fixed modification and oxidation of methionine and acetylation of lysine as variable modifications.

Scaffold (version Scaffold_3.6.4, Proteome Software Inc., Portland, OR) was used to validate MS/MS based peptide and protein identifications. Peptide identifications were accepted if they exceeded SEQUEST thresholds. Identifications required at least deltaCn scores of greater than 0.10 and XCorr scores of greater than 1.8, 2.5, 3.5 and 3.5 for singly, doubly, triply and quadruply charged peptides. Protein

identifications were accepted if they contained at least 2 identified peptides. Proteins that contained similar peptides and could not be differentiated based on MS/MS analysis alone were grouped to satisfy the principles of parsimony.

16. Promoter switch complementation assay

The putative promoter regions and ORFs of *hdr* isogenes were isolated from gDNA by PCR with primers (HDR1P1O, 1 and 6; HDR2P2O, 3 and 8; HDR1P2O, 1 and 2 and 7 and 8; HDR2P1O, 3 and 4 and 5 and 6) (Table 4). The PCR products were mixed with linearized pRK415 vector that digested by HindIII and BamHI, and the mixture was incubated to homologous recombination. After cloning, the PCR was repeated with each vector as template with following primers (HDR1P1O, 9 and 11; HDR2P2O, 10 and 12; HDR1P2O, 9 and 12; HDR2P1O, 10 and 11) and PCR was performed from gDNA using primers ($HDR1P_o1O$, 11 and 13; $HDR1P_o2O$, 2 and 13 and 7 and 12). The each PCR product was incubated with digested pLAFR6 by *Eco*RI and *Bam*HI. The cloned 6 different combination vectors were transformed into *E. coli* S17-1 strain. The vectors were transformed into HDR1KO by using double mating (Kim et al., 2004).

17. Hypersensitive reaction (HR) assay

The tobacco plants (*Nicotiana tabacum* cv. Xanthi) were grown for several weeks in chamber with a photoperiod of 12/12 h light-dark cycle at 26 ºC. BGR1, HDR1KO and HDR2KO were cultured in LB medium overnight and the cells were

washed and normalized with water to OD_{600} 0.5. The resuspended *B. glumae* was infiltrated to the reverse side of tobacco plants leaves using 1 mL syringe. After inoculation for 36 h in the above-mentioned chamber, the sizes of HR lesion were observed.

18. Gel mobility shift assay

The putative promoter region of *hdr2* gene, 131bp DNA fragment upstream of *hdr2*, was synthesized by PCR with the primers (HDR2promoter131-F, cgaattcCGATAGCGTTAAAATGCGATT; HDR2promoter131-R, cgaattcACAGGGCGAACTCCGAC). The fragment was labeld with [α-^{32}P]. The cloned vector of recombinant protein His-ToxR was kindly provided by professor I. K. Hwang (Kim et al., 2009). Then overexpression of ToxR was performed in the same procedure as the above-mentioned His-Hdr overexpression. The purified His-ToxR was mixed with labeled promoter region DNA fragment in binding buffer (20 mM HEPES-KOH pH 7.8, 50 mM KCl, 5 mM $MgCl_2$, 1 mM EDTA, 0.5 mM DTT, 5 μg BSA, 200 μg poly[dI-dC], 10 % glycerol) and incubated for 15 min at room temperature. The mixture was separated on 5 % polyacrylamide gel by the electrophoresis in half-strength TBE tank buffer (TBE: 89 mM Tris, 89 mM boric acid, and 2 mM EDTA) for the ToxR bound-DNA and free DNA.

19. Yeast 1 hybrid assay

ToxR ORF and putative *hdr2* promoter region (329 bp) were synthesized by PCR

from gDNA using following primers (ToxR-F: ggatccATGAATAATCTGAAGCGGATC, ToxR-R: gaattcTCAGCGGTCGCGCAC, HDR2promoter329-F: gaattcCGCCTGTTCGGCCGTGAGATT, HDR2promoter329-R: gaattcACAGGGCGAACTCCGACGACAAC). ToxR ORF PCR product was ligated with digested pGADT7-Rec2 (Clontech, USA) by *Eco*RI and *Bam*HI, and the promoter region PCR products was ligated with digested pHIS2 (Clontech, USA) by *Eco*RI. The 2 cloned vectors were co-transformed into *Saccharomyces cerevisiae* strain Y187 and selected on synthetic dropout glucose medium (SD) lacking Trp and Leu (DDO). The selected yeast was cultured in SD medium lacking Trp, Leu and His (TDO) with 0, 20, and 40 mM of AT (3-amino-1,2,4-triazole) for 3 days.

20. RT-qPCR

The 2 μg total RNA of BGR1 and ToxR knock-out mutant were reverse-trancribed with random hexamer. The synthesized cDNA was used for real-time quantitative PCR (RT-qPCR). PCR reactions were done for 40 cycles, in three biological replicates on a Rotor-gene 2000 Real Time Amplification System (Corbett Research, http://www.corbettesearch.com). The gene-specific sequences to RT-qPCR were as follows: HDR2-RT-F (5`-CCCAGGCCGTCGAGCAGGACG-3`), HDR2-RT-R (5`-CACCAGGATCACTTCGCCGGGAATT-3`).

21. Transcriptome analysis

The RNA was extracted in exponential phase from BGR1 and *hdr* isogene mutants. The quality and quantity of extracted total RNA of each strain were tested on Agilent 2100 Bioanalyzer to ensure RNA integrity number exceeded 9.0 (Schroeder et al., 2006). The mRNA was enriched by DSN method (Yi et al., 2011), and library was constructed by an Illumina mRNA-Seq sample preparation kit. The RNA sequence was read in single-end 36-bp using Illumina Genome Analyzer IIx, and the mapping was performed by genome sequence reference using CLC Genomics Workbench 4.0 (CLC bio). The RPKM (reads per kilobase of exon per million mapped sequence reads) was calculated by following formula and used to measure the relative transcript abundance.

RPKM = total matched reads / million reads × kilobase

22. Toxoflavin analysis

To measure the toxoflavin productivity of *B. glumae* BGR1 and mutants, each strains were cultured in LB medium at 37 ºC for 24 h, 5 mL of culture was centrifuged at 13000×*g* for 5 min. The cells were resuspended with 1 mL water and broken by sonication. The supernatant and broken cells were separately extracted 3 times with equal volume of $CHCl_3$ for absorbance measurement. After evaporation under the stream of N_2 gas, the dried residue was dissolved in 1 mL of chloroform, and measured at 260 nm. For TLC, supernatant was extracted and dried under the stream of N_2. The residue was dissolved in 20 μL of chloroform and developed on a TLC silica gel 60 F_{254} (Merck, Germany) with chloroform and methanol (95:5, v/v).

The spot was detected with 365 nm (Iiyama et al., 1995; Kim et al., 2004).

Table 3. Bacterial strains and plasmids used in this study.

Strain, plasmids	details	Source, Reference
Bacteria strain		
Escherichia coli		
BL21(DE3)	F–*ompT hsdSB*(rB–mB–)*gal dcm* (DE3)	Novagen
DH5a, DH10b	For Cloning	Clontech
DLYT1	FS1576 include pMMV22S l*ytB*::Km^R cassette	Kim et al. (2008)
S17-1	Mating helper Tra^+, *recA*, Sp^R	Simon et al. (1983)
Burkholderia glumae		
HDR1KO	BGR1 *hdr1*::Ω	Lee (2006)
HDR2KO	BGR1 *hdr2*::Ω	Lee (2006)
BGR1	Wild type, Rif^R	Kim et al. (2004)
BGS4	BGR1 *toxR*::Ω	Kim et al. (2004)
Saccharomyces cerevisiae		
Y187	MAT_{α}, *ura3-52, his3-200, ade2-101, trp1-901, URA3::GaL1*$_{UAS}$-GAL_{TATA}-*lacZ, leu2-3, 112, gal4*$_{\Delta}$, *met*$^-$, *gal80*$_{\Delta}$, *mEL1*	Harper et al. (1993)
Plasmids		
pBluescript II SK(+)	Cloning vector, pUC derivative, Amp^R	Fermentas
pET14b	T7 promoter-based expression vector, Amp^R	Kim et al. (2009)
pET-32a(+)	T7 promoter-based expression vector, Amp^R	Novagen
pGADT7-Rec2	*LEU2, pUC, ARS4,* P_{ADH1}, T_{ADH1}, Amp^R	Clontech

pGEMT®-T Easy	Cloning vector, *lac* Z, f1 Ori, Amp^R	promega
pHIS2	*ARS4, TRP1, Col E1,* $P_{minHIS3}$, Ka^R	Clontech
pHP45Ω	Ω cassette, Sm^R, Sp^R,	Kim et al. (2004)
pLAFR3	Mob^+, Tra^-, Tet^R, RK2 replicon	Kim et al. (2004)
pLAFR6	As pLAFR3 without lacZα, contains multilinker	Kim et al. (2004)
pMMV22S	Include MVA kinase, PMVA kinase and DPMVA decarboxylase, Amp^R	Kim et al. (2008)
pMW118	Cloning vector, Amp^R	Nippon gene
pRK2013	Helper plasmid, Tra^+, ColE1 replicon, Km^R	Kim et al. (2004)
pRK415	Broad host vector	Choi et al (2009)
pUC19	Cloning vector, *lac* Z, Amp^R	Fermentas
BgHdr1-pMW118	pMW118 with 1 kbp BamHI-BamHI fragment from pGEMTHDR1	This study
BgHdr2-pMW118	pMW118 with 0.9 kbp BamHI-BamHI fragment from pGEMTHDR2	This study
EcHDR-pMW118	pMW118 with 1 kbp BamHI-BamHI fragment from pGEMTEcHDR	This study
pBlueHDR1	pBluescript II SK(+) with 6.8 kbp HindIII-HindIII fragment obtaining *hdr1* from BGR1	This study
pBlueHDR1SP	pBlueHDR1 with 2 kb Sp^R cassette within *hdr1*	This study
pET32HDR1	pET-32a(+) with 1 kbp *hdr*1 ORF PCR product from BGR1	This study

pET32HDR2	pET-32a(+) with 0.9 kbp *hdr*2 ORF PCR product from BGR1	This study
pGADT7ToxR	pGADT7-Rec2 with 0.9 kbp PCR product from BGR1	This study
pGEMTHDR1	pGEMT-easy with 1 kbp *hdr*1 ORF PCR product from BGR1	This study
pGEMTHDR2	pGEMT-easy with 0.9 kbp *hdr*2 ORF PCR product from BGR1	This study
pHIS2HDR2-131	pHIS2 with 131 bp PCR product from BGR1	This study
pLAFRHDR1SP	pLAFR3 with 8.8 kbp HindIII-HindIII fragment from pBlueHDR1SP	This study
pLAFRHDR2SP	pLAFR3 with 11.2 kbp SmaI-SmaI fragment from pLAFRHDR2SP	This study
pLAFR6HDR1P1O	pLAFR6 with 1.3 kbp PCR product from pRK415HDR1P1O	This study
pLAFR6HDR1P2O	pLAFR6 with 1.2 kbp PCR product from pRK415HDR1P2O	This study
pLAFR6HDR2P1O	pLAFR6 with 1.4 kbp PCR product from pRK415HDR2P1O	This study
pLAFR6HDR2P2O	pLAFR6 with 1.3 kbp PCR product from pRK415HDR2P2O	This study
pLAFR6HDR1P$_o$1O	pLAFR6 with 2 kbp PCR product from BGR1	This study

pLAFR6HDR1P$_o$2O	pLAFR6 with 1 kbp and 1 kbp PCR product from BGR1	This study
pRK415HDR1P1O	pRK415 with 1.3 kbp PCR product from BGR1	This study
pRK415HDR1P2O	pRK415 with 1.2 kbp PCR product from BGR1	This study
pRK415HDR2P1O	pRK415 with 1.4 kbp PCR product from BGR1	This study
pRK415HDR2P2O	pRK415 with 1.3 kbp PCR product from BGR1	This study
pUCHDR2	pUC19 with 9.2 kbp SmaI-SmaI fragment obtaining *hdr2* from BGR1	This study
pUCHDR2SP	pUCHDR2 with 2 kb Sp^R cassette within *hdr2*	This study

Table 4. The primers for 6 combinatorial constructions of p*hdr*::hdr.

Primer name	Primer sequence	No.
HDR1P-pRK415-F	tgattacgccaagcttCATTCTGCTCGGCCTGAAGTC	1
HDR1P-pRK415-R	aagaatgactcgcatGGGTTACAGGATCCCGATGATTT	2
HDR2P-pRK415-F	tgattacgccaagcttCCTGTTCGGCCGTGAGATTC	3
HDR2P-pRK415-R	cggtggagctcatACAGGGCGAACTCCGACGA	4
HDR1O-pRK415-F	cggagttcgccctgtATGAGCTCCACCGATACGCTGTC	5
HDR1O-pRK415-R	cggtacccggggatccCGCTTTGGTAGGAGTCGATACCC	6
HDR2O-pRK415-F	cgggatcctgtaaccATGCGAGTCATTCTTGCCCAAC	7
HDR2O-pRK415-R	cggtacccggggatccCGGAATAGACAAGAGATGTCCTCCTC	8
HDR1P-pLAFR6-F	ttttttttccgaattcCATTCTGCTCGGCCTGAAGTC	9
HDR2P-pLAFR6-F	ttttttttccgaattcCCTGTTCGGCCGTGAGATTC	10
HDR1O-pLAFR6-R	cgactctagaggatccCGCTTTGGTAGGAGTCGATACCC	11
HDR2O-pLAFR6-R	cgactctagaggatccCGGAATAGACAAGAGATGTCCTCCTC	12
HDR1P$_o$-pLAFR6-F	ttttttttccgaattcCGATCGTCAGCCGCAGATAAT	13

RESULTS

1. Cloning and complementation assay

Genom analysis revealed a putative *hdr* gene on each *B. glumae* chromsome, one on chromosome 1 being named *hdr1* and anothe on chromosome 2 *hdr2*. The ORF of *hdr1* was predicted to be a 981 bp gene in size encoding a 36 kDa protein. The *hdr2* was composed of 942 bp in size and encoded a 34.5 kDa of protein. Both proteins had high homology with 4-hydroxy-3-methylbut-2-enyl diphosphate reductase. The *hdr1* has a neighboring gene encoding FKBP-type 16 kDa peptidyl-prolyl cis-trans isomerase (*slp*, bglu_1g28660), and DNA repair and recombination protein (*radC*, bglu_1g28660). The *hdr2* was neighbored by the gene encoding radical SAM domain-containing protein (*hpnH*, bglu_2g22180) and hopene-associated glycosyltransferase (*hpnB*, bglu_2g22160) (Fig. 8). Thus the *hdr1* and *slp* as well as *hdr2* and *hpnH* were predicted to be polycistronic. RT-PCR analysis confirmed that each of *hdr1* (*hdr1* and *slp*) and *hdr2* (*hdr2* and *hpnH*) operon was transcribed as single transcript (Fig. 9).

Both *B. glumae hdr1* and *hdr2* successfully complemented *hdr*-negative *E. coli* DLYT1 strain (Kim et al., 2008) (Fig. 10 and 11). It demonstrated that both *B. glumae* genes were expressed as functional Hdr proteins in *E. coli* (Fig. 11).

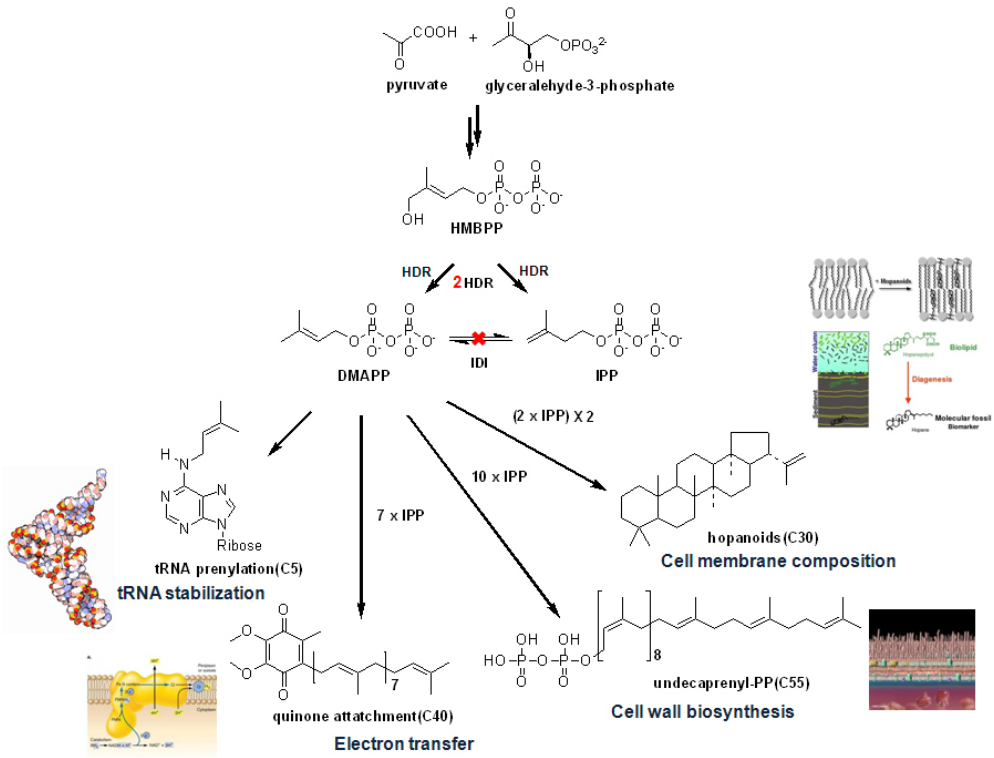

Figure 7. The terpenes of *B. glumae*.

The tepenoids in *B. glumae* were predicted by identifying enzymes in terpene metabolism through genome analysis. *B. glumae* only produces terpenoids as primary metabolites that are vital in cellular function: tRNA stabilization, cell membrane component, cell wall biosynthesis primer, and quinine side-chain.

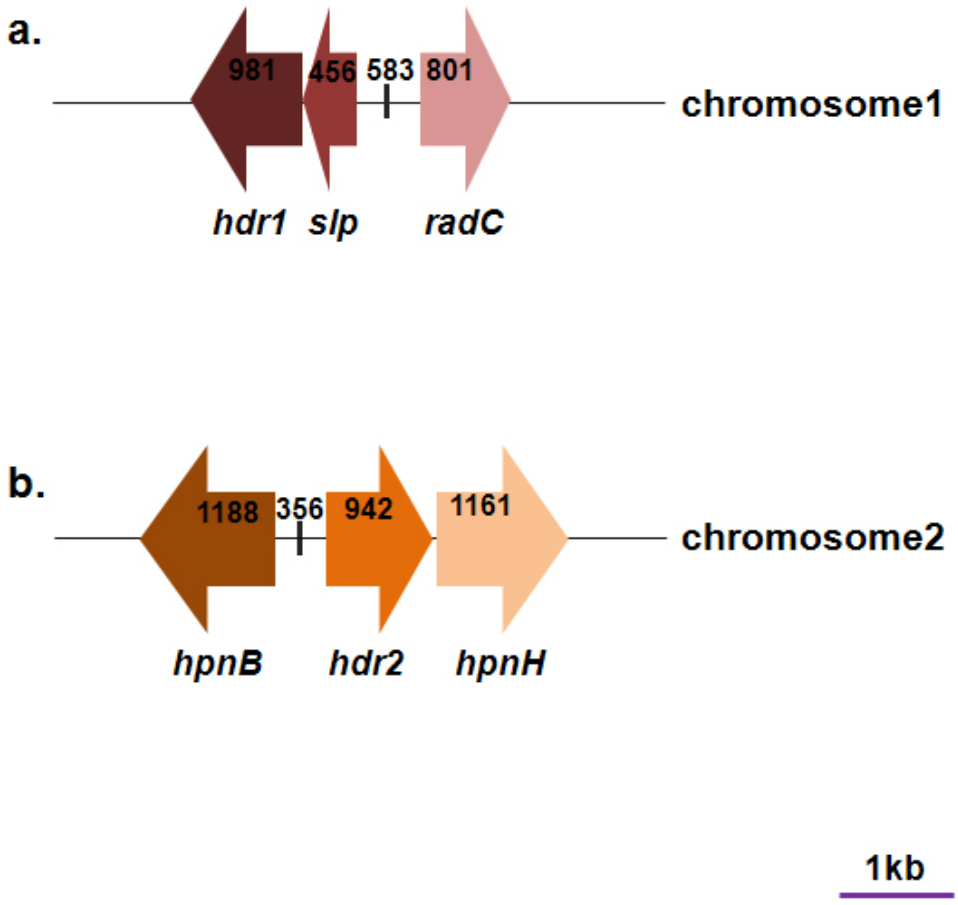

Figure 8. Organization of *hdr* isogenes.

Putatiave *hdr1* was neighbored by *slp* and *radC* at chromosome 1. On chromosome 2, putative *hdr2* was planked by *hpnH* and *hpnB*.

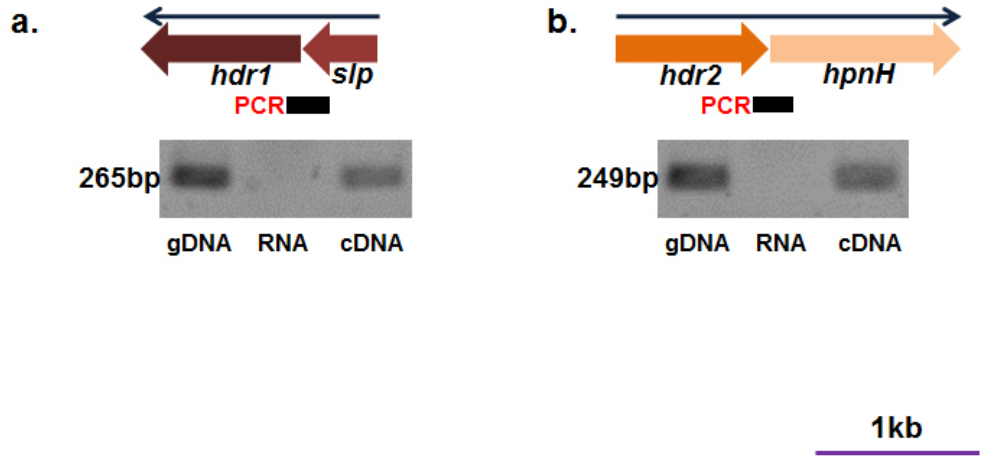

Figure 9. Transcriptional units in each *hdr* isogene operon.

Polycistronic *hdr1* and *slp* (a) as well as *hdr2* and *hpnH* (b) were shown by RT-PCR analysis. The black arrow indicates the transcription direction. The bars labeld as PCR indicates the RT-PCR product.

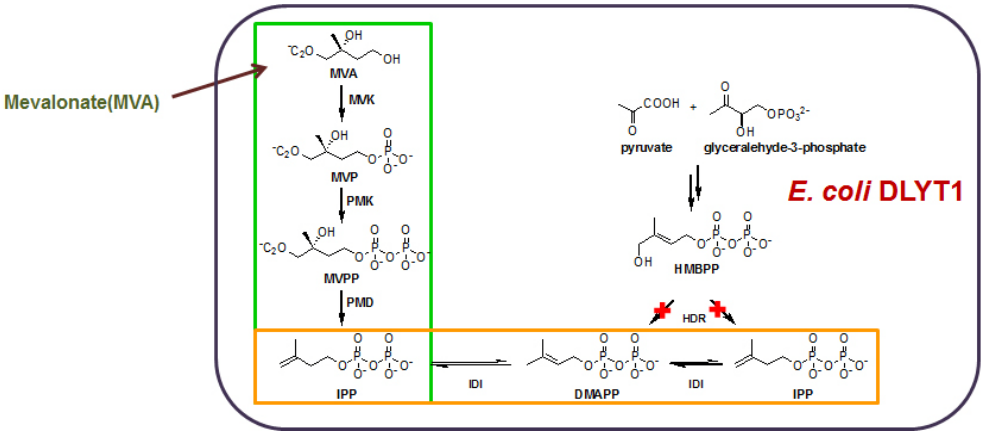

Figure 10. *E. coli* DLYT1.

The *hdr*-deficient *E. coli* mutant was engineered to harbore *mvk*, *pmk* and *pmd* genes of MVA pathway (Kim et al., 2008). The resulting mutant, DLYT1, could survive only in the presence of mevalonate (MVA).

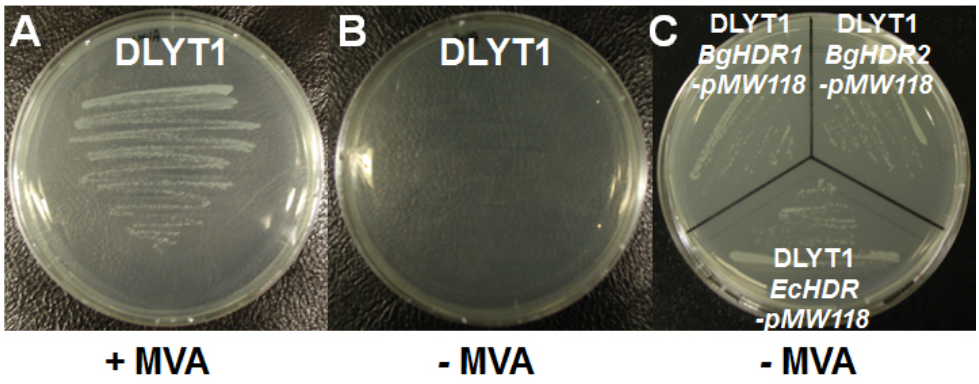

Figure 11. Complementation assay.

A. DLYT1 with MVA. B. DLYT1 without MVA. C. DLYT1 with BgHdr1-pMW118, BgHdr2-pMW118 and EcHDR-pMW118.

The LB plates were incubated at 37 ºC for 24 h. Both 2 *hdr* isogenes could rescue DLYT1. The EcHDR-pMW118 harboring the *E. coli hdr* gene was used as positive control.

2. Purification and characterization of Hdr isozymes

BgHdr proteins were expressed as fusion proteins with thioredoxin (17.8 kDa) at N-terminal and His-tag at C-terminal. The calculated molecular mass of the fused BgHdr1 and BgHdr2 were 51.33 and 49.9 kDa, respectively, as were confirmed by SDS-PAGE (Fig. 12). Both BgHdr1 and BgHdr2 have conserved regions in their amino acid sequences. For example, Cys27, 111, and 209 in BgHdr1 and Cys12, 96, and 194 in BgHdr2 are well-conserved, because they participate in iron-sulfur cluster formation (Fig. 13). In addition, His56, 89, and 139 of BgHdr1 and His41, 74, and 124 of BgHdr2 were also highly conserved (Fig. 13) for coordination with diphosphate group (Gräwert et al., 2009). Phylogenetic analysis showed that each isozyme belongs to different bacterial Hdr clade (Fig. 14).

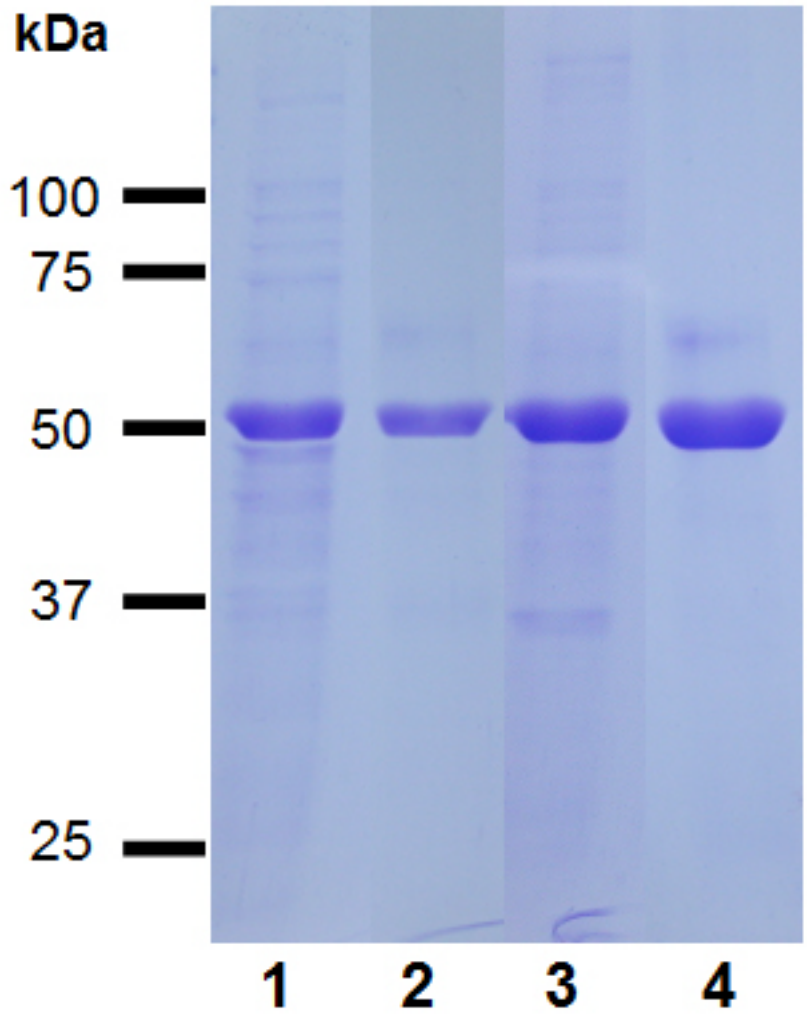
kDa
100
75
50
37
25
1
2
3
4

Figure 12. SDS-PAGE of the recombinant Hdr.

Lane 1, crude fused BgHdr1; Lane 2, purified fused BgHdr1; Lane 3, crude fused BgHdr2; Lane 4, purified fused BgHdr2.

Both recombinant proteins purified on Ni-NTA column.

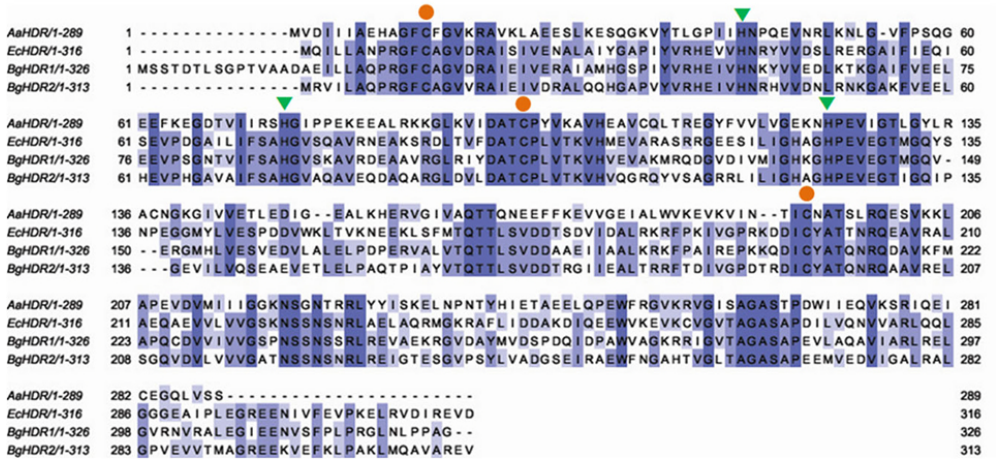

Figure 13. Homology among bacterial Hdr enzymes.

AaHDR (*Aquifex aeolicus,* aq1739), EcHDR (*E. coli,* Y75_p0029), BgHdr1 (*B. glumae,* bglu_1g28650), and BgHdr2 (bglu_2g22170). The residues marked with circle (Cys27, 111, and 209 in BgHdr1 and Cys12, 96, and 194 in BgHdr2) participate in iron-sulfur cluster. In addition, His56, 89, and 139 of BgHdr1 and His41, 74, and 124 of BgHdr2, marked with triangle, coordinate with diphosphate group (Gräwert et al., 2009).

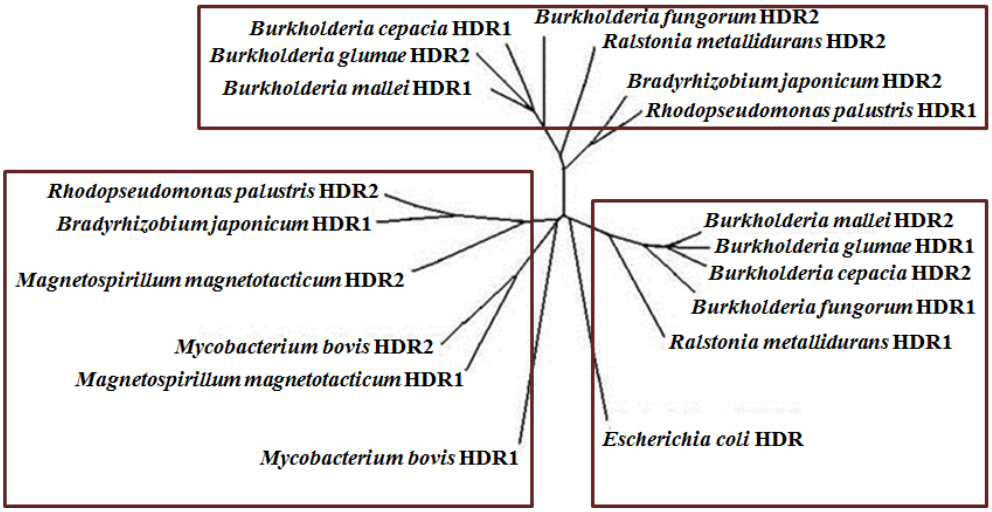

Figure 14. The phylogenetic tree of bacterial Hdr.

The each BgHdr isozyme belongs to the different clade.

3. Product ratio of BgHdr

IPP and DMAPP produced from HMBPP were cleaved to give corresponding alcohols, which were subsequently separated and identified by GC. The chromatogram of the alcohols showed R_t values at 7.12 and 8.05 min, which corresponded to those of standard 3M3B1ol and 3M2B1ol, respectively (Fig. 15). The peak area ratios of 3M3B1ol to 3M2B1ol, corresponding IPP to DMAPP ratio, were 2.28 for BgHdr1 and 2.22 for BgHdr2, indicating that the ratios were virtually identical in both isozymes (Fig. 15).

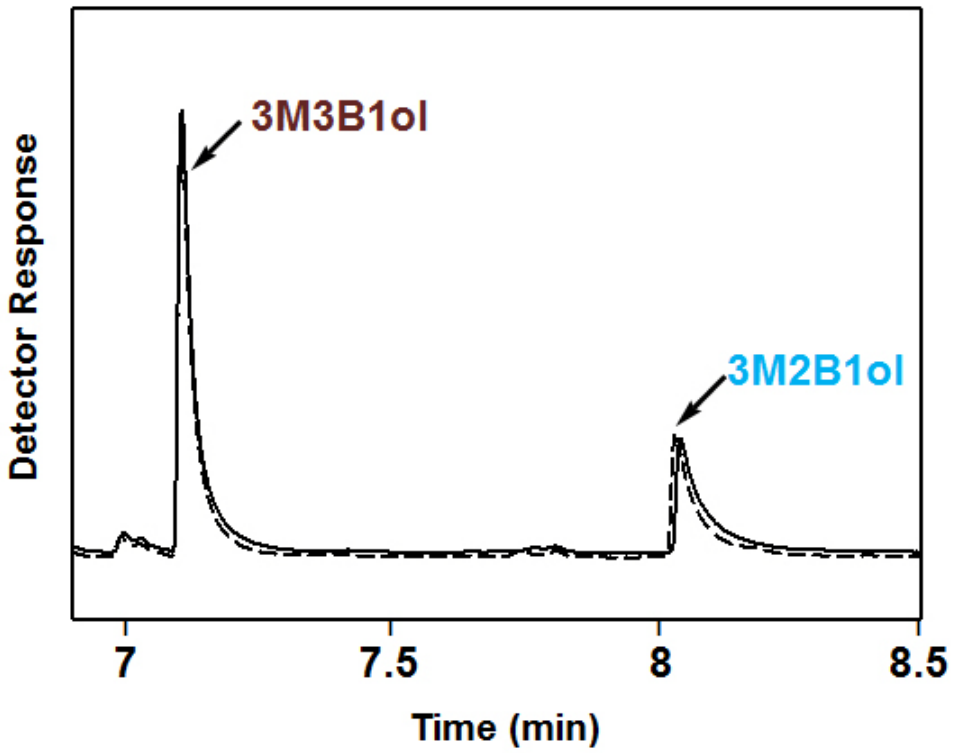

Figure 15. FID-GC analysis of products of *in vitro* reaction of BgHdrs.

3-Methyl-3-buten-1-ol (3M3B1ol) (Rt, 7.12 min) to 3-methyl-2-buten-1-ol (3M2B1ol) (Rt, 8.05 min) ratio, corresponding to IPP to DMAPP ratio, was about 2.2:1 for both BgHdr1 (black line) and BgHdr2 (broken line).

Table 5. The ratio of IPP and DMAPP.

AaHdr (*Aquifex aeolicus* Hdr), EcHdr (*E coli* Hdr), BgHdr1 (*B. glumae* Hdr1), BgHdr2 (*B. glumae* Hdr2). The product ratio of BgHdr was different from those of previous studied bacteria. *Aquifex aeolicus* and *E. coli* have only 1 *hdr* gene.

	IPP:DMAPP	**reference**
BgHdr1	2:1	This study
BgHdr2	2:1	This study
AaHdr	5:1	Altincicek et al., 2002
EcHdr	6:1	Gräwert et al., 2004

4. Kinetics properties of BgHdrs

To measure kinetic parameters of BgHdr, artificial electron donor MV and DT were used. MV has been used as electron donor for iron-sulfur clusters and was previously demonstrated that use of MV gave reaction kinetics of bacterial Hdr comparable to the reaction using the biological electron donor flavodoxin and NADPH (Gräwert et al., 2010, Wang et al., 2010).

Lineweaver-Burk plot of MV oxidation by BgHdr (Fig. 16) yielded k_{cat} and K_m values of BgHdrs (Table 4). BgHdr1 had 10-fold higher k_{cat}/K_m and 3.5-times lower K_m values than those of BgHdr2. This meant that two Hdr in *B. glumae* could differentially function under the various environmental conditions. It is possible that Hdr2 was expressed constitutively to function with high substrate concentration, while Hdr1 could be induced to cope with stress situation where carbon source is limiting.

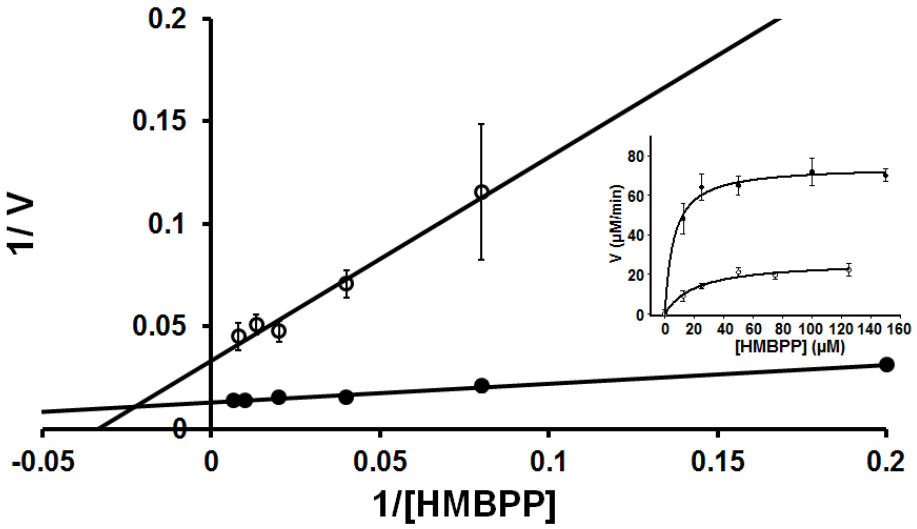

Figure 16. Lineweaver-Burk plot of BgHdr isozyme.

BgHdr1 (-●-); BgHdr2 (-○-).

The insert shows Michaelis-Menten plot.

Table 6. Kinetic parameters of bacterial Hdrs

Kinetic parameters of various bacterial Hdrs. BgHdr1 was 10 folds more efficient than BgHdr2.

	K_m (μM)	k_{cat} (min^{-1})	k_{cat}/K_m (μM^{-1} min^{-1})	Specific activity (μmol $min^{-1}mg^{-1}$)	Reference
BgHdr1	6.0 ± 1.1	187 ± 6	31.1 ± 6.2	3.66 ± 0.11	this study
BgHdr2	21.2 ± 5.5	66.6 ± 5.2	3.1 ± 0.8	1.39 ± 0.11	this study
AaHdr	590 ± 60	222 ± 12	2.66	6.6 ± 0.3	Altincicek et al., 2002
EcHdr	30	-	-	0.7~3.4	Gräwert et al., 2004

5. Expression pattern of *hdr* isogenes

To assess the temporal expression pattern of *hdr* isogenes during growth cycle, Northern blot analysis was performed using RNA from *B. glumae* BGR1 that was cultured for 10~19 h in M9 minimal medium (Fig. 17). Transcript message level of both *hdr1* and *hdr2* increased as culture progressed from lag (10~11 h) to exponential phase (12~14 h). After the growth reached stationary phase, the message level of *hdr* isogenes was dramatically reduced. The transcription was most active at the exponential phase (14 h), with higher transcription level of *hdr2* than *hdr1* throughout the growth (Fig. 17). These results were confirmed by transcriptome analysis of LB medium-grown bacterium (data from prof. I. Hwang, Seoul National University) (Table 5). The *hdr2* gene was transcribed 1.8 times higher at exponential phase (6 h) and 1.6 times at stationary phase (10 h) than *hdr1*.

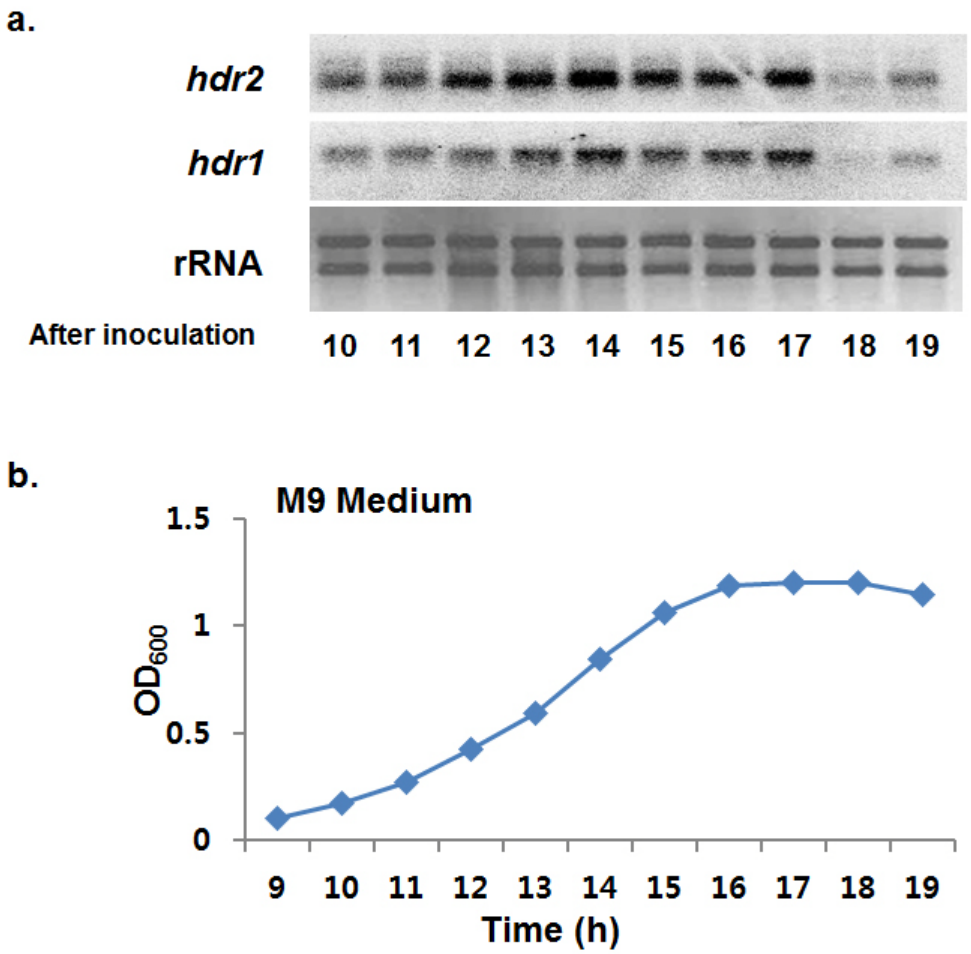

Figure 17. The expression pattern of *hdr* isogenes.

a. Nothern blot results of *hdr* isogenes. 2 μg of total RNA was loaded and blotted.

b. The RNA extraction time points after inoculation.

Both *hdr* genes were increasely transcribed to early stationary phase. The *hdr2* was more transcribed than *hdr1* in BGR1.

Table 7. The transcriptome analysis of MEP pathway genes.

The RNA sequencing data of MEP pathway genes were provided by prof. I. Hwang. The RNA of BGR1 was extracted at 6 h and 10 h after inoculation in LB medium. Like Nothern blot analysis, *hdr2* was transcribed more than *hdr1*.

	6hours	10hours
DXS1	461.8	241.8
DXS2	4.5	3
DXR	227.1	160.6
CMS	76.8	64.5
CMK	825.4	397.1
MECS	162.8	158.2
HDS	647.7	1381.2
HDR1	252.7	176.4
HDR2	453.3	288.9

6. Growth rates of *hdr* isogene knock-out mutants

The *hdr* isogene knock-out mutants were constructed by insertion of Ω cassette using triple mating (Lee, 2006). To observe phenotype of the knock-out mutants, the growth rates were measured under the various conditions. When grown in LB medium, the performance of BGR1, HDR1KO and HDR2KO were identical (Fig. 18). However, on LB plate, the colony size of HDR1KO was smaller than the others, while the number of colonies was the similar (data not shown). The mutants were cultured under the heat shock condition at 42 ºC. HDR1KO did not grow normally and colony size difference was larger than under 37 ºC incubation (Fig. 19). Susceptibillity of HDR1KO was again observed in culture grown at extreme pH. The difference in the growth rate was most obvious at pH 4 and 5. At alkaline pH, all the strains failed to grow (Fig. 20). The growth of HDR2KO was not different from BGR1 against heat and pH shock. When the strains were cultured in minimal M9 medium, the retarded growth of HDR1KO was more pronounced than in rich LB medium (Fig. 21). In the case of the inoculation on rice plants, the population of HDR1KO was 10~640 fold lower than that of HDR2KO and BGR1 (Fig. 22). This lower population of HDR1KO was probably due to inability to properly colonize the plant. In swimming test, the radius of HDR1KO was smaller by 28 % than HDR2KO and BGR1. The small radius again indicated the growth defect of HDR1KO (Fig. 23).

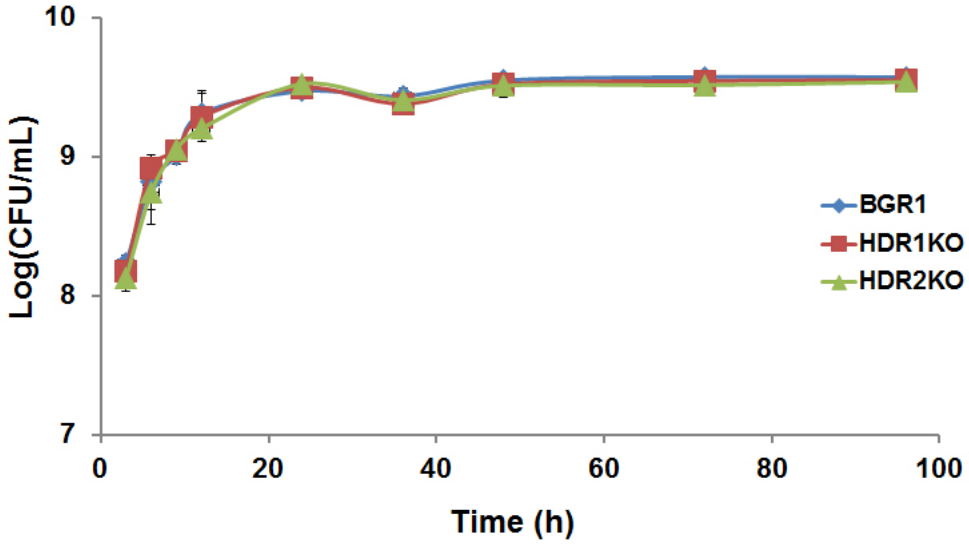

Figure 18. Growth of *B. glumae* starains in LB medium at 37 ºC.

Growth of both HDR1KO and HDR2KO mutants grew was not different from that of BGR1. Circle, BGR1; rectangle, HDR1KO; triangle, HDR2KO.

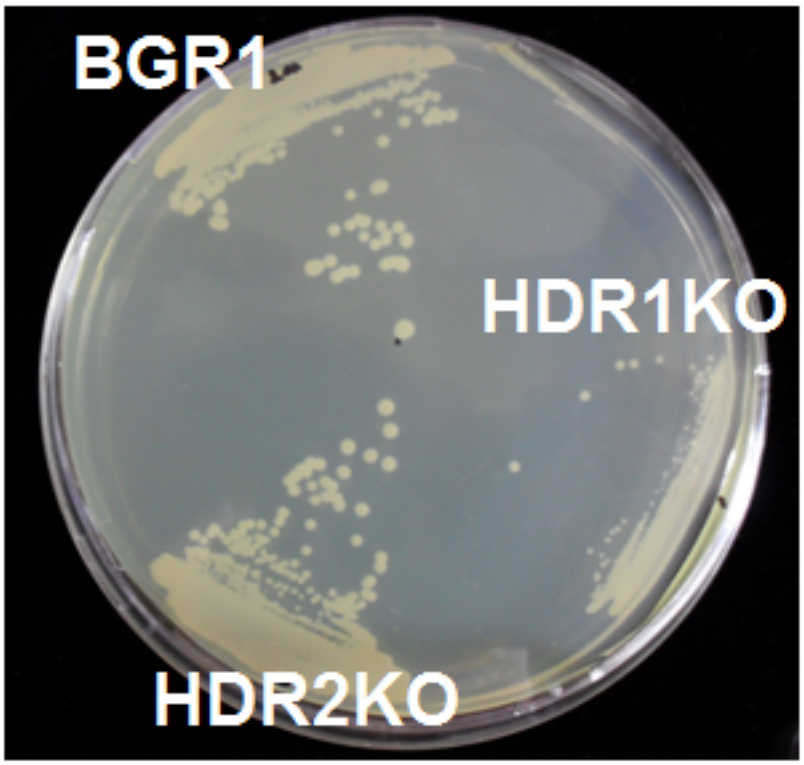

Figure 19. Growth under the heat shock condition at 42 ℃.

BGR1 and *hdr* knock-out mutants were incubated at 42 ℃ on LB medium.

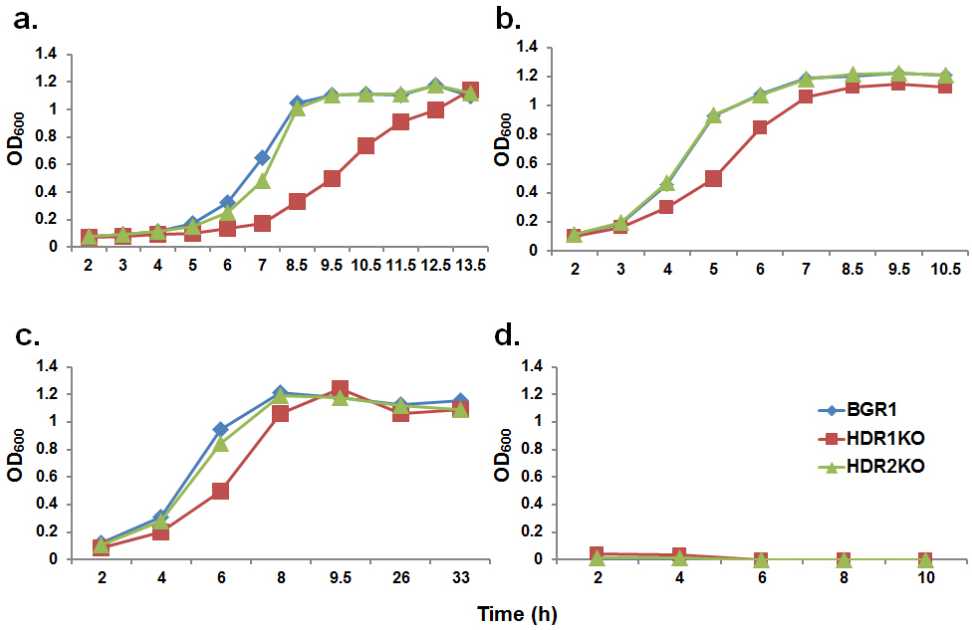

Figure 20. Growth under the pH shock condition.

Each *B. glumae* strains were cultured in LB medium with various pH conditions at 37 ºC. a. pH 4 buffer (100 mM MES); b. pH 5 buffer (100 mM MES); c. pH 7 buffer (100 mM MOPS); d. pH 8.5 buffer (100 mM bicine).

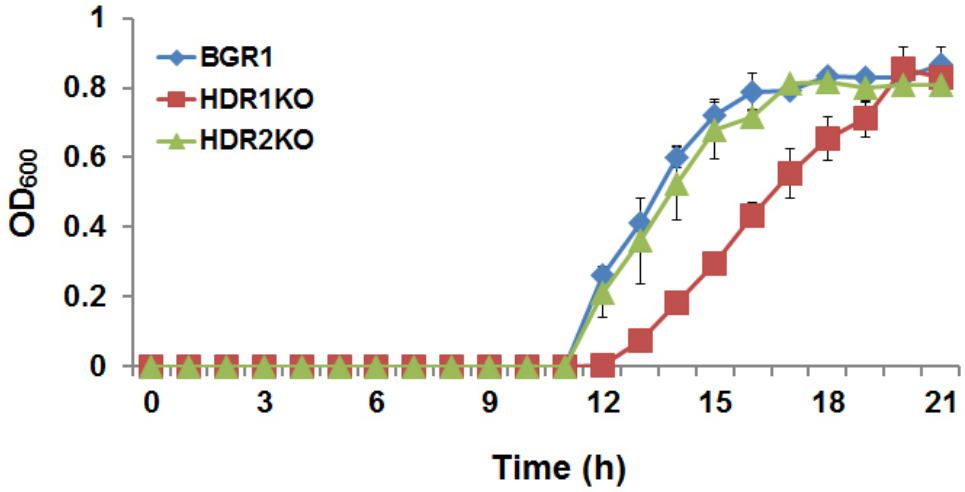

Figure 21. Growth in M9 minimal medium.

The *B. glumae* strains were cultured in M9 minimal medium (0.2 % glucose) at 37 ºC. Growth of HDR1KO lagged behind those of HDR2KO and BGR1.

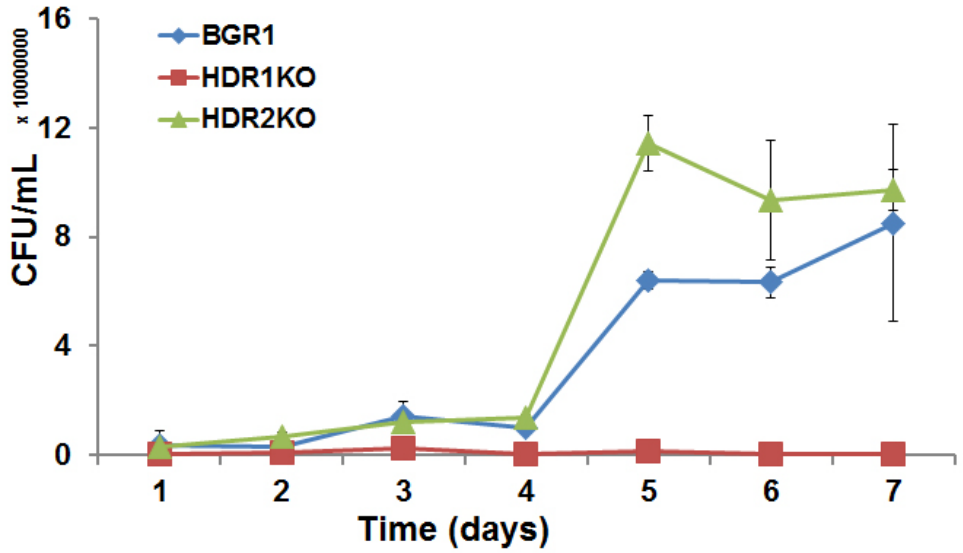

Figure 22. *B. glumae* cell densities in rice plant inoculated with the bacterium.

After B. glumae was inoculated to rice seedling, the cell bacterial cell density was meassured every day for a week. The cell density of HDR1KO was 1/10 ~ 1/640 of BGR1 and HDR2KO.

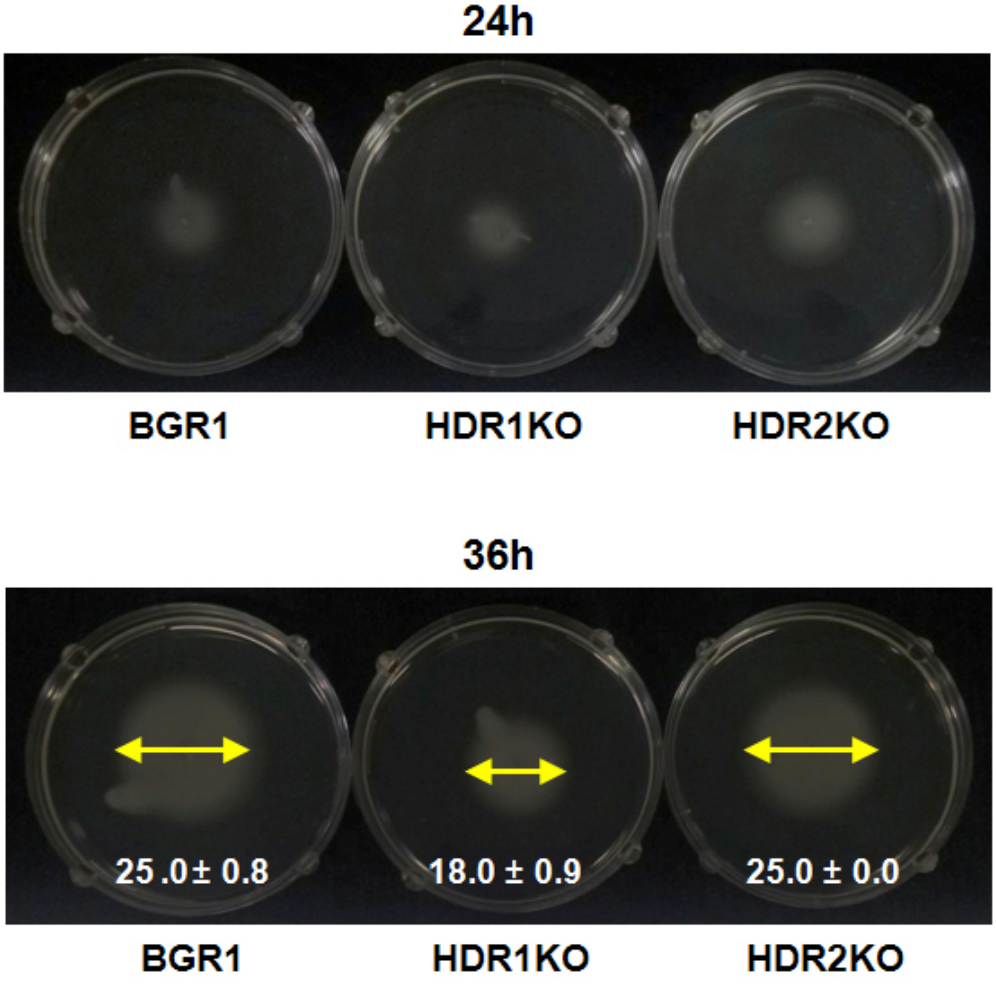

Figure 23. Effect of *hdr* knock-out on *B. glumae* swimming.

The swimming halo diameters were measured 36 h after inoculation on swimming plate (LB, 0.4 % agar) at 28 ºC. The reduced swimming ability of HDR1KO was caused by growth defect.

The halo radius (cm): 25.0 ± 0.8 for BGR1, 18.0 ± 0.9 for HDR1KO, and 25.0 ± 0.0 for HDR2KO.

7. Virulence of the knock-out mutants

The pathogenicity of the knock-out mutants was observed on rice plants at seedling and flowering stages. Rice seedling inoculated with BGR1 and HDR2KO developed wilt symptom accompanied by leaf browning. However, HDR1KO did not exhibit such symptom (Fig. 24). In the case of inoculated rice panicles at flowering stage, HDR1KO-inoculated rice exibited low of grain rot symptom (disease index 1.5), compared to the high pathogenicities of BGR1 (disease index 3.2) and HDR2KO (disease index 3.5) (Fig. 25). The low virulence of HDR1KO was compatible with the previously described low bacterial cell density (Fig. 22) of the strain upon inoculation.

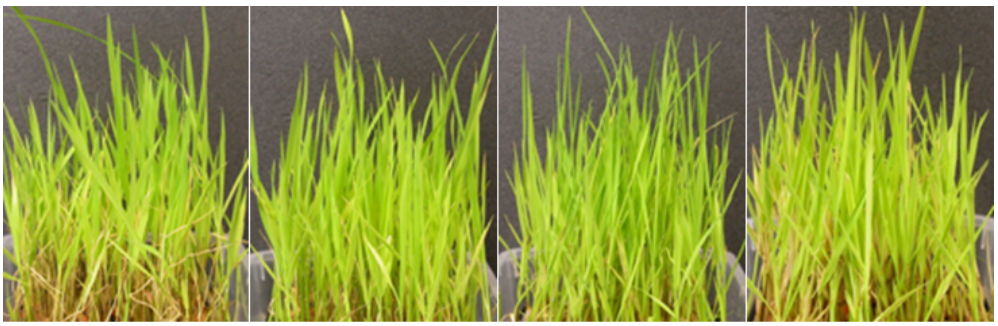

Figure 24. Rice seedlings inoculated with *hdr* knock-out mutants.

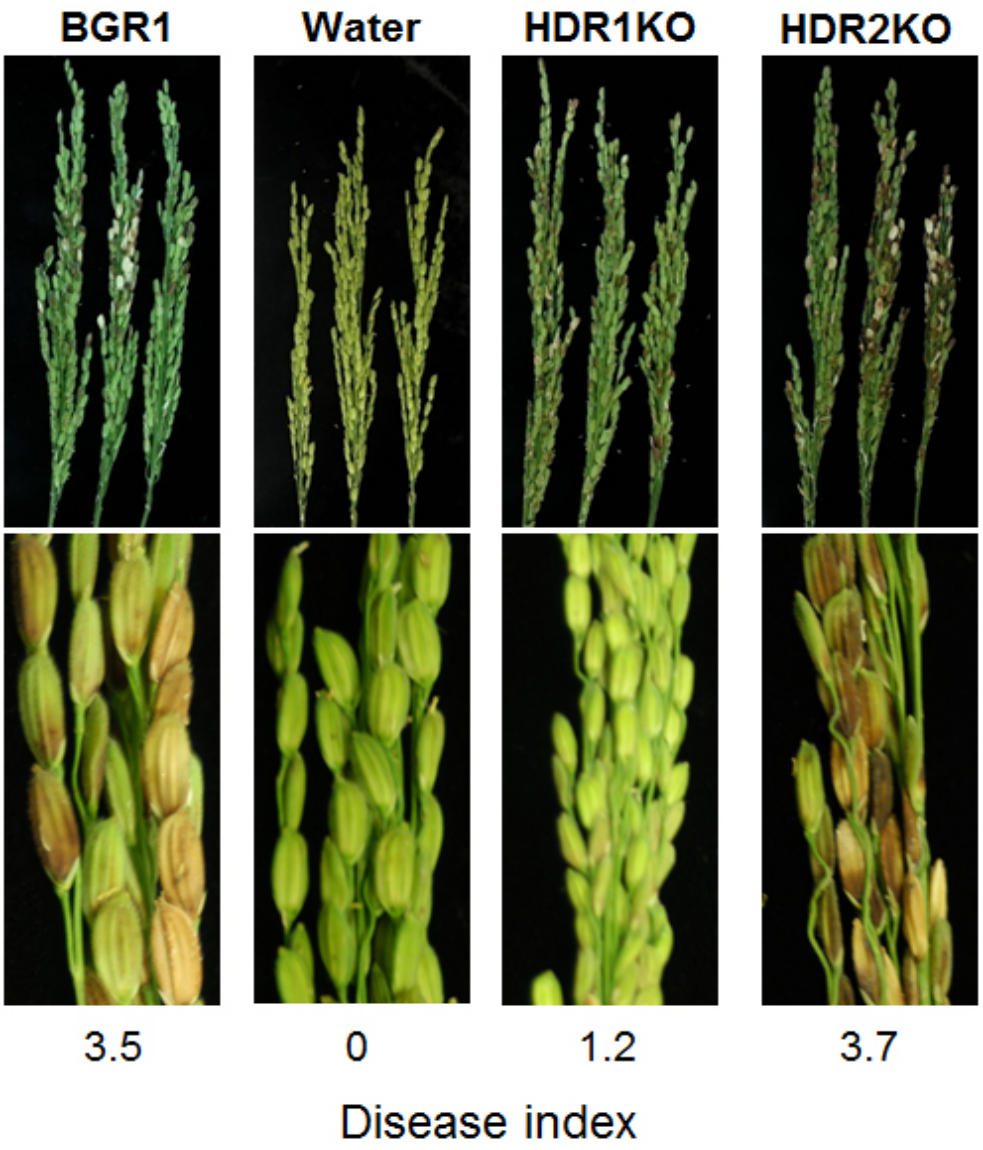

Figure 25. Rice panicle inoculated with *B. glumae hdr* mutants at the flowering stage.

8. Identification of cellular proteins modified in *hdr* isogene knock-out mutants

After the *hdr* isogene knock-out mutants and BGR1 were cultured in M9 medium, Cellular proteins were extracted from the strains at 6 h (exponential phase) and 10 h (stationary phase) after inoculation on M9 medium, and eletrophoresed on SDS PAGE. It was outstanding that 3 protein bands with apparent molecular mass of 36, 52, and 57 kDa of HDR1KO migrated faster than the corresponding bands of HDR2KO and BGR1 (Fig. 26). The bands were isolated, digested by trypsin, and identified by LC MS/MS analysis (Table 8). It was shown that the identities of proteins were the same in the corresponding bands. The most abundant protein, with molecular mass of 57 kDa, was identified as GroEL with 90 % coverage of peptide against Database (bglu_1g07150, bglu_2g19330) (Fig. 26). The protein band with 57 kDa reacted with GroEL antibody in Western blot (Fig. 27), further confirming the identity of the protein. The LC MS/MS analysis of GroEL band in HDR1KO harvested at exponential phase suggested that *m/z* value of Lys390 increased by 42, suggesting acetylation at the residue. .In contrast, GroEL of BGR1 and HDR2KO were not acetylated at this position (Fig. 28). However, at stationary phase, acetylation at Lys390 residue had also occured in BGR1 and HDR2KO.

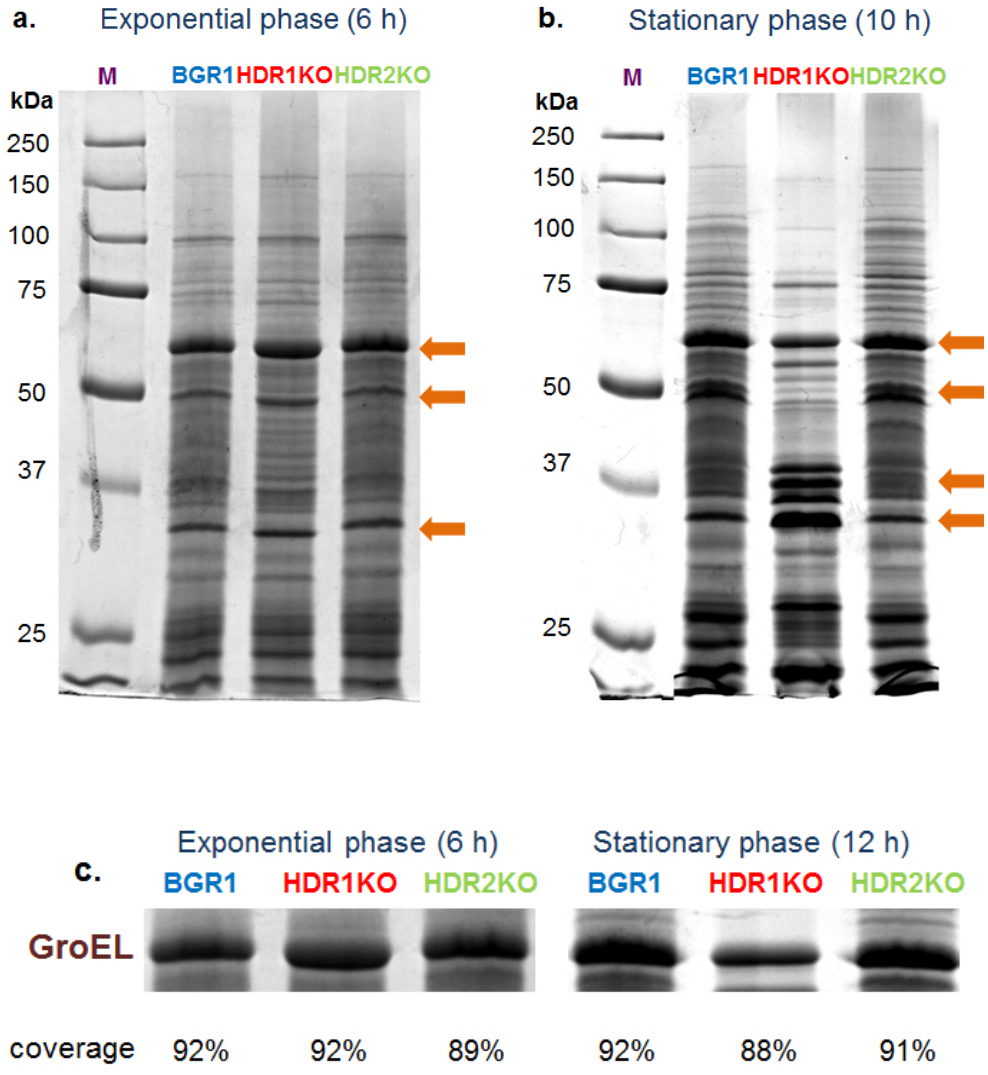
a.
Exponential phase (6 h)
M
BGR1
HDR1KO
HDR2KO
kDa
250
150
100
75
50
37
25
b.
Stationary phase (10 h)
M
BGR1
HDR1KO
HDR2KO
kDa
250
150
100
75
50
37
25
c.
Exponential phase (6 h)
Stationary phase (12 h)
BGR1
HDR1KO
HDR2KO
BGR1
HDR1KO
HDR2KO
GroEL
coverage
92%
92%
89%
92%
88%
91%

Figure 26. SDS-PAGE of cellular proteins at exponential (6 h) and stationary (10 h) phases.

The cellular proteins were separated on 10 % acrylamide gel. The yellow numbers indicate the analyzed protein bands by LC MS/MS.

a. SDS PAGE of cellular proteins at 6 h after inoculation. The 3 bands of HDR1KO migrated faster than those of other strains. The orange arrows indicate the isolated bands to LC MS/MS analysis.

b. SDS PAGE of cellular proteins at 10 h after inoculation. Expression of some proteins changed. The migration of 4 bands changed in comparision with protein migration pattern at 6 h. The 57 kDa protein of all strains migrated equally. The orange arrows indicate the isolated bands.

c. Among different migration bands, the 57 kDa protein was analyzed as GroEL. The coverage numbers means peptides coverages in LC MS/MS analysis. The GroEL of HDR1KO migrated faster than that of strains at exponential phase. But the difference of migration speed was disappeared at stationary phase, due to the faster migration of BGR1 and HDR2KO.

Table 8. Identification of isolated cellular proteins from bands

The cellular proteins were isolated from bands (B, BGR1; 1, HDR1KO; 2, HDR2KO) (Fig. 26). The proteins were analyzed by LC MS/MS.

Band name	Exponential phase (6h)	Stationary phase (10h)
B-57 kDa	GroEL (bglu_1g07150, bglu_2g19330)	GroEL (bglu_1g07150, bglu_2g19330)
1-57 kDa	GroEL (bglu_1g07150, bglu_2g19330)	GroEL (bglu_1g07150, bglu_2g19330)
2-57 kDa	GroEL (bglu_1g07150, bglu_2g19330)	GroEL (bglu_1g07150, bglu_2g19330)
B-52 kDa	ATP synthase F1, beta subunit (bglu_1g00770) ATP synthase subunit A (bglu_1g00750) *S*-adenosyl-L-homocysteine hydrolase (bglu_1g01990)	Isocitrate lyase (bglu_1g12420) S-adenosyl-L-homocysteine hydrolase (bglu_1g01990)
1-52 kDa	ATP synthase F1, beta subunit (bglu_1g00770) ATP synthase subunit A (bglu_1g00750) S-adenosyl-L-homocysteine hydrolase (bglu_1g01990)	Isocitrate lyase (bglu_1g12420) Histidine ammonia-lyase (bglu_1g25210)
2-52 kDa	ATP synthase F1, beta subunit (bglu_1g00770) ATP synthase subunit A (bglu_1g00750) S-adenosyl-L-homocysteine hydrolase (bglu_1g01990)	Isocitrate lyase (bglu_1g12420) S-adenosyl-L-homocysteine hydrolase (bglu_1g01990)
B-36 kDa	ABC-type phosphate transport	ABC-type phosphate transport

	system periplasmic component (bglu_1g11450)	system periplasmic component (bglu_1g11450) Translation elongation factor Ts (bglu_1g12730)
1-36 kDa	ABC-type phosphate transport system periplasmic component (bglu_1g11450)	ABC-type phosphate transport system periplasmic component (bglu_1g11450)
2-36 kDa	ABC-type phosphate transport system periplasmic component (bglu_1g11450)	ABC-type phosphate transport system periplasmic component (bglu_1g11450) Translation elongation factor Ts (bglu_1g12730)
B-44 kDa		ABC-type sugar transport system periplasmic component (bglu_1g08070)
1-44 kDa		ABC-type sugar transport system periplasmic component (bglu_1g08070)
2-44 kDa		ABC-type sugar transport system periplasmic component (bglu_1g08070)

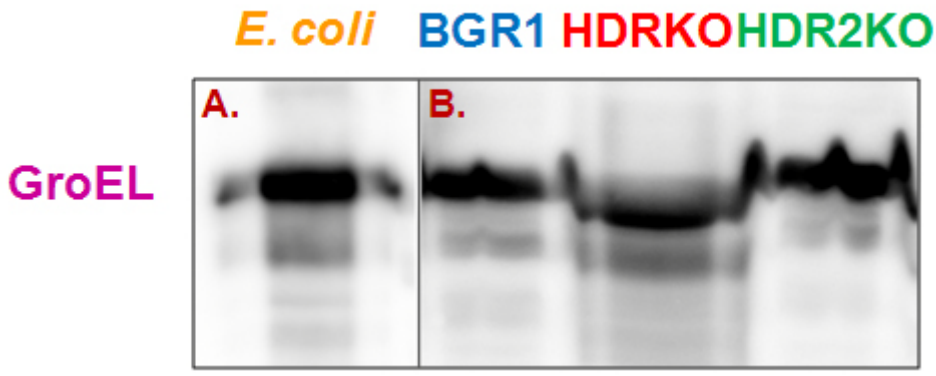

Figure 27. Western blot of cellular proteins with GroEL antibody.

The proteins, extracted from *B. glumae* at exponential phase, were separated by SDS-PAGE and was allowed to react with GroEL antibody.

A. *E. coli* GroEL .

B. *B. glumae* protein band near 57 kDa.

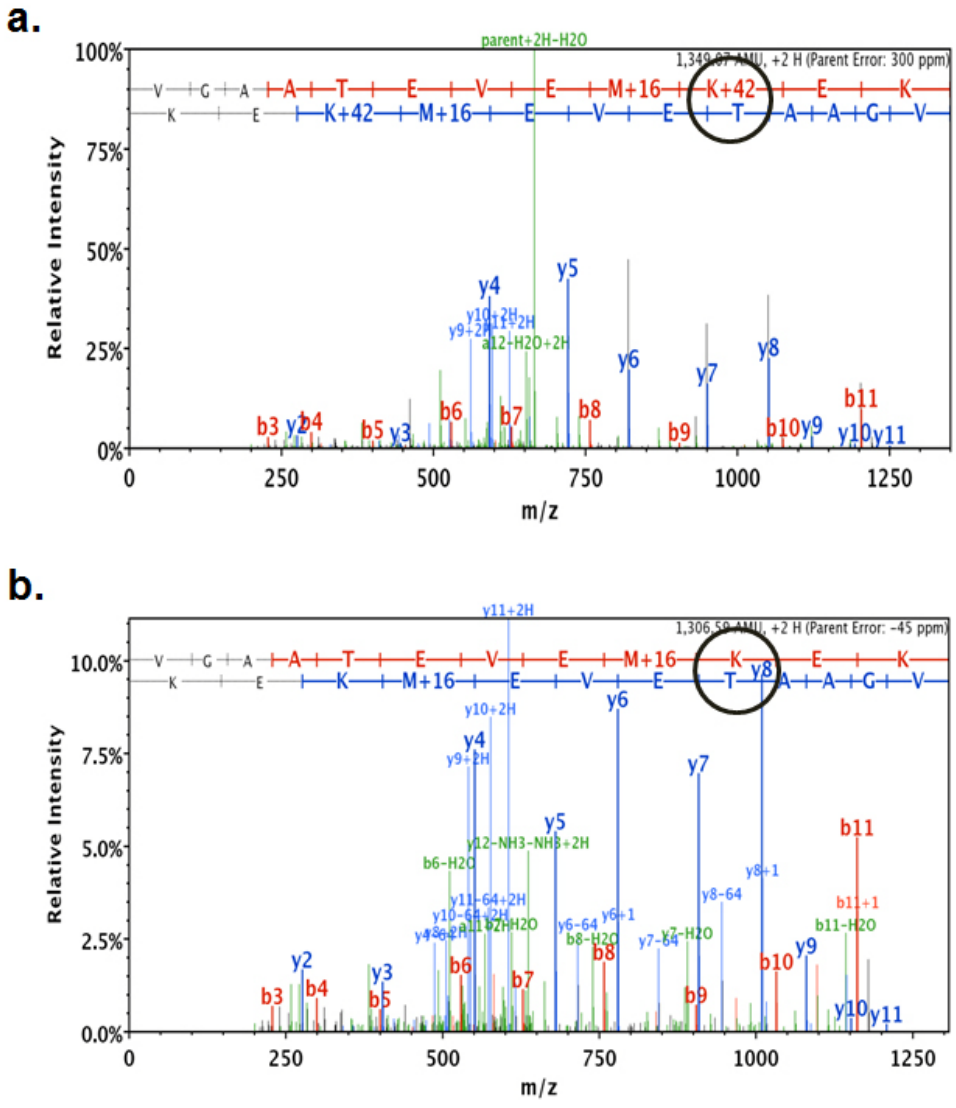
a.
parent+2H-H2O
1,349.97 AMU, +2 H (Parent Error: 300 ppm)
V G A A T E V E M+16 K+42 E K
K E K+42 M+16 E V E T A A G V
Relative Intensity
m/z
b.
y11+2H
1,306.59 AMU, +2 H (Parent Error: -45 ppm)
V G A A T E V E M+16 K E K
K E K M+16 E V E T y8 A A G V
Relative Intensity
m/z

Figure 28. Mass spectrum of 57 kDa-protein isolated from HDR1KO at exponential phase.

The decapetide fragment containing Lys390 (circled) is shown to be modified by acetylation as suggested by increase of m/z by 42 at Lys390.

a. HDR1KO GroEL. b. BGR1 GroEL.

9. Promoter switch experiment

The vector pLAFR6 was engineered to harbor 6 promoter::ORF combinations between 3 putative *hdr* promoters (1P: 300 bp upstream of *hdr1* translation starting point, 1Po: 576 bp upstream of *slp,* 2P: 327 bp upstream of *hdr2* translation starting point) and 2 *hdr* ORFs (1O and 2O for *hdr1* and *hdr2*, respectively) (Fig. 29). In practice, the putative operon promoter 1Po was used in tandem with *slp* to ensure polycistronic transcription of the operon. The vectors were transformed into HDR1KO, and then cellular proteins were analyzed by SDS PAGE. It became evident that the vector including putative *hdr1* operon promoter (1Po), regardless of identity of the *hdr* isogene, could only rescued the fast moving GroEL to wild type protein (Fig. 30). In other words, acetylated GroEL returned to deacetylated form upon complementation. The complementation experiment was further confirmed by hypersensitivity reaction (HR) test on tobacco leaf. HDR1KO that did not show HR became HR-active upon complementation with vector containing 1Po. However, *hdr2* promoter (2P) exerted little effect on HR (Fig. 31).

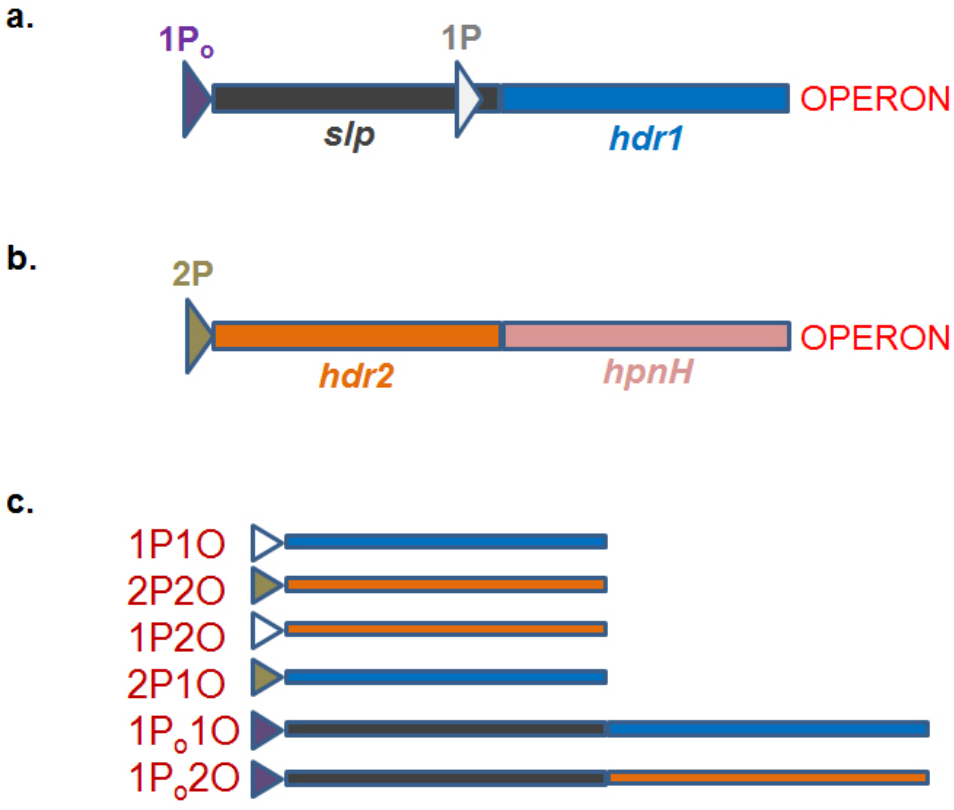
a.
1P$_o$
1P
slp
hdr1
OPERON
b.
2P
hdr2
hpnH
OPERON
c.
1P1O
2P2O
1P2O
2P1O
1P$_o$1O
1P$_o$2O

Figure 29. The construction of 6 vectors each harboring combination of *hdr* promoter and ORF.

a. Two putative promoters for *hdr1*.

b. Putative *hdr2* operon

c. Combination of promoters and *hdr*s cloned into pLAFR3. 1P1O, putative *hdr1* promoter and *hdr1* ORF; 2P2O, putative *hdr2* promoter and *hdr2* ORF; 1P2O, putative *hdr1* promoter and *hdr2* ORF; 2P1O, putative *hdr2* promoter and *hdr1* ORF; $1P_o1O$, putative *hdr1* operon promoter and *hdr1* operon; $1P_o2O$, putative *hdr1* operon promoter and *hdr2* operon.

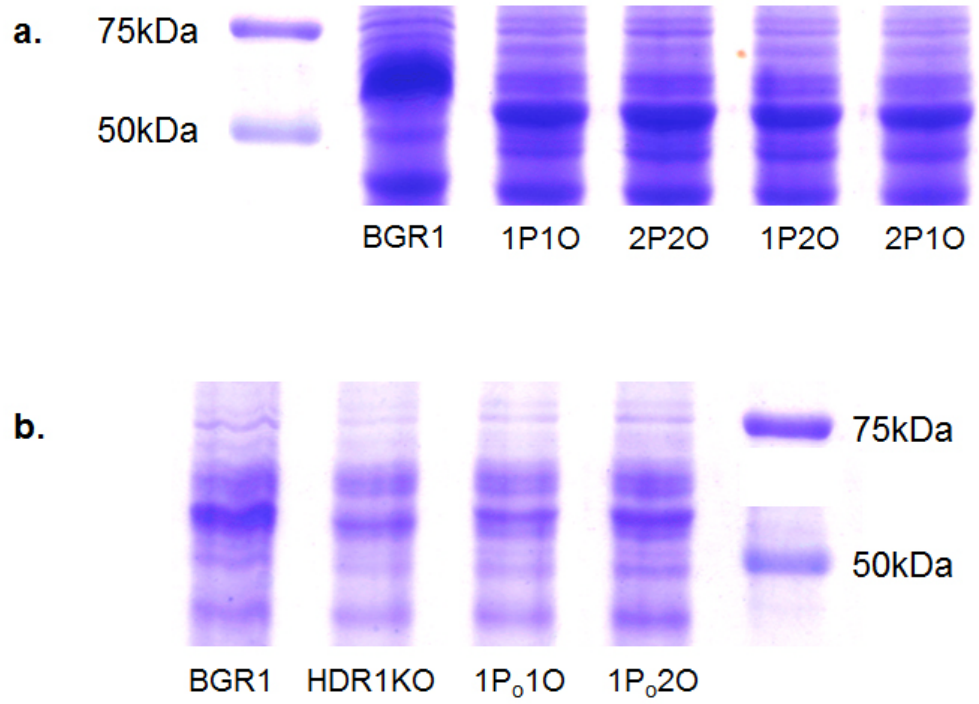

Figure 30. Electrophoretic mobility change of GroEL cuased by complementation of HDR1KO with 6 combinatorial vectors.

a. Complementation of DRR1KO with the promoter-*hdr* combination could not rescue the shifted GroEL mobility.

b. Combination of 1Po with either *hdr* could complement the HDR1KO in GroEL mobility.

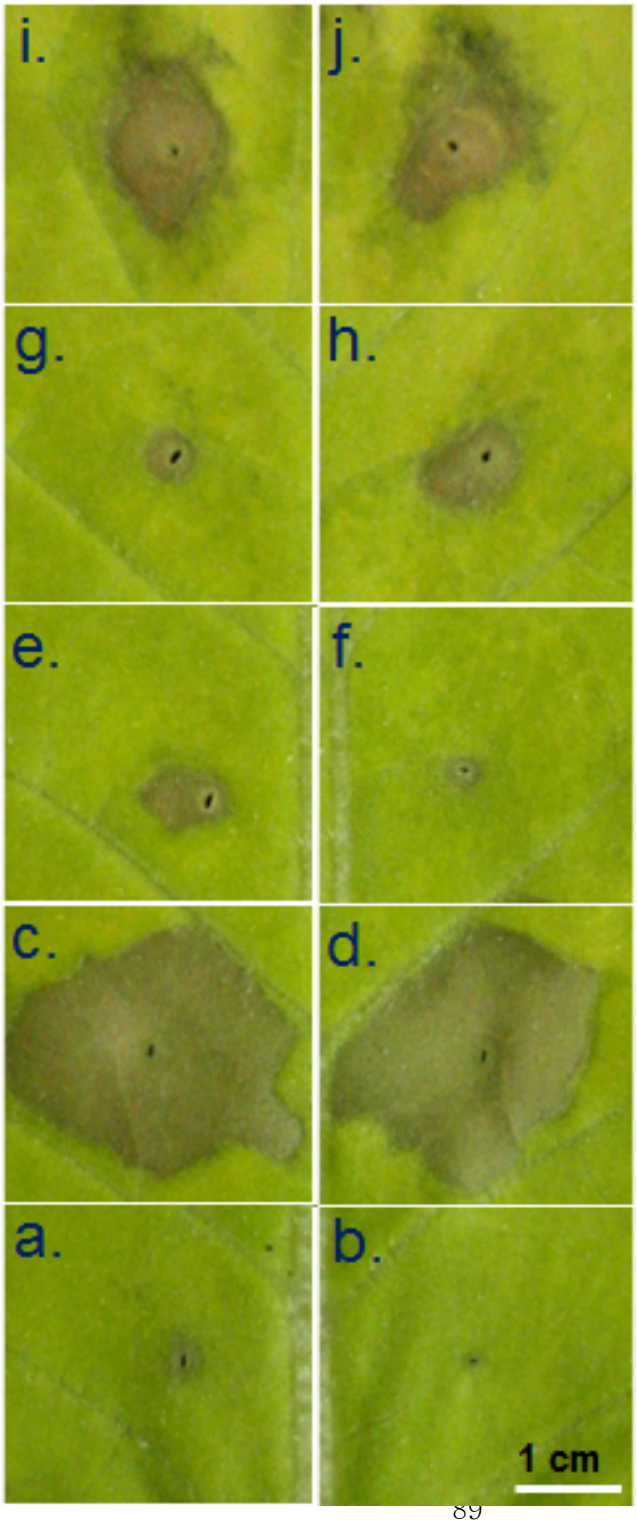
i.
j.
g.
h.
e.
f.
c.
d.
a.
b.
1 cm

Figure 31. Hypersesitivity reaction test after complementation of HDR1KO with 6 combinatorial vectors.

Complementation of HDR1KO with the *hdr* genes under the influence of 1Po could rescue the HR

a. HDR1KO; b. water; c. BGR1; d. HDR2KO; e. 1P1O; f. 1P2O; g. 2P1O; h. 2P2O; i. $1P_o1O$; j. $1P_o2O$

10. The seperated *hdr* isogene regulator and signal cascades.

To identify separate signal cascade respectively leading to transcription of *hdr1* and *hdr2* operon, the sequence of the putative promoter region of *hdr* isogenes were analyzed. In the putative promoter sequence of *hdr1*, there was no previously reported transcriptional factor-binding motif. However, in the putative *hdr2* promoter, 5 repeating ToxR binding sequences (T-N_{11}-A) were identified (Fig. 32). To determine whether ToxR binds to 131 bp-long putative *hdr2* promoter region, yeast-1-hybrid assay (Y1H) and Electrophoretic mobility shift assay (EMSA) were performed. The yeast harboring the vectors pHIS2HDR2-131 and pGADT7ToxR could survive, regardless concentration level of AT (3-amino-1,2,4-triazole, *his* gene inhibitor) (Fig. 33). Furthermore, recombinant ToxR was shown to bind to *hdr2* promoter in EMSA (Fig. 34). It was shown that the *hdr2* gene was down-regulated in the ToxR knock-out mutant than BGR1 by RT-qPCR (Fig. 35). Therefore, it was suggested that transcription of *hdr2* was regulated by ToxR independent of *hdr1*.

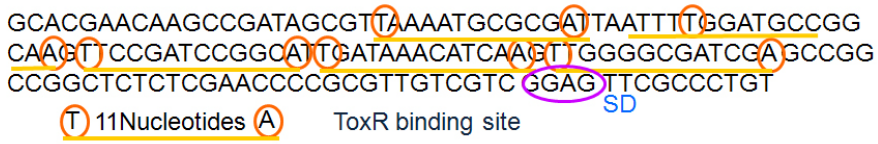

Figure 32. ToxR binding sites in putative *hdr2* operon promoter region.

The LysR-type regulator ToxR recognizes the specific T-N_{11}-A motif (underlined) and binds with that motif (Kim et al., 2009). The motif was repeated 5 times in the *hdr2* promoter. Nucleotides of GGAG in purple circle indicates is the ribosome binding site (SD = Shine-Dalgarno sequence). The promoter of *hdr1* did not have ToxR binding motif.

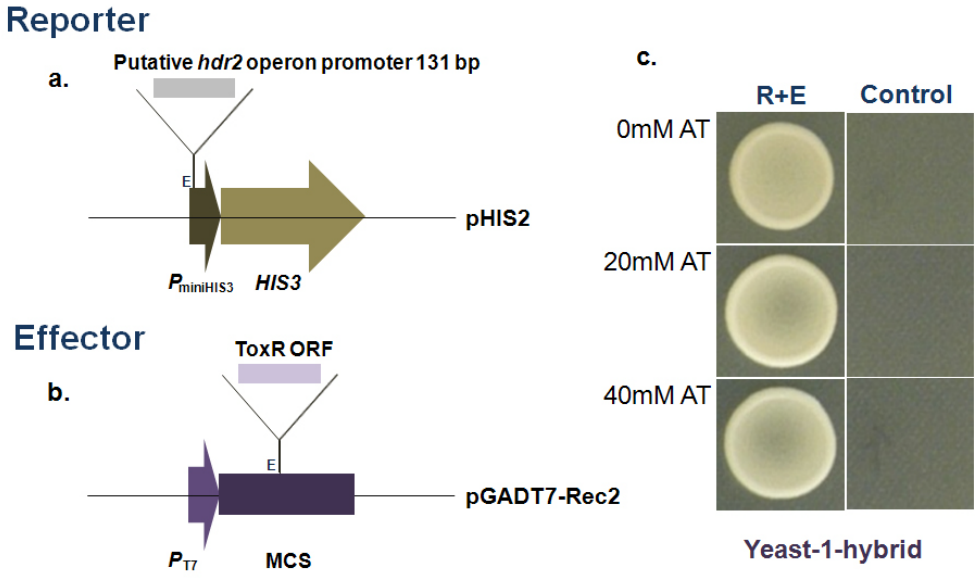

Figure 33. Yeast 1 hybrid assay.

a. The 329 bp-long putative *hdr2* promoter region was cloned into pHIS2 vector to construct pHISHDR2-131.

b. The ToxR ORF was cloned into pGAD7-Rec2 (pGADToxR).

c. The HIS3 inhibitor AT (3-amino-1,2,4-triazole) was added at 0, 20 and 40 mM. The yeast harboring both pHISHDR2-131 and pGADToxR could survive regardless of AT concentrations. The yeast only with pHISHDR2-131 or pGAD7-Rec2 could not survive without histidine.

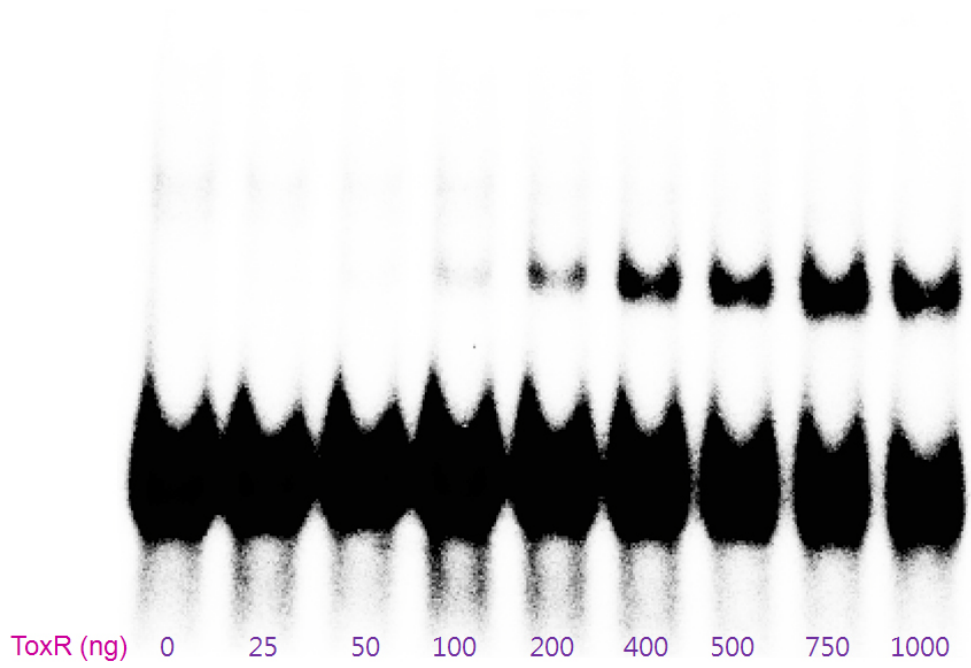

Figure 34. Electrophoretic mobility shift assay.

The recombinant ToxR protein was overexpressed by fusion protein with His_6 tag. The 131 bp putative *hdr2* promoter DNA was amplified by PCR and radio-labeled. The mixture of DNA and ToxR was separated on 5 % polyacrylamide gel by the electrophoresis and recorded on BAS-2010 (Fujifilm).

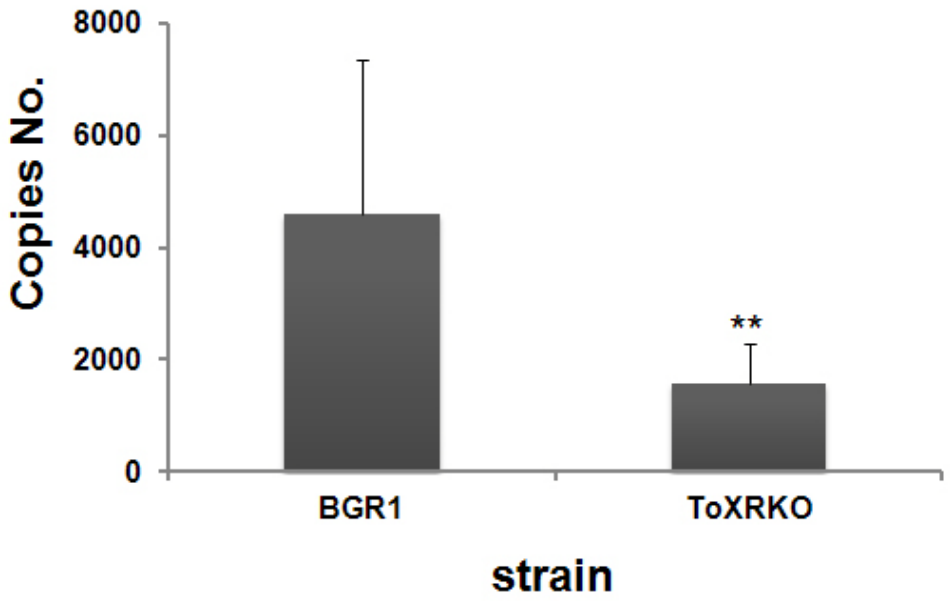

Figure 35. Transcript level of *hdr2* in BGR1 and ToxR knock-out mutant (TOXRKO).

The transcription of *hdr2* gene in ToxR knock-out mutant was down-regulated compared to that of BGR1 as shown by RT-qPCR analysis.

11. RNA sequencing analysis of *hdr* isogene mutants

To see consequence of *hdr* knock-out on a global scale, change in transcript distribution was assessed by Illumina sequencing. At first, genes associated with terpene biosynthesis were analyzed (Table 9). The significantly up-regulated gene was *cmk* in HDR1KO and down-regulated was squalene cyclase 2 (*sqc2*). However, in the HDR2KO, up-regulated genes were *cmk*, *hds*, undecaprenyl diphosphate synthase (*ups*) and undecaprenyl diphosphate phosphatase (*upp*), while *dxs2,* squalene synthase (*sqs*) 1 and 2, and *sqc2* were down-regulated. The most up-regulated gene in HDR1KO was *toxB, toxA* and *toxC* that constitute the toxoflavin biosynthesis operon. In the case of HDR2KO, *S*-adenosylmethionine decarboxylase proenzyme (*SAM-dcase*), stress response involved genes (superoxide dismutase, chaperonin Cpn10, cold-shock DNA-binding domain protein, co-chaperonin GroES, Heat shock protein and HSP20 family protein) and ribosomal genes (30S ribosomal protein S13, 50S ribosomal protein L36, L10, L32 and L34) were up-regulated (Table 10). The data suggested that toxoflavin biosynthesis-related genes were up-regulated in HDR1KO whereas stress associated and ribosomal proteins were upregulated transcribed in HDR2KO.

Table 9. Transcriptome analysis of the genes involved in terpene biosynthesis.

The color indicates the changes in expression level (red, 50~100 % increase; pale red, 25~50 % increase; white, -25~25 % increase; pale blue, 25~50 % decrease; blue, 50~100 % decrease). The RNA was cultured in M9 medium and extracted at exponential phase.

	BGR1	HDR1KO	HDR2KO	BGR1	HDR1KO	HDR2KO
DXS1	127.5616	136.3568	142.2936			
DXS2	75.81342	61.11541	32.24537			
DXR	178.414	143.5897	168.4546			
CMS	203.7422	199.0797	159.9799			
CMK	263.5041	416.7324	527.6976			
MCS	143.7831	131.2208	144.3782			
HDS	247.1115	300.578	560.2658			
HDR1	117.6529		118.2075			
HDR2	220.8763	269.9741				
GGPS,FPS	176.5485	207.3929	171.0901			
SQS1	128.5468	101.6812	67.85804			
SQS2	104.4671	74.06891	53.10258			
SQC1	85.04855	94.19989	62.5508			
SQC2	199.9091	120.779	127.3791			
UPS	156.4289	146.0094	252.806			
UPP	87.86908	103.8836	187.5408			

50~100% increase
25~50% increase
-25~25% increase
25~50% decrease
50~100% decrease

Table 10 The most up-regulated genes in *hdr* isogene mutants.

RNA was extracted at exponential phase.

HDR1KO

Gene	BGR1	HDR1KO	HDR2KO
ToxB	83.27378	4727.82	122.6149
ToxA	154.7964	2206.71	109.0899
ToxC	105.5687	1223.12	49.32788

HDR2KO

Gene	BGR1	HDR1KO	HDR2KO
hypothetical protein	213.9863	297.4899	2620.45
S-adenosylmethionine decarboxylase proenzyme	112.8782	132.589	1018.64
Superoxide dismutase	275.2781	449.9782	2278.33
Periplasmic binding protein/LacI transcriptional regulator	474.6757	312.0801	3685.2
Chaperonin Cpn10	163.8792	89.64414	1019.33
30S ribosomal protein S13	867.744	917.9687	4792.88
50S ribosomal protein L36	487.2402	639.8293	2608.7
translation initiation factor IF-1	846.1007	962.3885	4472.12
50S ribosomal protein L10	595.171	902.659	3122.03
50S ribosomal protein L32	6311.756	8183.38	30233.7
50S ribosomal protein L34	430.38	622.1788	1964.15
Cold-shock DNA-binding domain protein	6752.699	12188.15	30634.2
co-chaperonin GroES	994.7939	1148.068	4436.68
NADH:ubiquinone oxidoreductase, NADH-binding (51 kD) subunit	80.18455	108.6569	355.003
Heat shock protein, HSP20 family protein	202.6494	147.6234	858.291

12. Extracellular toxoflavin producticity

To confirm enhanced toxoflavin biosynthesis, toxoflavin production was semi-qunatitatively measured in *hdr* mutants and BGR1 by thin-layer chromatography (Fig. 36). The HDR1KO produced increased amounts of toxoflavin compared to the wild-type and HDR2KO. Fervenulin production was also increased in HDR1KO but not reumycin. The concentration of intracellular toxin was not changed (Fig. 36).

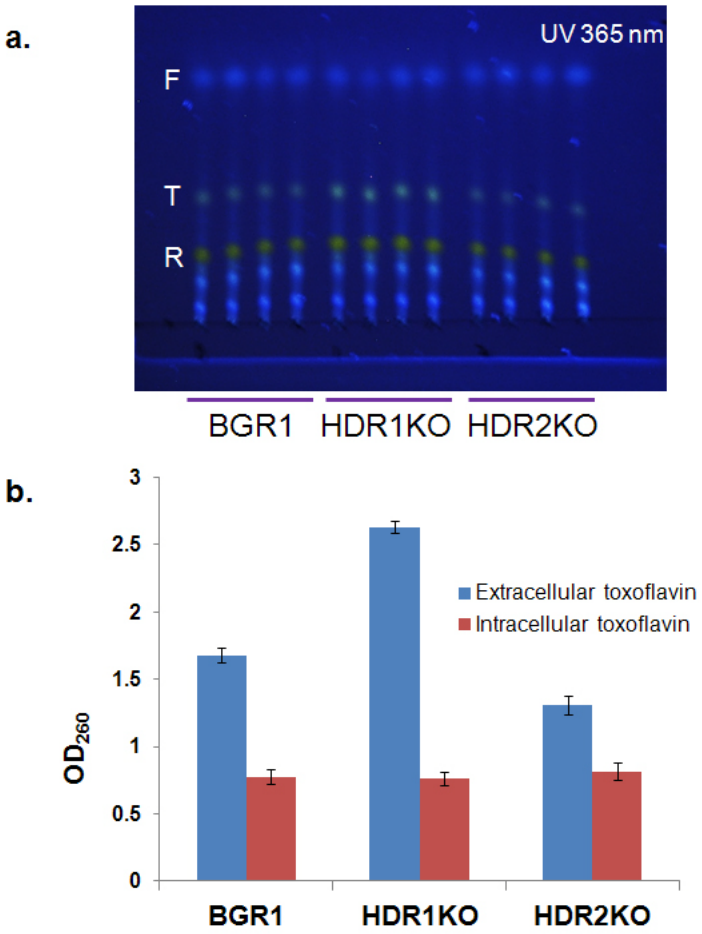

Figure 36. The production of toxoflavin in BGR1 and *hdr* isogene mutants.

The toxoflavin was extracted and separated after 24 h culture in LB medium.

a. TLC of extracted toxins The spots were visualized under the irradiation at 365 nm.

F, Fervenulin; T, Toxoflavin; R, Reumycin.

b. The toxoflavin contents measured at 260 nm.

DISCUSSION

Cartain bacterial genus, comprising free-living to host-specific species, has 2 *hdr* genes (Fig. 14). Despite genome size reduction occurred during evolution towards host-specific bacteria (Song et al., 2010), 2 *hdr* genes have been retained in the chromosome of *B. glumae*. Phylogenetic tree of bacterial two-gene Hdrs shows that there are three major Hdr clusters. For *Burkholderia*, two Hdrs are distributed in two different clades (Fig. 14). Interestingly, the interspecies homologies of Hdr sometimes are lower than that of intraspecies homologies.

Excluding 15 extra amino acid residues at the N-terminal position of BgHdr1, two BgHdrs bear only 56.1 % identities (Fig. 13). The phylogentic data and this low homology might imply that one of two *hdr* genes has been acquired by ancestral *Burkholderia* through horizontal gene transfer (Dutta et al., 2002).

Then why two Hdrs were retained during speciation of the genus Burkholderia. Do they have the same catalytic function? To understand the function of each Hdr, ORF of each *hdr* gene was isolated. The isolated genes complemented LytB (or Hdr) null *E. coli* mutant Therefore, both BgHdrs had identical catalytic function (Fig. 10, 11). *In vitro* enzyme assay also indicated that both Hdrs are catalytically active (Fig. 15). Interstingly, the ratio IPP to DMAPP was 2:1. This value is different from the ratio of other reported bacterial Hdr at 5:1 (Table 5). The finding that both Hdrs produced same IPP/DMAPP ratio defies the assumption that each isozyme would produce different ratio of IPP/DMAPP to cope with environmental and physiological need.

These facts connote the possibility that each isozyme has distinctive activity and function. We initially hypothesized that commonly observed 5-6:1 ratio of other bacterial species reflects natural "ideal" need towards these two isoprene precursors by the microorganisms, and each Hdr in *B. glumae* would produce products in varied ratio to meet the IPP:DMAPP ratio needed by shift of physiology to adapt in environment. The end product of MVA pathway is IPP, and it appears inevitable that any organism harboring this pathway should have isopentenyl diphosphate isomerase (Idi) to meet the need for DMAPP. However, *E. coli* is known to survive without Idi (Hahn et al., 1999). The 2.2:1 ratio could be justified if one assumes that the major intermediate of terpene biosythesis in *B. glumae* is farnesyl diphosphate (FPP), derived from one molecule of DMAPP and two molecules of IPP, as well as its dimeric derivative squalene, from which important bacterial membrane component hopanoids are synthesized (Rosenbaum et al., 1972, Daum et al., 2009). Slight excess of IPP at over 2:1 ratio could be used in minor metabolic flux such as further prenylation of FPP to form polyprenols (dolichols) that are essential cell wall synthesis starter (Ruize et al., 2008) and synthesis of quinone side chain. DMAPP alone could be used in reactions such as tRNA prenylation (Fig. 7).

Now, one can ask why *B. glumae* lacks Idi. The Idi enzyme could convert IPP into DMAPP favoring formation of DMAPP in various ratios of 1:2.2 to 1:13 (Ramos-Valdivia et al., 1997; Street et al., 1990; Rohdich et al., 2003). However, these values do not necessarily reflect *in vivo* IPP to DMAPP ratio. Feeding of radio-labeled CO_2 and glucose resulted in preferential labeling at IPP-derived moiety of

monoterpene in *Mentha piperita* (Jennewein et al., 2004). This could signify preexisting DMAPP pool. Idi would effectively replenish DMAPP pool from over-produced IPP. However, Hdrs were evolved to produce physiologically optimal ratio of IPP and DMAPP for *B. glumae* to survive without Idi. Then why do *E. coli* and *A. aeloicus* Hdrs produce 5-6:1 ratio of the products? One explanation is they have different demand for the precursors from *B. glumae*. To satisfactorily answer this question, we would have to wait until we gain more complete picture of terpene metabolism in eubacteria.

According to *in vitro* enzyme assay, BgHdr1 was not only more efficient enzyme but also had higher affinity towards the substrate than BgHdr2 (Table 4). The higher proportion of DMAPP compared to other Hdrs so far reported (Table 5) was possibly due to stronger interaction of the [4Fe-4S] cluster (Gräwert et al., 2010) with allylic C-2 of intermediate carbanion than with terminal methylene group. This led us to propose that BgHdr1 was evolved to cope with stringent environment where carbon source is limited, whereas BgHdr2 is designed to operate in the presence of reasonable supply of carbon source. Therefore, the presence of two Hdrs in *B. glumae* provides possible explanation for the adaptability of the bacterium in the environment. In contrast to that, raison d'être of multicopy Hdr in Ginkgo is to differentiate isoprene-related metabolic processes: housekeeping and the secondary metabolisms (Kim et al., 2008; Kang et al., 2012).

The function of both Hdr isozymes in *B. glumae* is identified through reverse genetics approach. First, *hdr* knock-out mutants were generated through tri-

parternal mating technique (data not shown). Growth of both Hdr knock-out mutants on LB medium seemed to show little difference from the growth of wild type BGR1 (Fig. 18), However, the growth of HDR1KO was retarded under the heat and pH shock compared to HDR2KO and BGR1 (Figs. 19, 20). In rice plants, the gap of growth rate was more significant and the pathogenecity was reduced (Figs. 22, 24, 25). To identify the cuase of the physiological defect in HDR1KO, the proteomics technique was used. One of the most significant changes was electrophoretic mobility change of GroEL (Hsp60s) (Figs. 26, 27), the charperonin that responses under the heat shock condition. Generally, protein folding is important to keep cellular function of protein maintained under adverse environment (Vabulas et al., 2010). Most small proteins, consisting about 70 % of total protein, spontaneously fold correctly (Anfinsen, 1973). In the folding of larger size proteins, about 20 % of total protein, helping instrument, i.e. chaperones DnaK (Hsp70) and DnaJ (Hsp40), are needed especially under stress and heat shock condition (Hartl, 1996). Chaperones assist corrected folding of misfolded proteins and prevent aggregation of proteins (Hayer-Hartl et al., 2006; Vabulas et al., 2010). The proteins that still evade intervention of DnaJ and Dnak are caged into GroEL chaperonin. When GroES binds with GroEL by consuming ATPs, the conformational change of GroEL could correctly fold inner caged polypeptides, leading prevention of proteins from misfolding (Kerner et al., 2005; Vabulas et al., 2010).

The increased electrophoretic mobility of HDR1KO compared to HDR2KO and

BGR1 suggested post-translational modification (Table 8). The protein band mobility shift was often due to phosphorylation, prenylation or acetylation. The LC MS/MS analysis of GroEL showed additional acetylation of lysine residue (Lys390) in GroEL protein (Fig. 28). There are several reports on bacterial acetylation and deacetylation system that regulates protein function. Acetylation and deacetylation of acetyl-CoA synthetase (AcsA) respectively leads to deactivation and activation of the enzyme in *Salmonella enterica* (Starai et al., 2004; Starai et al., 2005) and *Bacillus subtilis* (Grdner et al., 2006; Gardner et al., 2008). Since bacteria consumes 40 % of whole energy in ribosome function, bacteria under the energy limit must regulate gene expressions and enzyme functions at the time of need, especially in sudden response against stress (Slonczewski et al., 2009). In *E. coli*, GroEL is one of the acetylated heat shock-mediated proteins. Therefore, it is not suprizing that GroEL in *B. glumae* was acetaylated. Now the question is reduced as to why knock out of Hdr1 caused acetylation of GroEL while HDR2KO shows same phenotype as wild-type with less degree of acetylation. To paraphrase this, why each isogene has separated regulation although the enzymes encoded by the genes have the same catalytic function? There are two possible regulation points, one after translation and the other before transcription. The former explanation cannot stand because two Hdr isozymes catalyze same chemical reaction. Two *hdr* genes constitute separate operons consisted of different proteins, and the promoter of each operon was disctinctive from each other. To confirm regulation before gene transcription, the promoter switch experiment was performed (Fig. 29). If it is structural gene that is

more important than regulation, expression of either *hdr1* or *hdr2* would result in same phenotype. It was found that complementation of HDR1KO mutant with *hdr1* operon promoter linked to either tye of *hdr* rescued the phenotype mutant to result in restoration of GroEL protein mobility. The experiment clearly indicated that it is regulation of *hdr* expression but not the kind of Hdr protein that caused GroEL band shift in electrophoretic mobility (Fig. 30). The complementation was reconfirmed by HR in tobacco plant (Fig. 31). Therefore, it is possible that 2 isogenes had a different course of evolution. It is natural to think that *Burkholderia* originally had an operon consisted of *hdr* gene and hopanoid biosynthesizing gene. Hdr is an upstream enzyme in biosynthesis of triterpene hopanoid, an essential bacterial cell-membrane component (Welander et al., 2009). Later in the course of evolution, through horizontal gene transfer, *Burkholderia* acquired another *hdr* gene that somehow formed an operon with stress related genes. Because the lately acquired gene was able to function under substrate-limiting stress condition, the new gene was useful to expand its biological niche and became essential for a species such as *B. glumae*.

The ensuing question is the identity of signal cascade and transcriptional factor involved in activation of each *hdr* isogene. The *hdr2* operon promoter region possessed ToxR binding motif characterized by the sequence T-N11-A (Fig. 32). By EMSA and Y1H analysis (Fig. 33, 34), ToxR was shown to act as transcriptional factor of *hdr2* gene. It was further shown that ToxR knock-out mutant had the reduced *hdr2* mRNA level (Fig. 35).

Transcriptome analysis further revealed that knock out of *hdr* resulted in the altered terpene flux (Table 9). A kinase, *cmk*, in MEP pathway was up-regulated in both of HDRKOs. In the case of HDR2KO, only *hds*, one step upstream of *hdr*, was upregulated. At the same time, down-regulation of *sqs* and *sqc* that respectively make squalene and hopene, the precursors of hopanoids, was observed. Overall, when *hdr2* was knocked out, hopanoids biosynthetic genes were down-regulated while the MEP pathway genes were upregulated. One way to explain this observation is that the failure to transcribe *hdr2* operon resulted in accumulation of hopanoid precursors and feedback loop caused diminished biosynethesis of squalene and hopene. On the other hand, the diminished hopanoid level sends signal to MEP pathway to produce more hopanoid precursors by upregulating essential catalytic points such as *cmk* and *hds*. Another explanation is that the decreased terpene flux, due to knock-out of *hdr2* operon in HDR2KO, resulted in deficiency of FPP. Because FPP level became low, *sqs* and *sqc*, encoding the subsequent reaction enzymes, were down-regulated. At the same time, *hds* was up-regulated because the low level of hopanoids calls for more isoprenoids precursors. It is thus possible that *hds* was regulated under the same signal as *hdr2*. Decreased hopanoid level in cell membrane could make cell to strengthen cell wall as compensation by increasing expression of *ups* and *upp*, which are essential parts of cell wall biosynthesis (Fig. 37).

The genes tht experienced most dramatic transcription level change (Table 10) could help provide explanation for the *hdr* isogene regulation mechanisms. The tox

operon was up-regulated 10~56 folds in HDR1KO than BGR1 and HDR2KO. The amount of toxoflavin was actually increased 2-3 folds in HDR1KO as a result of activation of *tox* operon (Fig. 36). It is possible that mobilization of tox operon is a part of stress-overcoming mechanism, which was directly or indirectly disrupted by knock-out of *hdr1*.

The increased mRNA transcription message in HDR2KO was found among stress-mediated genes encoding ribosomal proteins, stress signal sensor (Bell et al., 1988; VanBogelen et al., 1990) and SAM-decarboxylation enzyme, whose product decarboxylated SAM was known as inhibitor of protein acetylation (Pegg et al., 1986). Up-regulation of SAM-decarboxylation enzyme would end up at accumulation of decarboxylated SAM that is GroEL acetylation inhibitor. As a result of inhibited acetylation of GroEL, GroEL remains in active form that is essential for overcoming the stress. Once the hopanoids biosynthesis declined, the bacterium becomes vulnerable to environmental stress. At this point, because HDR2KO have normal *hdr1* operon and signal cascades, stress-related mechanisms become active to overcome the stress by up-regulating stress-mediated genes (Fig. 37).

A mechanism to explain the observaed data is presented in Fig. 38. Despite both of 2 Hdr isozymes have identical catalytic function, reduction of HMBPP to IPP and DMAPP, each isogene encoding Hdr was transcribed as a separate operon and regulated by independent signal. The *hdr1* operon contained stress-related genes and disruption of this operon resulted in GroEL inactivation by acetylation, which

partly explains sensitivity of HDR1KO towards environmental stress. Nevertheless, the exact function of each *hdr* is not clear not only in the biosynthesis of hopanoids but also in the stress mechanism. Here two possibilities are presented. One is that isoprenylation of certain small molecule make the molecule active in a signal cascade. In fact, terpenoids and prenlyated peptide is known to be used as signal molecules. In *Candida*, farnesoic acids transmittes quorum sensing signal (Oh et al., 2001). It is possible that certain terpene can be used as stress-associated signal molecule in *B .glumae*. In Gram-positive bacteria, prenylated peptide is used as pheromones (Ansaldi et al., 2002). Moreover, a gene associated with protein prenylation is found in *B. glumae* (bglu_1g09110). Therefore, *hdr1* gene could provide material for small molecule prenylation. The other possibility is that certain isoprenoid itself might be synthesized as stress-defense molecule. ME-cPP, a MEP pathway intermediate, accumulates under the stress condition and signals carotenoids pigmentation of corybacteria (Ostrovsky et al., 1998). The caretenoids is stress-defense molecules. Therefore, stress signal might regulate *hdr1* operon for accumulation of stress-bearing molecule in adition to inducing GroEL activation.

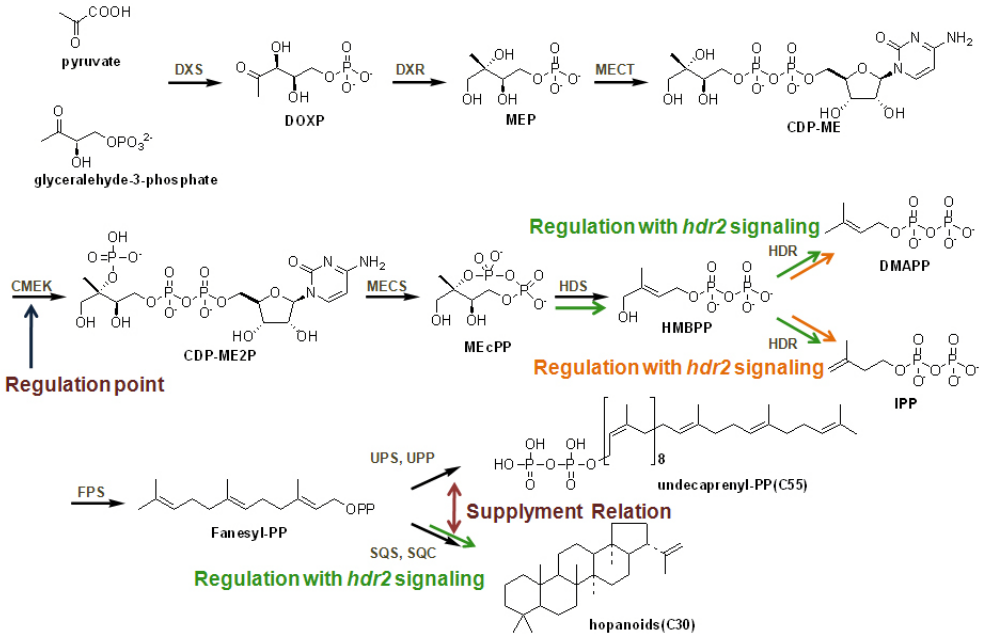

Figure 37. The proposed regulation signals in MEP pathway.

The Cmk was shown to be a whole regulation point of MEP pathway in *B. glumae*, because transcription of *cmk* in both *hdr* isogene mutants was up-regulated.

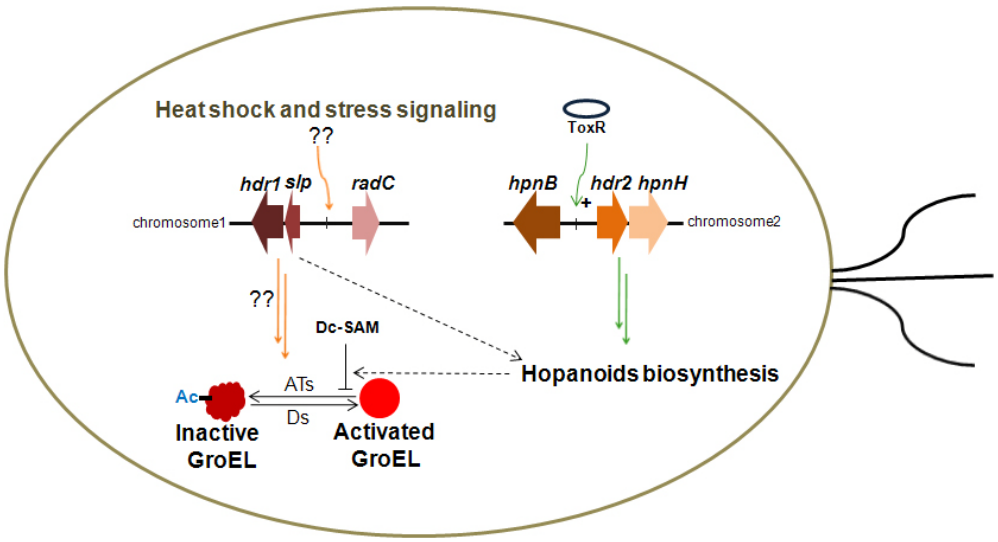

Figure 38. The proposed mechanisms of Hdr isozyme regulation.

REFERENCES

Adam P, Hecht S, Eisenreich W, Kaiser J, Gräwert T, Arigoni D, Bacher A, Rohdich F (2002) Biosynthesis of terpenes: studies on 1-hydroxy-2-methyl-2-(E)-butenyl 4-diphosphate reductase. *Proc Natl Acad Sci USA*, **99**, 12108-12113.

Altincicek B, Duin EC, Reichenberg A, Hedderich R, Kollas AK, Hintz M, Wagner S, Wiesner J, Beck E, Jomaa H (2002) LytB protein catalyzes the terminal step of the 2-c-methyl-d-erythritol-4-phosphate pathway of isoprenoid biosynthesis. *FEBS Lett*, **532**, 437-440.

Anfinsen CB (1973) Principles that govern the folding of protein chains. *Science*, **181**, 223-230.

Ansaldi M, Marolt D, Stebe T, Mandic-Mulec I, Dubnau D (2002) Specific activation of the *Bacillus* quorum-sensing systems by isoprenylated pheromone variants. *Mol Microbiol*, **44**, 1561-1573.

Araki N, Kusumi K, Masamoto K, Iba K (2000) Temperaturesensitive arabidopsis mutant defective in 1-deoxy-D-xylulose 5-phosphate synthase within the plastid non-mevalonate pathway ofisoprenoid biosynthesis. *Physiologia Plantarum*, **108**, 19–24.

Bell J, Neilson L, Pellegrini M (1988) Effect of heat shock on ribosome synthesis in *Drosophila melanogaster*. *Mol Cell Biol*, **8**, 91-95.

Briskin DP (2000) Medicinal plants and phytomedicines. Linking plant biochemistry and physiology to human health. *Plant Physiol*, **124**, 507-514.

Bhattacharya D, Archibald JM, Weber AP, Reyes-Prieto A (2007) How do endosymbionts become organelles? Understanding early events in plastid evolution. *Bioessays*, **29**, 1239-1246.

Bradford MM (1976) A rapid and sensitive method for the quantitation of microgram quantities of protein utilizing the principle of protein-dye binding. *Anal Biochem*, **72**, 248-254.

Chang HC, Tang YC, Hayer-Hartl M, Hartl FU (2007) Snap Shot: molecular Shot: Molecular chaperones, Part I. *Cell*, **128**, 212.

Chappell J (1995) The Biochemistry and Molecular Biology of Isoprenoid Metabolism. *Plant Physiol*, **107**, 1-6.

Christianson DW (2008) Unearthing the roots of the terpenome. *Curr Opin Chem*

Biol, **12**, 141-150.

Cordoba E, Salmi M, León P (2009) Unravelling the regulatory mechanisms that modulate the MEP pathway in higher plants. *J Exp Bot*, **60**, 2933-2943.

Cottyn B, Cerez MT, Van Outryve MF, Barroga J, Swings J, and Mew TW (1996) Bacterial diseases of rice. I. Pathogenic bacteria associated with sheath rot complex and grain discoloration of rice in the Philippines. *Plant Dis*, **80**, 429–437.

Cunningham FX Jr, Lafond TP, and Gantt E (2000) Evidence of a role for *lytb* in the nonmevalonate pathway of isoprenoid biosynthesis. *J Bacteriol*, **182**, 5841-8.

Daum M, Herrmann S, Wilkinson B, and Bechthold A (2009) Genes and enzymes involved in bacterial isoprenoid biosynthesis. *Curr Opin Chem Biol*, **13**, 180-188.

Disch A, Schwender J, Müller C, Lichtenthaler HK, Rohmer M (1998) Distribution of the mevalonate and glyceraldehyde phosphate/pyruvate pathways for isoprenoid biosynthesis in unicellular algae and the *cyanobacterium Synechocystis* PCC 6714. *Biochem J*, **333**, 381-388.

Durr IF, Shwayri AN (1964) Metabolism of mevalonic acid by *lactobacillus*

plantarum. *J Bacteriol*, **88**, 361-366.

Dutta C, and Pan A (2002) Horizontal gene transfer and bacterial diversity. *J Biosci*, **27**, 27-33.

Eisenreich W, Bacher A, Arigoni D, Rohdich F (2004) Biosynthesis of isoprenoids via the non-mevalonate pathway. *Cell Mol Life Sci*, **61**, 1401-1426.

Flagel LE, Wendel JF (2009) Gene duplication and evolutionary novelty in plants. *New Phytol*, 183, 557-564.

Flesch G, Rohmer M (1988) Prokaryotic hopanoids: the biosynthesis of the bacteriohopane skeleton. Formation of isoprenic units from two distinct acetate pools and a novel type of carbon/carbon linkage between a triterpene and D-ribose. *Eur J Biochem*, **175**, 405-411.

FraenkeL GS (1959) The raison dêtre of s econdary plant substances; these odd chemicals arose as a means of protecting plants from insects and now guide insects to food. *Science*, **129**, 1466-1470.

Gardner JG, Escalante-Semerena JC (2008) Biochemical and mutational analyses of AcuA, the acetyltransferase enzyme that controls the activity of the acetyl

coenzyme a synthetase (AcsA) in *Bacillus subtilis*. *J Bacteriol*, **190**, 5132-5136.

Gardner JG, Grundy FJ, Henkin TM, Escalante-Semerena JC (2006) Control of acetyl-coenzyme A synthetase (AcsA) activity by acetylation/deacetylation without NAD(+) involvement in *Bacillus subtilis*. *J Bacteriol*, **188**, 5460-5468.

Gophna U, Thompson JR, Boucher Y, Doolittle WF (2006) Complex histories of genes encoding 3-hydroxy-3-methylglutaryl-CoenzymeA reductase. Mol Biol Evol **23**, 168-178.

Goodwin TW (1958) Studies in carotenogenesis 25. The incorporation of 14CO2, [2-14C] acetate and [2-14C]mevalonate into beta-carotene by illuminated etiolated maize seedings. *Biochem J*, **70**, 612-617.

Gould SB, Waller RF, McFadden GI (2008) Plastid evolution. Annu *Rev Plant Biol*, **59**, 491-517.

Grochowski LL, Xu H, White RH (2006) *Methanocaldococcus jannaschii* uses a modified mevalonate pathway for biosynthesis of isopentenyl diphosphate. *J Bacteriol*, **188**, 3192-3198.

Grunstein M (1997) Histone acetylation in chromatin structure and transcription.

Nature, **389**, 349-352.

Gräwert T, Kaiser J, Zepeck F, Laupitz R, Hecht S, Amslinger S, Schramek N, Schleicher E, Weber S, Haslbeck M, Buchner J, Rieder C, Arigoni D, Bacher A, Eisenreich W, Rohdich F (2004) IspH protein of *Escherichia coli*: studies on iron-sulfur cluster implementation and catalysis. *J Am Chem Soc*, **126**, 12847-12855.

Gräwert T, Rohdich F, Span I, Bacher A, Eisenreich W, Eppinger J, Groll M (2009) Structure of active IspH enzyme from *Escherichia coli* provides mechanistic insights into substrate reduction. *Angew Chem Int Ed Engl*, **48**, 5756-5759.

Gräwert T, Span I, Eisenreich W, Rohdich F, Eppinger J, Bacher, Groll M (2010) Probing the reaction mechanism of IspH protein by X-ray structure analysis. *Proc Natl Acad Sci USA*, **107**, 1077-1081.

Gräwert T, Groll M, Rohdich F, Bacher A, and Eisenreich W (2011) Biochemistry of the non-mevalonate isoprenoid pathway. *Cell Mol Life Sci*, **68**, 3797-3814.

Hahn FM, Hurlburt AP, and Poulter CD (1999) *Escherichia coli* open reading frame 696 is *idi*, a nonessential gene encoding isopentenyl diphosphate isomerase. *J Bacteriol*, **181**, 4499-4504.

Ham JH, Melanson RA, and Rush MC (2011) *Burkholderia glumae*: next major pathogen of rice? *Mol Plant Pathol*, **12**, 329-339.

Hartl FU (1996) Molecular chaperones in cellular protein folding. *Nature*, **13**, 571-579.

Hayer-Hartl M, Minton AP (2006) A simple semiempirical model for the effect of molecular confinement upon the rate of protein folding. *Biochemistry*, **45**, 133356-13360.

Hayden HS, Lim R, Brittnacher MJ, Sims EH, Ramage ER, Fong C, Wu Z, Crist E, Chang J, Zhou Y, Radey M, Rohmer L, Haugen E, Gillett W, Wuthiekanun V, Peacock SJ, Kaul R, Miller SI, Manoil C, Jacobs MA (2012) Evolution of *Burkholderia pseudomallei* in recurrent melioidosis. *PLoS One*, **7**, e36507.

Hemmerlin A, Gerber E, Feldtrauer JF, Wentzinger L, Hartmann MA, Tritsch D, Hoeffler JF, Rohmer M, Bach TJ (2004) A review of tobacco BY-2 cells as an excellent system to study the synthesis and function of sterols and other isoprenoids. *Lipids*, **39**, 723-735.

Hemmerlin A, Harwood JL, Bach TJ (2012) A raison d'être for two distinct pathways in the early steps of plant isoprenoid biosynthesis? *Prog Lipid Res*, **51**, 95-148

Hintz M, Reichenberg A, Altincicek B, Bahr U, Gschwind RM, Kollas AK, Beck E, Wiesner J, Eberl M, Jomaa H (2001) Identification of (E)-4-hydroxy-3-methyl-but-2-enyl pyrophosphate as a major activator for human gammadelta T cells *in Escherichia coli*. *FEBS Lett*, **509**, 317-322.

Hunter WN (2007) The Non-mevalonate pathway of isoprenoid precursor biosynthesis. *J Biol Chem*, **282**, 21573-21577.

Iannuzzi C, Adinolfi S, Howes BD, Garcia-Serres R, Clémancey M, Latour JM, Smulevich G, Pastore A. (2011) The role of CyaY in iron sulfur cluster assembly on the *E. coli* IscU scaffold protein. *PLoS One*, **6**, e21992.

Jacobsen W, Kirchner G, Hallensleben K, Mancinelli L, Deters M, Hackbarth I, Benet LZ, Sewing KF, Christians U (1999) Comparison of cytochrome P-450-dependent metabolism and drug interactions of the 3-hydroxy-3-methylglutaryl-CoA reductase inhibitors lovastatin and pravastatin in the liver. *Drug Metab Dispos*, **27**, 173-179.

Jennewein S, Wildung MR, Chau M, Walker K, and Croteau R (2004) Random sequencing of an induced *Taxus* cell cDNA library for identification of clones involved in Taxol biosynthesis. *Proc Nat. Acad Sci USA*, **101**, 9149-9154.

Jung KH, Lee J, Dardick C, Seo YS, Cao P, Canlas P, Phetsom J, Xu X, Ouyang S, An K, Cho YJ, Lee GC, Lee Y, An G, Ronald PC (2008) Identification and functional analysis of light-responsive unique genes and gene family members in rice. *PloS Genet*, **4**, e1000164.

Kang MK, Nargis S, Kim SM, and Kim SU (2012) Distinct expression patterns of two *Ginkgo biloba* 1-hydroxy-2-methyl-2-(*E*)-butenyl-4-diphosphate reductase/isopentenyl diphospahte synthase (Hdr/IDS) promoters in Arabidopsis model. *Plant Physiol Biochem,* **62**, 47-53.

Keasling JD (2012) Synthetic biology and the development of tools for metabolic engineering. *Metab Eng*, **14**, 189-195.

Kellogg BA, Poulter CD (1997) Chain elongation in the isoprenoid biosynthetic pathway. *Curr Opin Chem Biol*, **1**, 570-578.

Kennedy MC, Kent TA, Emptage M, Merkle H, Beinert H, and Münck E (1984) evidence for the formation of a linear [3Fe-4S] cluster in partially unfolded

aconitase. *J Biol Chem*, **259**, 14463-14471.

Kerner MJ, Naylor DJ, Ishihama Y, Maier T, Chang HC, Stines AP, Georgopoulos C, Frishman D, Hayer-Hartl M, Mann M, Hartl FU (2005) Proteome-wide analysis of chaperonin-dependent protein folding in *Escherichia coli*. *Cell*, **122**, 209-220.

Kobayashi K, Suzuki M, Tang J, Nagata N, Ohyama K, Seki H, Kiuchi R, Kaneko Y, Nakazawa M, Matsui M, Matsumoto S, Yoshida S, Muranaka T (2007) Lovastatin insensitive 1, a Novel pentatricopeptide repeat protein, is a potential regulatory factor of isoprenoid biosynthesis in Arabidopsis. *Plant Cell Physiol*, **48**, 322-31

Kim BR, Kim SU, Chang YJ (2005) Differential expression of three 1-deoxy-D-xylulose-5-phosphate synthase genes in rice. *Biotechnol Lett*, **27**, 997–1001.

Kim J, Kim JG, Kang Y, Jang JY, Jog GJ, Lim JY, Kim S, Suga H, Nagamatsu T, Hwang I (2004) Quorum sensing and the LysR-type transcriptional activator ToxR regulate toxoflavin biosynthesis and transport in *Burkholderia glumae*. *Mol Microbiol*, **54**, 921-934.

Kim J, Oh J, Choi O, Kang Y, Kim H, Goo E, Ma J, Nagamatsu T, Moon JS,

Hwang I (2009) Biochemical evidence for ToxR and ToxJ binding to the *tox* operons of *Burkholderia glumae* and mutational analysis of ToxR. *J Bacteriol*, **191**, 4870-4878.

Kim SM, Kuzuyama T, Chang YJ, Song KS, Kim SU (2006) Identification of class 2 1-deoxy-D-xylulose 5-phosphate synthase and 1-deoxy-D-xylulose 5-phosphate reductoisomerase genes from *Ginkgo biloba* and their transcription in embryo culture with respect to ginkgolide biosynthesis. *Planta Med*, **72**, 234-240.

Kim SM, Kim YB, Kuzuyama T, Kim SU (2008a) Two copies of 4-(cytidine 50-diphospho)-2-C-methyl-D-erythritol kinase (CMK) gene in *Ginkgo biloba*: molecular cloning and functional characterization. *Planta*, **228**, 941–950.

Kim SM, Kuzuyama T, Kobayashi A, Sando T, Chang YJ, and Kim SU (2008b) 1-Hydroxy-2-methyl-2-(E)-butenyl 4-diphosphate reductase (IDS) is encoded by multicopy genes in gymnosperms *Ginkgo biloba* and *Pinus taeda*. *Planta*, **227**, 287-298.

Kim YB, Kim SM, Kang MK, Kuzuyama T, Lee JK, Park SC, Shin SC and Kim SU. (2009) Regulation of resin acid synthesis in Pinus densiflora by differential transcription of genes encoding multiple 1-deoxy-D-xylulose 5-phosphate synthase and 1-hydroxy-2-methyl-2-(E)-butenyl 4-diphosphate reductase

genes. *Tree Physiology*, 29, 737–749.

Kirby J, and Keasling JD (2009) Biosynthesis of plant isoprenoids: Perspectives for microbial engineering. *Annu rev plant biol*, **60,** 335-355.

Kuzuyama T, Seto H (2003) Diversity of the biosynthesis of the isoprene units. *Nat Prod Rep*, **20**, 171-183.

Lange BM, Rujan T, Martin W, and Croteau R (2000) Isoprenoid biosynthesis: The evolution of two ancient and distinct pathways across genomes. *Proc Natl Acad Sci USA*, **97**, 13172–13177.

Learned RM, Connolly EL (1997) Light modulates the spatial patterns of 3-hydroxy-3-methylglutaryl coenzyme A reductase gene expression in *arabidopsis thaliana*. *Plant J*, **11**, 499-511.

Lee JK (2006) Molecular characterization of two isopentenyl diphosphate / dimethylallyl synthases (IDS) from *Burkholderia glumae*. Master's thesis, Seoul National University.

Lim J, Lee TH, Nahm BH, Choi YD, Kim M, Hwang I (2009) Complete genome sequence of *Burkholderia glumae* BGR1. *J.Bacteriol*, **191**, 3758-3759.

Lohr M, Im CS and Grossman AR (2005) Genome-Based Examination of Chlorophyll and Carotenoid Biosynthesis in *Chlamydomonas reinhardtii*. *Plant Physiol*, **138**, 490-515.

López-Juez E (2007) Plastid biogenesis, between light and shadows. *J Exp Bot*, **58**, 11-26.

Maldonado-Mendoza IE, Vincent RM, Nessler CL (1997) Molecular characterization of three differentially expressed members of the *Camptotheca acuminata* 3-hydroxy-3-methylglutaryl CoA reductase (HMGR) gene family. *Plant Mol Biol*, **34**, 781-790.

Mandel MA, Feldmann KA, Herrera-Estrella L, Rocha-Sosa M, Leo´n P (1996) CLA1, a novel gene required for chloroplast development, is highly conserved in evolution. *Plant J*, **9**, 649–658.

Merret R, Cirioni J, Bach TJ, Hemmerlin A (2007) A serine involved in actin-dependent subcellular localization of a stress-induced tobacco BY-2 hydroxymethylglutaryl-CoA reductase isoform. *FEBS Lett*, **581**, 5295-5299.

Modi VV, Patwa DK (1961) Occurrence of mevalonic acid in carrots. *Nature*, **191**,

1202.

Odom AR (2011) Five questions about non-mevalonate isoprenoid biosynthesis. *PLoS Pathog*, **7**, e100232.

Oh KB, Miyazawa H, Naito T, Matsuoka H (2001) Purification and characterization of an autoregulatory substance capable of regulating the morphological transition in *Candida albicans*. *Proc Natl Acad Sci USA*, **98**, 4664-4668.

Ohyama K, Suzuki M, Masuda K, Yoshida S, Muranaka T (2007) Chemical phenotypes of the hmg1 and hmg2 mutants of Arabidopsis demonstrate the in-planta role of HMG-CoA reductase in triterpene biosynthesis. *Chem Pharm Bull*, **55**, 1518-1521.

Oldfield E, and Lin FY (2012) Terpene biosynthesis: Modularity rules. *Angew Chem Int Ed Engl*, **51**, 1124-1137.

Ostrovsky D, Diomina G, Lysak E, Matveeva E, Ogrel O, Trutko S (1998) Effect of oxidative stress on the biosynthesis of 2-C-methyl-D-erythritol-2,4-cyclopyrophosphate and isoprenoids by several bacterial strains. *Arch Microbiol*, **171**, 69-72.

Pegg AE, Wechter RS, Clark RS, Wiest L, Erwin BG (1986) Acetylation of decarboxylated S-adenosylmethionine by mammalian cells. *Biochemistry*, **28**, 379-384.

Phillips MA, D'Auria JC, Gershenzon J, Pichersky E (2008a) The Arabidopsis thaliana type I Isopentenyl Diphosphate Isomerases are targeted to multiple subcellular compartments and have overlapping functions in isoprenoid biosynthesis. *Plant Cell*, **20**, 677-696.

Phillips MA, Leo´ n P, Boronat A, Rodrı´guez-Concepcio´n M (2008b) The plastidial MEP pathway: unified nomenclature and resources. *Trends Plant Sci*, **13**, 619–623.

Phillips MA, Walter MH, Ralph SG, Dabrowska P, Luck K, Urós EM, Boland W, Strack D, Rodríguez-Concepción M, Bohlmann J, Gershenzon J (2007) Functional identification and differential expression of 1-deoxy-D-xylulose 5-phosphate synthase in induced terpenoid resin formation of Norway spruce (*Picea abies*). *Plant Mol Biol*, **65**, 243–257.

Penuelas J, Llusia J, Estiarte M (1995) Terpenoids: a plant language. *Trends Ecol Evol*, **10**, 289.

Pichersky E, Gang DR (2000) Genetics and biochemistry of secondary metabolites in plants: an evolutionary perspective. *Trends Plant Sci*, **5**, 439-445.

Puan KJ, Wang H, Dairi T, Kuzuyama T, Morita CT (2005) *fldA* is an essential gene required in the 2-C-methyl-D-erythritol 4-phosphate pathway for isoprenoid biosynthesis. *FEBS Lett*, **579**, 3802-3806.

Rodríguez-Concepción M (2004) The MEP pathway: A new target for the development of herbicides, antibiotics and antimalarial drugs. *Curr Pharm Design*, **10**, 2391-2400.

Ramos-Valdivia AC, Van der Heijden R, and Verpoorte R (1997) Isopentenyl diphosphate isomerase: A core enzyme in isoprenoid biosynthesis. A review of its biochemistry and function. *Nat Prod Rep*, **14**, 591-603.

Rohdich F, Hecht S, Gartner K, Adam P, Krieger C, Amslinger S, Arigoni D, Bacher A, Eisenreich W (2002) Studies on the non-mevalonate terpene biosynthetic pathway: Metabolic role of IspH (LytB) protein. *Proc Natl Acad Sci USA*, **99**, 1158-1163.

Rohdich F, Zepeck F, Adam P, Hecht S, Kaiser J, Laupitz R, Gräwert T,

Amslinger S, Eisenreich W, Bacher A Arigoni D (2003) The deoxyxylulose phosphate pathway of isoprenoid biosynthesis: Studies on the mechanisms of the reactions catalyzed by IspG and IspH protein. *Proc Natl Acad Sci USA*, **100**, 1586-1591.

Rohmer M (1999) The discovery of a mevalonate-independent pathway for isoprenoid biosynthesis in bacteria, algae and higher plants. *Nat Prod Rep*, **16**, 565-574.

Rohmer M, Grosdemange-Billiard C, Seemann M, Tritsch D (2004) Isoprenoid biosynthesis as a novel target for antibacterial and antiparasitic drugs. *Curr Opin Investig Drugs*, **5**, 154-162.

Rohmer M, Knani M, Simonin P, Sutter B, Sahm H (1993) Isoprenoid biosynthesis in bacteria: a novel pathway for the early steps leading to isopentenyl diphosphate. *Biochem J*, **295**, 517-524.

Rosenbaum N, and Gefter ML (1972) Δ^2-Isopentenylpyrophosphate: Transfer ribonucleic acid Δ^2-isopentenyltransferase from *Escherichia coli*. *J Biol Chem*, **247**, 5675-5680.

Ruiz N (2008) Bioinformatics identification of MurJ (MviN) as the peptidoglycan

lipid II flippase in *Escherichia coli*. *Proc Natl Acad Sci USA*, **105**, 15553-15557.

Sacchettini JC, Poulter CD (1997) Creating isoprenoid diversity. *Science*, **277**, 1788-1789.

Sancho J (2006) Flavodoxins: sequence, folding, binding, function and beyond. *Cell Mol Life Sci*, **63**, 855-864.

Sando T, Takeno S, Watanabe N, Okumoto H, Kuzuyama T, Yamashita A, Hattori M, Ogasawara N, Fukusaki E, Kobayashi A (2008) Cloning and characterization of the 2-C-methyl-D-erythritol 4-phosphate (MEP) pathway genes of a natural-rubber producing plant, *Hevea brasiliensis*. *Biosci Biotechnol Biochem*, **72**, 2903-2917.

Seetang-Nun Y, Sharkey TD, Suvachittanont W (2008) Molecular cloning and characterization of two cDNAs encoding 1-deoxy-D-xylulose 5-phosphate reductoisomerase from *Hevea brasiliensis*. *J Plant Physiol*, **165**, 991-1002.

Slonczewski, JL, Foster JW (2009) In *Microbiology: An Evolving Science*. W. W. Norton & Company Inc., New York.

Smith JS, Brachmann CB, Celic I, Kenna MA, Muhammad S, Starai VJ,

Avalos JL, Escalante-Semerena JC, Grubmeyer C, Wolberger C, Boeke JD (2000) A phylogenetically conserved NAD+-dependent protein deacetylase activity in the Sir2 protein family. *Proc Natl Acad Sci USA*, **97**, 6658-63.

Soppa J (2010) Protein acetylation in archaea, bacteria, and eukaryotes. *Archaea*, **pii**, 820681.

Starai VJ, Escalante-Semerena JC (2004) Identification of the protein acetyltransferase (Pat) enzyme that acetylates acetyl-CoA synthetase *in Salmonella enterica*. *J Mol Biol*, **340**, 1005-1012.

Starai VJ, Gardner JG, Escalante-Semerena JC (2005) Residue Leu-641 of Acetyl-CoA synthetase is critical for the acetylation of residue Lys-609 by the Protein acetyltransferase enzyme of *Salmonella enterica*. *J Biol Chem*, **280**, 26200-26205.

Street IP, Christensen DJ, and Poulter CD (1990) Hydrogen exchange during enzyme-catalyzed isomerization of isopentenyl diphosphate and dimethylally diphosphate. *J Am Chem Soc*, **112**, 8577-8578.

Struhl K (1998) Histone acetylation and transcriptional regulatory mechanisms. *Genes Dev*, **12**, 599-606.

Suzuki F, Zhu Y, Sawada H, and Matsuda I (1998) Identification of Proteins Involved in Toxin Production by *Pseudomonas glumae*. *Ann Phytopathol Soc Jpn*, **64**, 75–79.

Suzuki M, Kamide Y, Nagata N, Seki H, Ohyama K, Kato H, Masuda K, Sato S, Kato T, Tabata S, Yoshida S, Muranaka T (2004) Loss of function of 3-hydroxy-3-methylglutaryl coenzyme A reductase 1 (HMG1) in Arabidopsis leads to dwarfing, early senescence and male sterility, and reduced sterol levels. *Plant J*, **37**, 750-761.

Tan F, Zhang Y, Wang J, Wei J, Cai Y, and Qian X (2008) An efficient method for dephosphorylation of phosphopeptides by cerium oxide. *J Mass Spectrom*, **43**, 628-632.

Tang YC, Chang HC, Hayer-Hartl M, Hartl FU (2007) Snap Shot: molecular chaperones, Part II. *Cell*, **128**, 412.

Thai L, Rush JS, Maul JE, Devarenne T, Rodgers DL, Chappell J, Waechter CJ (1999) Farnesol is utilized for isoprenoid biosynthesis in plant cells via farnesyl pyrophosphate formed by successive monophosphorylation reactions. *Proc Natl Acad Sci USA*, **96**, 13080-13085.

Vabulas RM, Raychaudhuri S, Hayer-Hartl M, Hartl FU (2010) Protein folding in the cytoplasm and the heat shock response. *Cold Spring Harb Perspect Biol*, **2**, a004390.

Van der Fits L, Memelink. J (2000) ORCA3, a jasmonate-responsive transcriptional regulator of plant primary and secondary metabolism. *Science*, **289**, 295-7.

VanBogelen RA, Neidhardt FC (1990) Ribosomes as sensors of heat and cold shock in *Escherichia coli*. *Proc Natl Acad Sci USA*, **87**, 5589-5593.

Vranová E, Coman D, and Gruissem W (2012) Structure and dynamics of the isoprenoid pathway network. *Mol Plant*, **5**, 318-333.

Vranová E, Hirsch-Hoffmann M, Gruissem W (2011) AtIPD: a curated database of Arabidopsis isoprenoid pathway models and genes for isoprenoid network analysis. *Plant Physiol*, **156**, 1655-1660.

Walter MH, Hans J, Strack D (2002) Two distantly related genes encoding 1-deoxy-d-xylulose 5-phosphate synthases: differential regulation in shoots and apocarotenoid-accumulating mycorrhizal roots. *Plant J*, **31**, 243-254.

Wang K, Wang W, No JH, Zhang Y, Zhang Y, and Oldfield E (2010) Inhibition of the Fe_4S_4-cluster-containing protein IspH (LytB): EPR, metallacycles, and mechanisms. *J Am Chem Soc*, **132**, 6719-6727.

Welander PV, Hunter RC, Zhang L, Sessions AL, Summons RE, Newman DK (2009) Hopanoids play a role in membrane integrity and pH homeostasis in *Rhodopseudomonas palustris* TIE-1. *J Bacteriol*, **191**, 6145-6156.

Wiberley AE, Donohue AR, Westphal MM, Sharkey TD (2009) Regulation of isoprene emission from poplar leaves throughout a day. *Plant Cell Environ*, **32**, 939–47.

Wink M (2003) Evolution of secondary metabolites from an ecological and molecular phylogenetic perspective. *Phytochemistry*, **64**, 3-19.

Wu S, Schalk M, Clark A, Miles RB, Coates R, Chappell J (2006) Redirection of cytosolic or plastidic isoprenoid precursors elevates terpene production in plants. *Nat Biotechnol*, **24**, 1441-1447.

Wolff M, Seemann M, Tse Sum Bui B, Frapart Y, Tritsch D, Estrabot AG, Rodríguez-Concepción M, Boronat A, Marquet A, Rohmer M. (2003) Isoprenoid biosynthesis via the methylerythritol phosphate pathway: the (E)-4-

hydroxy-3-methylbut-2-enyl diphosphate reductase (LytB/IspH) from *Escherichia coli* is a [4Fe–4S] protein. *FEBS Lett*, **541**, 115-120.

Yazaki K, Sasaki K, Tsurumaru Y (2009) Prenylation of aromatic compounds, a key diversification of plant secondary metabolites. *Phytochemistry*, **70**, 1739-1745.

Yu BJ, Kim JA, Moon JH, Ryu SE, Pan JG (2008) The diversity of lysine-acetylated proteins in *Escherichia coli*. *J Microbiol Biotechnol*, **18**, 1529-1536.

Zhang J, Sprung R, Pei J, Tan X, Kim S, Zhu H, Liu CF, Grishin NV, Zhao Y (2009) Lysine acetylation is a highly abundant and evolutionarily conserved modification in *Escherichia coli*. *Mol Cell Proteomics*, **8**, 215-225.

Zhou D, White RH (1991) Early steps of isoprenoid biosynthesis in *Escherichia coli*. *Biochem J*, **273**, 627-634.

국문 요약

아이소프렌 단위는 생물종에 따라 메발론산 경로 (MVA pathway) 또는 비메발론산 경로 (MEP pathway)를 통해 만들어지며, 생존에 필요한 물질인 터핀 생합성의 주 재료가 된다. 전세계 벼 생산에 큰 영향을 주는 벼 병원균인 *Burkholderia glumae*는 비메발론산 경로만을 이용하는 그람 음성 세균으로, 특히 경로에 존재하는 총 7개의 유전자중, 처음과 마지막 유전자인 *dxs*와 *hdr*를 각각 2벌씩 가지고 있다. 비메발론산 경로에서 여러 벌 존재하는 유전자는 각각 터핀 생합성 흐름을 조절하는 고유의 역할을 가지는 타입별로 분류가 되어있으나, 식물에서 연구가 주로 이루어지고, 더욱이 *hdr* 유전자 연구는 거의 전무하다. 그럼에도, 없는 유전자는 버리려고 하는 세균의 진화상 특징을 고려할 때, 두 벌의 *hdr*도 고유의 역할을 각각 가질 것으로 생각되며, 더욱이 식물에서, *hdr*도 타입이 존재하는 것이 밝혀짐에 따라, 세균에서 두 벌의 *hdr* 기능이 각각 분화되어 있는지를 연구하게 되었다.

우선, 효소의 기본 특성을 알아보기 위해, 과발현을 통해 재조합 효소를 획득하여, 기질과 반응시켰다. 두 효소 모두 IPP와 DMAPP를 지금까지 보고된 바와 다른 2:1의 비율로 생산하며, 특히 Hdr1은 Hdr2보다 10배 효율적인 효소였다. 이는 Hdr1은 보다 어려운 환경에서 재빠른 반응을 통해 물질을 생산하기 위한 효소이기 때문이라고 생각되며 Hdr2에 비해 상시 발현양이 낮은 이유의 원인이라고 생각된다, 또한 두 효소가 56.1 %만의 상동관계를 가지고, 서로 다른 계통 분기를 가지는 것으로 볼 때 한 유전자는 수평적 유전자 이동에 의하여 습득되었음을 추론할 수 있다. 염기서열 분석을 통해, 각각의 상동유전자가 스트레스관련 유전자 그리고 호파노이드 합성 관련 유전자와 각각 오페론을 이루고, promoter를 공

유하는 것을 발견하였고, 이는 두 벌의 유전자가 각기 다른 쓰임새를 가지는 증거라고 생각되었다. 보다 정확한 두 유전자의 차이를 확인하기 위하여, 각각 유전자의 기능을 knock-out 시켜, 표현형을 관찰하였다. 37 ºC 배양에서는 생장이 차이가 없었으나, 열, pH 스트레스를 주었을 때, HDR1KO 에서 생장이 늦어졌으며, 최소배지 배양과, 벼에 접종하였을 때 생장의 차이가 심화되고, 제대로 군체를 형성하지 못하였다. 열악한 환경에 처해질수록 벌어지는 생장의 차이는 오직 Hdr1이 기능을 수행하지 못할 때, 스트레스 대처능력이 저하되어 나타나는 현상이라 생각되며, 이는 두 벌의 Hdr 역할이 분화되어 있음을 뜻한다. 더욱이 저하된 스트레스저항성과 군체형성능력으로 말미암아, 유묘와 출수기 벼에 병을 내는 능력 또한 저하됨을 관찰할 수 있었다. 이러한 현상을 설명하기 위하여, 각각의 돌연변이체의 세포질 단백질 패턴을 관찰하였고, HDR1KO에서만 보이는 몇몇 단백질들의 이동성 차이가 발견되었고 LC MS/MS 분석을 통해 그 중 스트레스 관련 단백질인 GroEL의 아세틸레이션을 발견하고, 이것이 단백질의 활성화를 이끌어낸 다는 결론을 내렸다. 오직 *hdr1* promoter이 포함된 조합만이 HDR1KO의 GroEL 디아세틸레이션과 표현형을 회복시킬 수 있었고, 이로써 상동유전자가 각기 다른 조절 기작을 가지며 유전자의 전사에 관여하는 요소를 찾아야 했다. Promoter 분석으로 *hdr2*는 ToxR의 조절을 받으며, Y1H와 EMSA 그리고 RT-qPCR 실험으로 ToxR은 *hdr2*의 activator임을 알아내었다. *hdr1*은 아마도 스트레스 관련 신호에 의해 전사가 개시되지 않을까 생각 된다. 또한 전사체 분석을 통해, 세포 내에 발생하는 전반적인 변화를 감지하였는데, HDR1KO는 Toxoflavin 생합성 유전자가, HDR2KO는 스트레스관련, 리보솜 단백질 합성, *SAM-decarboxylase*가 발현량이 현저히 증가함을 발견하였다. 이를 토대로, *hdr1* 오페론은 스트레스에 연관

된 신호를 받아, acetylation을 통하여 GroEL의 활성화 조절에 관여하며, *hdr2* 오페론은 ToxR의 조절에 의해, 호파노이드 합성에 관련한 기능을 가지며, 특정 호파노이드 생산이 차질을 빚을때, 나타나는 스트레스를 decarboxlated-SAM을 이용한 GroEL의 활성화로 극복하는 모델을 창안하였다. 더불어 Toxoflavin 생산 증가는 HDR1KO의 낮은 생장밀도로 인해 밀도를 유지하려는 성질 때문으로 생각된다. *hdr1* 오페론에서 *hdr1*이 가지는 역할에 두 가지 가설을 제시한다. 첫째는 그람양성 세균의 밀도조절 기작에서 이미 페로몬으로 이용되는 prenylated-peptide가 스트레스 반응에서 신호전달 물질로 작용하는 기작이다. 둘째는 효소는 일종의 복합체를 이루어, 특정 물질을 생산하는 경우가 많은데, 각각의 Hdr은 연관되어 있는 다른 효소와의 복합으로 Hdr1 복합체는 스트레스 반응에 관련하는 새로운 물질을 만들어 내는 기작이다.

주요어; *Burkholderia glumae*, GroEL acetylation, *hdr* 상동유전자 오페론, 분화된 신호전달, 비메발론산 경로

학 번; 2005-21628

CURRICULUM VITAE

Name : Moonhyuk Kwon

Sex : Male

Date of Birth : 23 Dec, 1979

Place of Birth : Pusan, Korea

Present Address : Graduate School of Agricultural Biotechnology

Seoul National University

Seoul, 151-921, Korea

Phone; 82-2-880-4652, Fax; 82-2-873-3112

E-mail; ardrid04@snu.ac.kr

Education : Seoul National University

Seoul, Korea

B. S. In Agricultural Chemistry (’05)

Seoul National University

Seoul, Korea

Ph. D. in Agricultural Biotechnology (’13)

PUBLICATIONS

1. **Moonhyuk Kwon,** Bok-Kyu Shin, Jaekyoung Lee, Jaehong Han and Soo-Un Kim (2012) Characterization of *Burkholderia glumae* BGR1 4-Hydroxy-3-methylbut-2-enyl Diphosphate Reductase (Hdr), the Terminal Enzyme in 2-*C*-Methyl-D-erythritol 4-Phosphate (MEP) Pathway. *ABC*. Accepted for publication.

PATENTS

ACKNOWLEDGEMENTS

생물과 화학, 이 두 단어는 어느 순간부터인가 내게 선망의 대상이었고, 늘 이두 과목을 사이에 두고 어떤 것과 내 인생의 마지막까지 함께 할 것인가에 대해 고민이 있었던 것으로 기억한다. 고등학교 무렵이었을 것이다. 생물은 그 자체로써 매력을 물씬 풍기는 분야였고, 화학은 장선영 선생님이라는 은사 덕분에 무척 신선하고, 재미있는 분야였다. 졸업하면 고스톱 치러 놀러라 하시던 선생님은 졸업 후 몇 해가 지나지 않아 불의의 병으로 돌아가셨지만, 화학의 기초를 다져주신 고마운 분으로 기억하며, 비록 보잘 것 없지만, 이 논문의 첫 감사를 드리고 싶은 분이라, 서두에 미리 감사의 말씀을 드린다. 이 두 분야를 대학 전공에서 선택하여야 하는 고민은 하지만 이내 더 이상 고민이 되지 않게 되었다. 맙소사, 생물과 화학 모두 전공으로 공부할 수 있는 곳이 있을줄이야. 서울대학교 응용생물화학부는 내게 그래서 선택한 소중한 배움의 터전이었다. 장학생으로 당당히 입학하여, 비록 중간 중간 많은 일탈과 사건들이 있었지만, 훌륭히 공부하였고, 열정적으로 생활하였으며, 누구보다도 더 열심히 대학생활을 했음을 자부한다. 아직 1, 2학년때 받은 몇 가지 과목의 C, D 가 눈에 거슬릴때도 있지만, 한편으로는 공부외의 다른 소중한 경험들이 지금의 내가 있게 해준 밑거름일 수 있기에, 후회없는 대학생활을 보낼 수 있었다. 지금도 세상 누구보다 더 친한 김상우, 신혜철, 윤상식, 이동주, 정우철, 정재훈, 최희규, 홍순찬 (이상 가나다 순), 이 친구들과의 피보다 진하진 않지만 가족을 제한다면 누구보다 소중한 우정은 좋은 추억들과 멋진 에피소드를 간직하며 7년간을 잘 지내게 해준 원동력이었다. 앞으로도 더 좋고 멋진 인간관계가 되

리라 의심하지 않는다. 모두에게 말로 못할 최대의 감사의 인사를 전한다. 그리고 양해조(97). 친구들 보다 오히려 더 오랫동안 어려움을 나누고, 서로 격려하며, 많은 도움을 주고 받았던 형에게 당연한 감사의 말씀을 드린다. 같은 무리인 김정훈, 최혁준, 그리고 김경완 모두 고맙다. 앞으로 각각의 분야에서 최선을 다해 끌어주고 당겨주도록 하자. 후배 박상욱(99). 오갈 곳 없던 시절, 흔쾌히 받아주었던 네 마음, 형이 절대로 잊지 않도록 할게. 고맙다.

사실 대학원에 오려는 생각은 입학할 때부터 생각하고 있었다. 하지만, 사실 막상 어떤 선생님의 사사를 받으며, 어떠한 분야를 연구할 지 구체적으로 생각해 본 적은 그리 길지 않았던 것 같다. 하지만, 돌이켜보면 늘 나는 운이 좋은 사람인 것 같다. 항상 돈은 필요한 만큼 필요한 때에 생겼으며, 자연스레 시기에 맞는 인연이 나타나 반드시 결정이 필요할 때에 큰 도움을 받거나 혹은 내가 가고자 하는 방향으로 잘 이끌어 준 것 같다. 내가 한참 대학원 생각에 고민할 때, 인연처럼 만난 그런 사람이 김상민 박사이다. 수업으로 들었던 배구 수업에서 조교로 활동하였던 형을 만나, 비록 세세한 조언을 듣지 못했지만, 형의 인품과 능력은 천연물화학을 공부하겠다는 생각에 쐐기를 박아주게 된다. 감사드리며 앞으로도 좋은 동료, 선후배로써 잘 부탁드리는 바이다. 이렇게 이야기하면 김수언 교수님께서 섭섭하게 생각하실 지 모르겠지만, 당연히 천연물 화학실에 입학하게 된 동기는 선생님의 인품과 명성, 그리고 연구분야 때문이었다. “김수언 교수님. 정말 감사드리며 또 감사의 인사 드립니다. 선생님 덕분에 제가 졸업장을 받을 수 있게 되었고, 또 인생을 배우게 되었습니다. 선생님의 많은 지식과 연륜을 널리 세상을 이롭게 하는데 사용할 수 있도록 꼭 성공하겠습니다. 꾸벅.” 그리고 부족한 제자 가르쳐 주시고, 실험에 도

움을 많이 주신 최양도, 김정한, 노희명, 김민균, 이상기, 배의영 교수님들께 감사와 존경을 보내드린다. 특히 바쁘신 와중에도 심사를 흔쾌히 허락해 주시고, 조언을 많이 해 주신 오기봉, 신찬석 교수님께 진심으로 감사의 인사를 드린다. 이 졸업 논문의 시작은 사실 조그마한 흥미와 궁금증에서 비롯되었다. 하지만 이 작은 호기심에도 관심 가져주시며, 지원을 아끼지 않으셨던 황인규 교수님께 감사의 인사를 드리며, 낮에는 실험의 기초를 다져주고, 밤에는 가상의 공간에서도 함께했던 진우형과 사소한 골칫거리부터 큰 고민 해결에 도움을 준 내 친구 홍섭이에게도 감사를 전한다. 그리고, 실험실에서 같이 생활하며, 웃고 또 웃었던 미향누나, 순희누나, 희영누나, 김연복, 이광일, 전율택, 이철호, 김보라, 이재경, 김용경, 이영섭, 전은미, 김지영, 최고은, 나르기스, 라보니, 홍성호, 김철호, 손영진 모두 감사하며 특히 8년간 함께 한 민경이와 진희는 특별히 더 감사인사 전한다. 그리고, 옆방 사람들. 정말 고마웠다. 삶의 재충전, 인생의 활력소가 되어준 서주석, 이한용, 서준성, 심재성, 이상준, 엄태영 모두 노던블랏 한 장이라도 데이터를 만드는데 도움을 준 바 감사하게 생각한다.

앞으로 또 어떤 인연과 새로운 어떤 일들이 벌어질까 모르겠지만, 과거에 실험을 함께 하였으며 앞으로도 함께할 소중한 선후배 과학자들, 박시형 박사님, 한재홍 박사님, 신복규 군 그리고 제 심사를 기꺼이 수락해 주신 권형진 박사님께 감사드리고, Kist의 강경수, 정우석, 박진수, 강석우 모두 잊지 말고 좋은 동료 과학자로써 앞으로도 잘 부탁드린다. 선후배로써도 좋은 사람들이다. 특히 판철호 박사님과 송대근 군에게 무한한 감사와 존경을 바친다. 그리고, 내 능력을 믿고, 내가 사회로의 첫 발을 내딛는데 기회를 주신 노대균 교수님, 예

전부터 그리고 앞으로도 존경했고, 존경하며, 멋지게 연구 한 번 해 보도록 하겠습니다.

고등학교부터 대학원 졸업때까지 많은 도움을 준 여러 사람들께 먼저 인사를 드렸지만, 마지막으로 소중한 가족들과 아내에게 말을 전하는 것이 도리일 듯 싶다. 늘 든든한 뒷 모습을 보이시며 가족을 위해 살아오신 아버지, 고생하시며 아들 걱정과 교육에 한 평생 희생하신 어머니, 언제봐도 의지가 되고 힘이 되는 사랑하는 우리 누나, 그런 누나를 사랑해주는 우리 매형, 오빠를 말없이 걱정해주는 많이 못 챙겨줘 미안한 우리 동생, 지갑을 열게 만드는 귀엽고 예쁜 조카 유진 지우 모두 사랑하고, 고맙다. 우리 부모님 희생이 아니었으면 뭐하고 있었을까 생각이 들 때가 많다. 앞으로 정말 건강히 오래 사셨으면 좋겠다. 그리고 늘 특별히 생각해주고, 많이 사랑해 준 차동기, 서미영 부부와 김원국, 차남희 부부에게 감사드린다. 뒤늦게 부모자식의 연이 생겼으나, 해 드린건 없어도 늘 사위 챙겨주시는 장모님, 나리 키워주시고, 저 사랑해 주셔서 감사드리며, 하나밖에 없는 사랑하는 처제 김유리와 그의 남편이자 훌륭한 인격의 소유자 이룡에게도 감사드린다.

그리고 누구보다 늦게 일해도, 졸업이 좀 늦어져도, 내가 힘들어도, 기뻐도 늘 이해해주고 사랑으로 감싸주는 내 소중한 아내 김나리 박사, 비록 내가 당신보다 졸업이 좀 늦었지만, 보란듯이 성공하여 갚아주도록 열심히 살게. 늘 부족하지만 날 믿어줘서 고맙고, 사랑하고 또 사랑한다.

감사의 글이 뭐이리 기냐고 생각할지도 모르지만, 감사한다는 생각을 가지고 살아온 것이 좋은 인연과 좋은 길을 걸을 수 있는 원동력이 되었는지도 모른다. 모두들 감사합니다.